Bedload transport in rivers: from the flume to the field

A. Recking

HAL Id: tel-02598769

https://hal.inrae.fr/tel-02598769v1

Submitted on 16 May 2020

UNIVERSITY OF GRENOBLE

Dissertation submitted to obtain

L'HABILITATON A DIRIGER DES RECHERCHES

In

Mechanics

by

Alain RECKING

Irstea (Cemagref), Research Unit Torrential Erosion, Snow and Avalanches
Grenoble

Bedload transport in rivers: from the flume to the field

JURY

Gary Parker	Examiner
John Pitlick	Examiner
Philippe Belleudy	Examiner
Mohamed Naaim	Examiner
François Charru	Reviewer
Alain Crave	Reviewer
Stuart Lane	Reviewer

August 2012

TABLE OF CONTENT

NOTATIONS

A *Cross-section area*

C *Chezy resistance coefficient*

C_f *Bed resistance coefficient*

d *Flow depth*

D *Grain diameter*

D_x *Grain diameter (subscript denotes % finer)*

f *Darcy-Weisbach friction coefficient*

Fr *Froude number $Fr=U/(gH)^{1/2}$*

F_s *Sand fraction at the bed surface*

k_s *Bed roughness*

n *Manning resistance coefficient*

$\overline{P}$ *Width averaged value of parameter P: $\overline{P} = \dfrac{1}{W}\int_{y=0}^{W} P\,dy$*

Q *Flow discharge*

q *Specific discharge (q=Q/W)*

Q_s *Sediment discharge at equilibrium flow condition*

q_s *Bedload transport rate per unit width ($q_s=Q_s/W$)*

q_{sv} *Volumetric bedload transport rate per unit width ($q_{sv}=Q_s/[W\rho_s]$)*

R *Hydraulic radius*

Re *Reynolds number $Re=UR/\nu$*

$Re*$ *Roughness Reynolds number $Re*=u*D/\nu$*

S *Geometric slope*

S_e *Energy slope*

s *Relative density ($s=\rho_s/\rho$)*

$tan\alpha$ *Dynamic coefficient of internal friction*

U *Vertically averaged flow velocity*

$u(z)$ *Mean flow velocity at z level*

$u*$ *Shear velocity:* $u* = \sqrt{\tau / \rho}$

W *Channel width*

z *Height above the bed*

α *Bed roughness to grain diameter ratio* k_s/D_x

Φ *Dimensionless transport rate:* $\Phi = q_{sv}/[g(s\text{-}1)D^3]^{0.5}$

κ *Von Karman coefficient (0.4)*

ρ *Fluid density*

ρ_s *Sediment density*

τ *Bed roughness shear stress* $[N/m^2]$

τ' *Grain shear stress* $[N/m^2]$

τ'' *Shear stress induced by form resistance* $[N/m^2]$

$\tau*_c$ *Critical Shields stress corresponding to grain entrainment [ ]*

$\tau*_m$ *Mobility Shields stress corresponding to the transition from partial to full mobility [ ]*

$\tau*$ *Shields parameter calculated for diameter* D_x *[ ]:* $\tau*_x = \tau/[(\rho_s\text{-}\rho)gD_x]$

ABSTRACT

Because it is difficult to measure bedload sediment transport in rivers during flooding, flume experiments have been widely used for studying the mechanisms involved and for constructing bedload transport equations. However, flume experiments usually involve several simplifications concerning the sediment material (usually a uniform grain size distribution is used) and the flow conditions (usually maintained high for one-dimensional transport and no bed meandering), which can have strong consequences when the flume-derived equations are used in the field. This manuscript presents the results of my research on this topic and aims to fill the gap between the flume and the field. The three parts of the manuscript concern the hydraulics, the threshold conditions for bedload transport, and bedload transport rates. It is shown that large diameters such as D_{84} are recommended for matching the results obtained in the flume and in the field, both for flow resistance and threshold dimensional shear stress. The comparison is less trivial for bedload transport as (i) most flume bedload transport were measured for high shear stress and almost full mobility of the bed sediments, whereas in the field, measurements usually correspond to partial transport (the finer fractions are transported whereas the coarsest fractions are maintained at rest) and (ii) because of nonlinearity, 1D flume derived equations tend to underestimate bedload transport when they are used with width averaged data.

RESUME

En raison de la difficulté à mesurer le charriage dans les rivières en crue, l'expérimentation en canal a très largement été utilisée pour étudier les mécanismes impliqués et pour élaborer des équations. Cependant, les expériences en canal impliquent généralement plusieurs simplifications concernant les sédiments (généralement une distribution uniforme est utilisée) et les conditions d'écoulement (généralement maintenues élevées pour un transport unidimensionnel), ce qui peut avoir des conséquences fortes lorsque les équations qui en sont issues sont utilisées sur le terrain. Ce manuscrit présente les résultats de ma recherche sur ce sujet et vise à faire le lien entre le laboratoire et le terrain. Les trois parties du manuscrit concernent l'hydraulique, les conditions de début de mouvement, et la modélisation du charriage. Il est montré que les grands diamètres tels que le D_{84} sont recommandés pour comparer les résultats obtenus au laboratoire et sur le terrain, à la fois pour la résistance à l'écoulement et pour la contrainte adimensionnel de mise en mouvement. La comparaison est moins triviale pour charriage car (i) le charriage au laboratoire a souvent été mesuré pour des

contraintes de cisaillement fortes et une mobilité quasi totale des sédiments du lit alors que sur le terrain, les mesures correspondent habituellement à un transport partiel (les fractions les plus fines sont transportées alors que le fractions plus grossières sont maintenus au repos) et (ii) en raison de la non-linéarité du phénomène, les équations 1D issues du canal ont tendance à sous-estimer le charriage lorsqu'elles sont utilisées sur le terrain avec grandeurs moyennées sur la section.

1. INTRODUCTION

Bedload prediction is of primary importance for river engineering, fluvial geomorphology, eco-hydrology, environmental surveys and management, and hazard prediction. For instance bedload transport impacts the bed morphology, the banks stability, and the safety of associated infrastructures. Sediment transport is also of first-order importance for the quality and complexity of in-channel habitats in the aquatic environment (Pitlick and Van Steeter, 1998).

Policies and guidelines are being developed to limit adverse impacts of sediment, whether too much or too little. One recent example is the European Water Framework Directive (WFD), issued by the EU in 2000 with the specific goal of establishing a framework for protecting water resources in member states (*EU*, 2000). Among the attributes of rivers required to maintain *high* ecological status, the WFD lists several environmental quality standards related directly to sediment transport and geomorphology: *"The continuity of the river is not disturbed by anthropogenic activities and allows undisturbed migration of aquatic organisms and sediment transport"* (*EU*, 2000, *p*. 40) and, *"Channel patterns, width and depth variations, flow velocities, substrate conditions and both the structure and condition of the riparian zones correspond totally or nearly totally to undisturbed conditions"* (*EU*, 2000, *p*. 40).

This is why prediction of sediment mobility (in quantity and quality) has become a central question in numerous river restoration projects, as for instance for the Rhone river (Gaydou, 2012) or the Rhine river (Schmitt et al., 2012): when will the sediment move? What will be the river response when adding sediments? Which size should be used to obtain a stable channel, or a channel of ecological interest? For instance Figure 1a shows the reinjection of sediments in the Rhine River near Kembs (France) in October 2010, for ecological restoration. In mountain streams, sediments can impact directly the safety of populations, as shown in Figure 1b. Despite almost one century of research dedicated to this topic, even in the most developed countries, management agencies still lack the resources to effectively predict bedload transport in rivers and associated river morphodynamic.

Figure 1: (a) Injection of 25000m3 of sediments for ecological restoration of the Rhine River near Kemb (photo Alsace.fr) (b) Sediment deposition on the Domenon River and its impacts on population safety (Photo Belleudy)

Sometimes, practitioners can use field measurements to calibrate a sediment curve, but most of the time such data do not exist because measuring bedload in the field is a difficult and time-consuming task. This is why they must employ computational methods, often established with flume experiments. Usually experiments were performed with appropriate Froude (Fr) and grain Reynolds number (Re*), for similitude. But the major simplifications differentiating the flume and the field is that most materials used in the laboratory are either artificial materials or natural sediments of nearly uniform grain size distribution. Doing so, it is implicitly considered that bedload transport is only the result of the flow and sediment interaction. This is not true: when sediments of different grain sizes are mixed, their strongly interact during their movement (either by gravity in dry flows or under the action of water), through complex grain sorting phenomenon (Frey and Church, 2011).

A good understanding of bedload transport also necessitates having a good description of the flow, and more particularly of the shear stress exerted by the flow on the bed. This is why flow resistance equations have also widely been studied in the flume. However, except for a few studies, both topics (flow resistance and bedload transport) were studied in independent research. In addition, for long, results derived from fluid mechanics (especially the law of the wall) has served as a basis for river engineering. However, the flow hydraulics change with the bed sediments and morphology, and flume measurements validated for lowland sandy rivers are not necessarily valid for gravel and cobble-bed rivers, especially on steep slopes mountain streams (Figure 2).
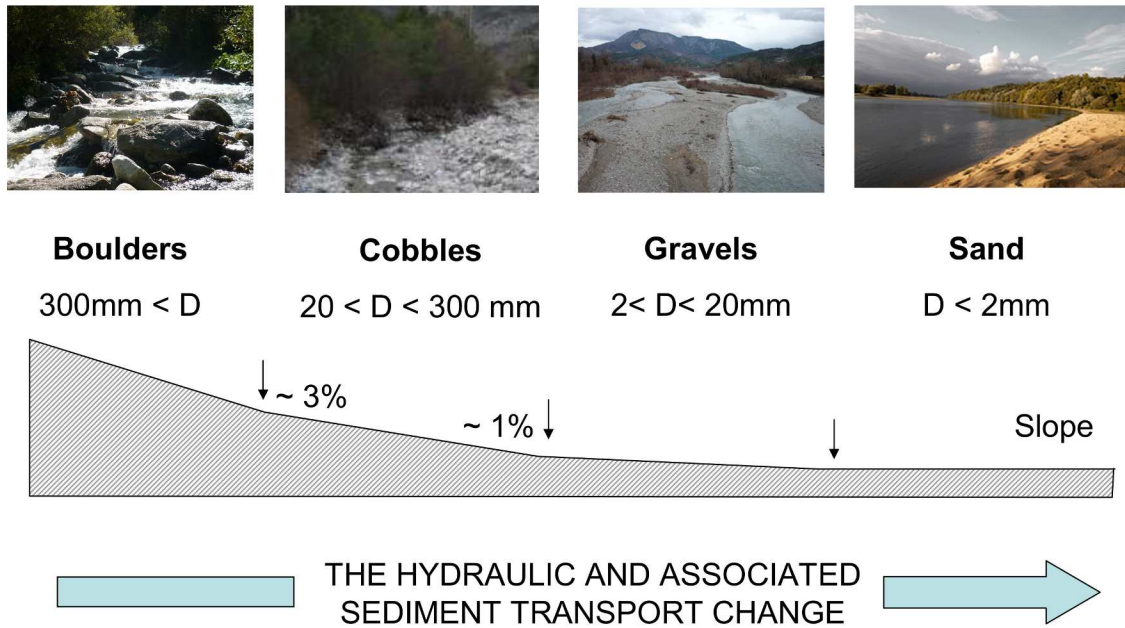
Figure 2 : Changes in bed characteristics with the slope, from lowland sandy-rivers (on the right) to steep slopes boulder streams (on the left).

Width-averaged flow parameters are usually considered in field operations (except when a 2D-numerical or a physical model is used). However, another major difference between the flume and the field is that flume observations and measurements are one-dimensional (usually the flow is chosen such that local depositions can not form) whereas in the field, transport of sediments is usually the response to a two-dimensional flow field associated with a large variance in the bed and flow conditions over the section. This has strong consequences when section-averaged data are used (which is often the case) because relations linking bedload transport and the flow conditions are non-linear.

What are the consequences of flume simplifications on the measured bedload transport and, consequently, how long can the flume derived equations be used in field applications? Figure 3 compares flume and field data sets (10,257 values, the x-axes plots the dimensionless shear τ^* and the y-axes plots the dimensionless bedload transport Φ; both terms are defined latter in this manuscript) and the Meyer-Peter and Mueller equation (Meyer-Peter and Mueller, 1948), probably the most widely used bedload transport equation. Three conclusions can be drawn from this figure: (1) the flume and the field data collapse only for a limited flow range, (2) the scatter is large (to a given shear stress bedload transport can cover almost 6 order of magnitude) and (3) a single equation can not reproduce the wide range of flow condition.
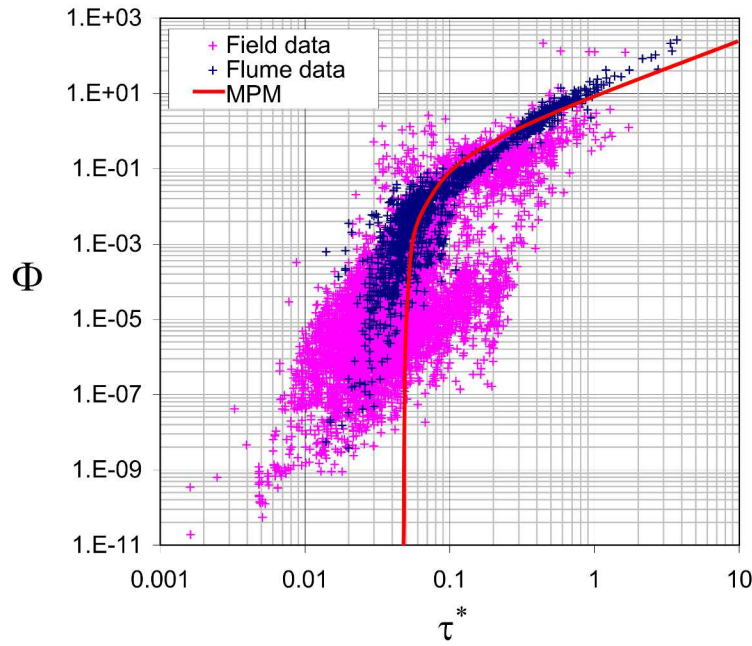
Figure 3 : Comparison between bedload measured in the flume and in the field (dimensionless shear stress on the x-axes and dimensionless bedload on the y-axes) and the well know bedload equation from Meyer-Peter and Mueller (1948)

The validity of flume derived equations when used in field applications has motivated dozens of research programs, and despite results are contrasted, most studies have concluded that flume derived equations can lead to large over or under bedload prediction. So, should we conclude that flume experiments are not suitable for investigating bedload transport and the associated morphodynamics? This is an important issue considering that flume experiments are still widely used in many labs all around the world. This manuscript aims to fill the gap between the flume and the field. The physical processes are considered, and analyzed with consideration of simplifications introduced in the flume. In a first part, the hydraulics is considered because the way the shear stress is computed is the first source of difference that can exist between the flume and the field results. I also examine how hydraulic changes with changing bed substrate and slope, from lowland sandy rivers to steep boulder streams (Figure 2). In a second part, I present the state of the art and the results of my research on incipient bedload motion, with emphasis on the impact of changing flow hydraulics with changing slope. In the third part, the link between the flume and the field bedload transport is investigated with consideration of partial transport and nonlinearity, and consequences for bedload prediction are discussed. Finally outlooks of this research are discussed.

2. SHEAR STRESS AND FLOW RESISTANCE

Since hydraulic considerations can be a large source of error in bedload prediction, this part reviews   the physics involved and the methods that have been proposed in the literature for computing the bed shear stress.

2.1. General considerations

2.1.1. Bed shear stress τ' and friction law

Let consider a rough turbulent flow (considered two-dimensional for simplicity's sake), over a flat bed constituted of uniform grains. In such flow the bottom roughness is greater than the viscous sub-layer and the shear stress τ' near the wall is given by its turbulent component $\rho u'v'$ (where ρ is the water density and u' and v' are the turbulent velocities in the flow and the vertical directions, respectively), ignoring the viscous term $\rho v \partial u/\partial y$ (where v is the water viscosity and $\partial u/\partial y$ is the velocity gradient in the vertical). This turbulent shear stress was modelled with the eddy viscosity concept v_t (Boussinesq, 1872) and the Prandtl mixing length empirical model $v_t = l^2 \partial u/\partial y$, where $l = \kappa y$ ($\kappa = 0.4$ is the Von Karman coefficient). Mass conservation imposes $u'^2 = v'^2 = u^{*'2}$ at the wall ($u^{*'}$ [ms^{-1}] is called the shear velocity), which finally gives:

$$\tau' = \rho v \frac{\partial u}{\partial y} + \rho \overline{u'v'} \approx \rho \overline{u'v'} = \rho v_t \frac{\partial u}{\partial y} = \rho \left[\kappa y \left(\frac{\partial u}{\partial y} \right) \right]^2 = \rho u^{*'2} \tag{1}$$

In field applications, turbulence is generally not available and the indirect approach consists in integrating $u^{*'} = \kappa y (\partial u/\partial y)$, which gives the well-known logarithmic velocity profile:

$$\frac{u(y)}{u^{*'}} = \frac{1}{\kappa} \ln \left(\frac{y}{y_0} \right) \tag{2}$$

where y_0 is the value of y where u is zero. Assuming this profile is verified, two flow velocities u_1 and u_2 measured at two different depths y_1 and y_2 close to the bed can be used to calculate the boundary shear stress $\tau' = \rho u^{*'2}$:

$$\tau' = \rho \left(\frac{u_1 - u_2}{2.5 \ln(y_1/y_2)} \right)^2 \tag{3}$$

One can also determine y_0 graphically. This method, called the Clauser method, has been successfully tested in the field (Bridge and Jarvis, 1982; Petit, 1994; Sime et al., 2007).

13

Depth-averaging Eq.2, and defining the zero level with $y_0 = k_s/30$ (where k_s is the bed roughness; Nikuradse, 1933) gives (for $d \gg y_0$) the friction law:

$$\frac{U}{u^{*'}} = \frac{1}{\kappa} \ln\left(\frac{11d'}{k_s}\right) \tag{4}$$

Keulegan (1938) first proposed this equation for describing natural flows in canals, with a constant of 12.2 instead of 11 for a trapezoidal section. Considering Eq.1 the bed shear stress can be calculated with the measured flow depth d' and velocity U:

$$\tau' = \rho \left(\frac{\kappa}{\ln(11d'/k_s)}\right)^2 U^2 \tag{5}$$

The roughness k_s is often considered proportional to the grain diameter D (see *Yen, 2002* for an exhaustive review). In rivers, the bed shear stress and associated friction law can be used in bedload modelling only for the ideal situation where the flow is controlled exclusively by the wall friction (i.e. interaction with the bed sediment roughness). In reality, to move downstream the flow must overcome additional 'form' resistance (drag forces), including lateral and vertical channel irregularities, bank and bed vegetation, or transported solids. As a consequence, for a given velocity U, the measured flow depth d is higher than d', and the equations presented above must be used with caution.

2.1.2. Boundary shear stress τ and flow resistance

In fluid mechanics, the drag force exerted on a solid immersed in a flow is $F = \frac{1}{2}\rho A C_D u^2$, where $\frac{1}{2}\rho u^2$ is the dynamic pressure exerted by the local mean flow velocity u on the exposed surface A of the solid, and C_D is a dimensionless drag coefficient. By analogy, the depth-averaged flow velocity U exerts on the river boundary (grain and form roughness) a mean drag force, which is, per unit bed area:

$$\tau = \rho C_f U^2 \tag{6}$$

where C_f is a bed resistance coefficient.

On the other hand, assuming a uniform flow, a force balance applied to the water column links the bed shear stress to the mean flow depth d and the slope (the bed slope S is considered assuming the flow is uniform at the reach scale):

$$\tau = \rho g d S \tag{7}$$

Equalling Eq.6 and 7 gives the flow resistance equation:

$$\frac{U}{gdS} = \left(\frac{1}{C_f}\right)^{1/2}$$

<div align="right">(8)</div>

where C_f is related to the well-known Chezy C [$L^{1/2}s^{-1}$], Manning n [$L^{-1/3}s$] and Darcy-Weisbach (dimensionless) coefficients by the relation:

$$C_f = \frac{g}{C^2} = \frac{gn^2}{d^{1/3}} = \frac{f}{8}$$

<div align="right">(9)</div>

These coefficients can be calibrated for the given flow condition or deduced from nomographs (see *Yen* 2002 for an exhaustive review). The water depth and the slope may be difficult to measure (and even to define) in an irregular cross-section, especially in cobble and boulder beds with large grain sizes.

2.1.3. Relation between τ and τ'

In natural channels, 'form' resistances can be fairly large and the boundary shear stress τ computed with the measured d and U can be much higher than the actual bed shear stress τ' acting on the grains. In that case the use of τ in bedload computation can lead to over-prediction, and a correction is needed to deduce τ' from τ.

Although Einstein and Barbarossa (1952) recognised that there are "*very serious theoretical objections due to the basic nonlinearity of the problem*", one widely accepted approach has considered that the total friction loss is simply the sum of the different friction losses, as is usually (and successfully) done in pipe flows. This led to a linear decomposition $\tau = \tau' + \tau''$ of the bed shear stress $\tau = \rho u^{*2}$ between the boundary shear stress $\tau' = \rho u^{*'2}$ (Eq.1) and the form drags $\tau'' = \rho u^{*''2}$. This linear separation is accomplished through $C_f = C_f' + C_f''$ in Eq.6 and $d = d' + d''$ (Einstein, 1950) or $S = S' + S''$ (Meyer-Peter and Mueller, 1948) in Eq.7, and a friction equation derived for flows over a flat grain surface (as described in paragraph 2.1.1).

Meyer-Peter and Muller (1948) suggested calculating d' with the Manning equation and the Strickler (1923) grain roughness n' deduced for flat beds in the laboratory ($n' = D_{90}^{1/6}/26$):

$$d' = \left(\frac{n'U}{S^{0.5}}\right)^{3/2}$$

<div align="right">(10)</div>

Alternatively, when the total flow roughness n is known ($n = S^{0.5}d^{2/3}/U$), this equation becomes:

$$d' = \left(\frac{n'}{n}\right)^{3/2} d$$

<div align="right">(11)</div>

A second method uses a Keulegan-type flow resistance equation (Eq.4), written in the following form, considering $u*'= \sqrt{gSd'}$ (from Eq.1 and 7) :

$$\frac{U}{\sqrt{gSd'}} = 6.25 + 5.75\log\left(\frac{d'}{k_s}\right)$$

(12)

This equation can be solved iteratively for estimating the depth *d'* associated with the mean velocity *U* (Einstein and Barbarossa, 1952; Wilcock, 2001), such that $\tau'=\rho gd'S$.

Both approaches presented above are identical, except that the Manning equation is explicit. Note that instead of iteratively solving Eq.12 for *d'*, Eq.5 is sometimes used with the measured flow depth *d* and velocity *U* (Ackers and White, 1973; Carling, 1983; Duan and Scott, 2007; Sime et al., 2007). Doing so the method is simplified (no iterations); however, if k_s is defined for the grain roughness, it implicitly considers that the bed shear stress τ associated with measured *d* and *U* is such that $\tau=\tau'$ (i.e. no form resistance).

In the following, only the bed friction is considered (*d'*, τ') but all parameters are written without a note for simplicity (*d*, τ). In addition the flow hydraulic radius *R* is considered in place of the flow depth *d* for the case where the bank friction can not be neglected (with $d \approx R$ when the channel width-to-depth ratio is higher than ~20).

2.2. Roughness layer and bedload roughness

2.2.1. The roughness layer

All the above methods come from the law of the wall in fluids mechanics and consider a logarithmic velocity profile. However the logarithmic profile is not always verified in rivers as shown in Figure 4 (Marchand et al., 1984; Nikora et al., 2004).
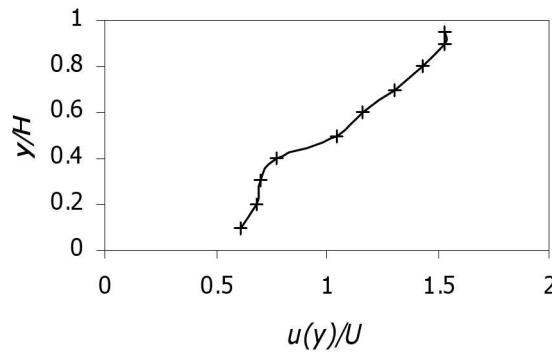

Figure 4 : Velocity profile measured over gravel bed (from Marchand et al. 1984, Lake Creek).

16

Because the wakes shed at the leading edge of the bed elements produce a roughness layer that develops well above the rough surface, the logarithmic profile (when it exists) cannot be extended to the wall (O'Loughlin and Annambhotla, 1969; Christensen, 1971; Ashida and Bayazit, 1973; Day, 1977; Mizuyama, 1977; Nowell and Church, 1979; Marchand et al., 1984; Bathurst, 1988; Nakagawa et al., 1988; Aguirre-Pe and Fuentes, 1990; Jarrett, 1990; noWiberg and Smith, 1991; Robert, 1991; Tsujimoto, 1991; Pitlick, 1992; Ferro and Baiamonte, 1994; Byrd and Furbish, 2000; Byrd et al., 2000; Nikora et al., 2001; Katul et al., 2002; Franca, 2005). Instead, a more complicated pattern was generally described, with a roughness layer close to the bed where the velocity profile was nearly constant, and a second zone (above the former), where the velocity profile was logarithmic (Figure 5).
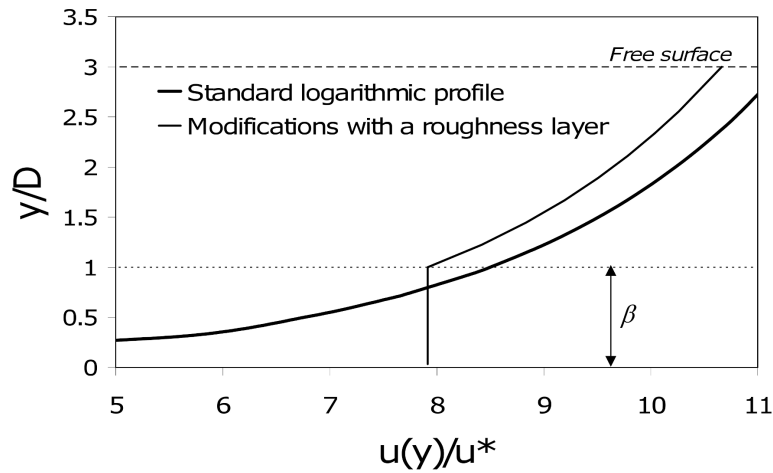
Figure 5 : The standard logarithmic profile compared to the roughness layer profile for the same mean velocity U

This velocity profile can be written (Aguirre-Pe and Fuentes, 1990):

$$\frac{u(y)}{u*} = \frac{1}{\kappa} \ln \frac{y}{\alpha D} + 8.5 \qquad \text{in the logarithmic zone} \tag{13}$$

and

$$\frac{u(y)}{u*} = \frac{1}{\kappa} \ln \frac{\beta}{\alpha} + 8.5 \qquad \text{in the roughness layer} \tag{14}$$

where β is the ratio between the roughness layer thickness and the grain diameter, α is a grain diameter factor in the Nikuradse equivalent roughness $k_s = \alpha D$ used for the logarithmic part of the profile (in the exemple of Figure 5, Eq. 13 and 14 are used with α fitted for the case $\beta = 1$ and $R/D = 3$).

The roughness layer corresponds to zones of intense shear downstream of each roughness element (grains and particle clusters, producing Kelvin-Helmholtz instabilities) where the kinetic energy of the mean flow is transformed into turbulence energy. This turbulence thus produced intensifies the mixing or transfer of momentum, resulting in a continuous adjustment in the velocity profile close to the bed (O'Loughlin and Annambhotla, 1969). The roughness layer thickness is the grain diameter in order of magnitude (Nowell and Church, 1979; Tsujimoto, 1991; Carollo et al., 2005; Manes et al., 2007), but it is likely to vary with slope and relative depth, especially for the wake zone because the wake's frequency and size are related to the mean flow velocity and sediment size (through the Strouhal number). Several studies showed that the mean flow velocity and turbulence intensity near the bed decreased with decreasing relative depth *R/D* (Bayazit, 1976; Tsujimoto, 1991; Wang et al., 1993; Dietrich and Koll, 1997; Carollo et al., 2005; Lamb et al., 2008). The roughness layer also varies with the concentration of protruding sediments (the ratio between the number of grains and the maximum number of grains that can be arranged in the reference area). An optimum concentration was observed over which the roughness layer effects stabilized (Carollo et al., 2005) or even decreased with bed smoothing (Nowell and Church, 1979). However, the measurements available indicate that the roughness layer still exists with a maximum concentration, i.e., with a gravel bed of near-uniform sediment distribution (Aguirre-Pe and Fuentes, 1990; Tsujimoto, 1991; Wang et al., 1993; Manes et al., 2007).
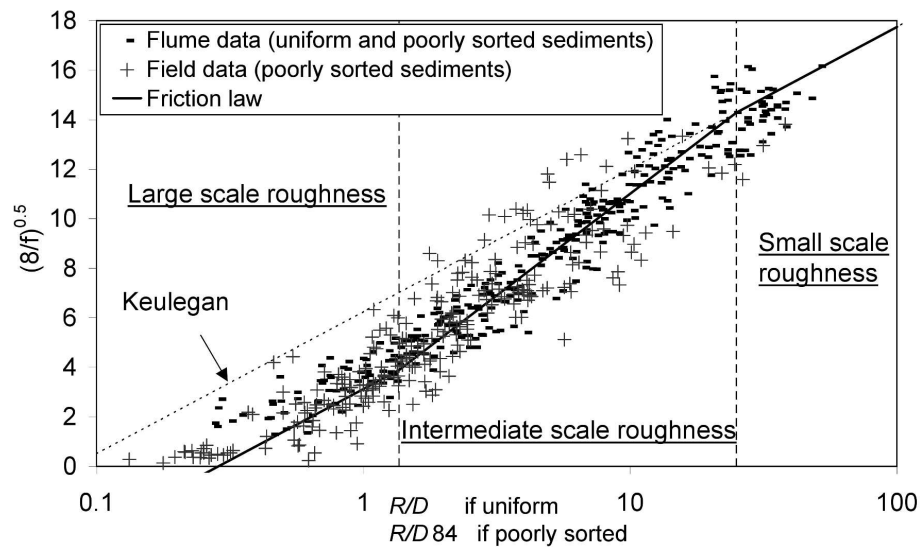

Figure 6 : Selection of flume and field flow resistance values measured over flat beds, with no bedload transport (Recking, 2009)

Figure 6 plots a selection of flume and field Darcy coefficients $(8/f)^{0.5}$ measured over a flat bed. A deviation from the keulegan equation is clearly observed when the relative depth is smaller than 10 approximately. It is important to insist here on the fact that all the flume data used in Figure 6 were measured with a nearly uniform sediment over flat beds. Consequently, the deviation from the Keulegan law is not due to form resistance as define in paragraph 2.1.2, but to additional turbulent energy dissipation. *Bathurst et al.* (1981) proposed to classify flows according to the relative depth and defined a large-scale roughness (*R/D84 < 2*, the roughness features affect the free surface and the flow distortions and drag effects are important), an intermediate-scale roughness (*2 < R/D84 < 7*) and a small-scale roughness (*R/D84 > 7* and the flow can be described by the boundary layer theory).

2.2.2. Bedload and flow resistance interactions

Except rare exception (Smart and Jaeggi, 1983) bedload equations are used with a friction equation established for flows over a fixed bed. Combining two formulas established independently may dissociate the physics of the two phenomena (flow resistance and bed load transport). This can mean that the final relations may not take into account, or at least underestimate, a possible feedback mechanism between bed load and flow resistance. Indeed, several studies have clearly demonstrated that, over flat beds, bed load can dramatically increase flow resistance when compared to clear water flows (Smart and Jaeggi, 1983; Rickenmann, 1990; Baiamonte and Ferro, 1997; Song et al., 1998; Bergeron and Carbonneau, 1999; Carbonneau and Bergeron, 2000; Omid et al., 2003; Calomino et al., 2004; Gao and Abrahams, 2004; Mahdavi and Omid, 2004; Campbell et al., 2005; Hu and Abrahams, 2005).

This was investigated with a series of 144 flume experiments with uniform materials, for a wide range of flow conditions (slope, flow and solid discharge) (Recking et al., 2008). For a given slope, we observed three distinct regimes (Figure 7):

- Regime 1: no transport, $\sqrt{8/f}$ increases (flow resistance decreases) with increasing flow depth.

- Regime 2: bedload transport is low and $\sqrt{8/f}$ is nearly constant for increasing flow depth. This plateau was maintained with increasing bedload transport for a range of flow conditions.

- Regime 3: bedload transport is intense and $\sqrt{8/f}$ increases again for increasing flow depth. This last regime was referred as the 'sheet flow' regime in several of the data sets considered.
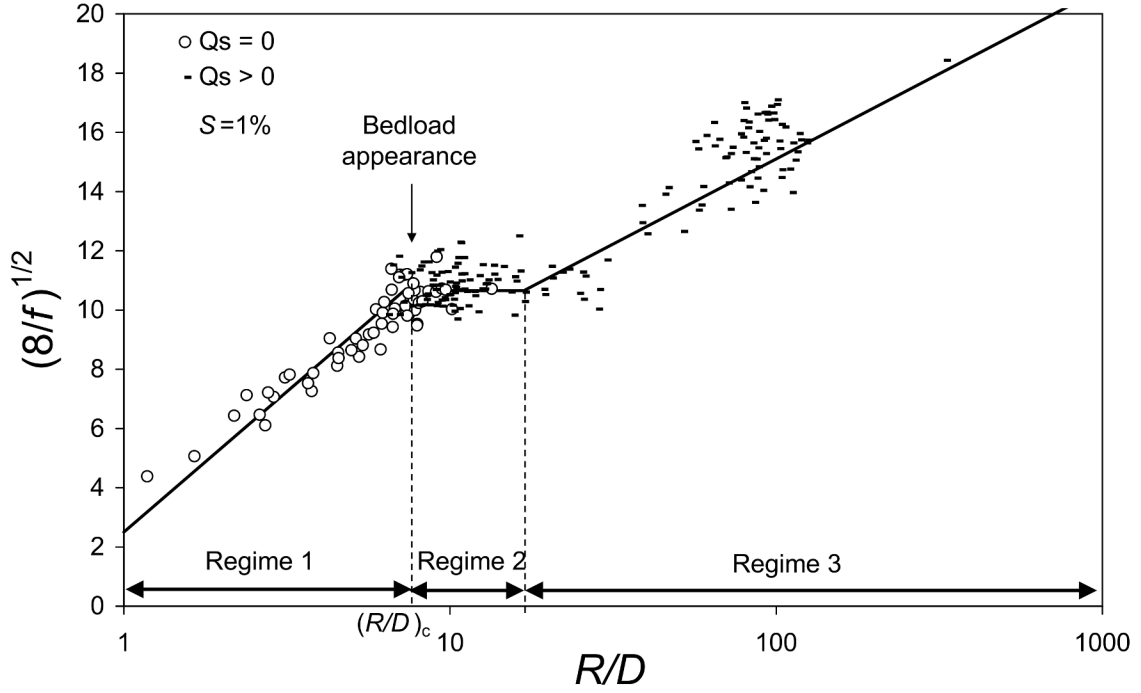
Figure 7 : Effects of bedload transport on flow resistance measured in a flume for slope 1% (Recking, 2007)

2.2.3. Consequences for friction equations

Specific equations were proposed for the roughness layer. For instance Aguirre-Pe and Fuentes (1990) integrated Eqs. 13 and 14 to produce:

$$\sqrt{\frac{8}{f}} = \frac{U}{u*} = \frac{1}{\kappa}\ln\left(\frac{R}{\alpha D}\right) + 8.5 - \frac{1}{\kappa} + \frac{1}{\kappa}\frac{\beta D}{R} \tag{15}$$

However most approaches use conventional friction equations such as Eq. 4 despite the logarithmic profile can not be extended to the wall, but with an apparent roughness length greater than the actual grain dimensions and given in the form $k_s = \alpha D$, with $\alpha > 1$ (see *Yen 2002* for an exhaustive review).

A data set comprising 1567 friction values of the literature measured in a flume over flat bed, with nearly uniform sediments, and for a wide range of slope and relative depth, was used to derive a friction equation reproducing the roughness layer and the interactions with bedload (Recking et al., 2008). It is written:

$$\frac{U}{\sqrt{gRS}} = 6.25 + 5.75\log\left(\frac{R}{\alpha_{RL}\alpha_{BR}D}\right) \tag{16}$$

where U is the vertically averaged flow velocity and

$$\alpha_{RL} = 4\left(\frac{R}{D}\right)^{-0.43} \quad \text{with } 1 \le \alpha_{RL} \le 3.5 \tag{17}$$

$$\alpha_{BR} = 7S^{0.85}\frac{R}{D} \quad \text{with } 1 < \alpha_{BR} \le 2.6 \tag{18}$$

where α_{RL} is a roughness layer coefficient taking into account deviation from the logarithmic profile in small relative depth flows (with an increasing influence of the roughness layer) and α_{BR} is a bedload roughness coefficient taking into account additional flow resistance caused by bedload. Equation 16 was validated with an independent data set (Recking et al., 2008) and is compared to flume and field data in Figure 6 for flows without bedload ($\alpha_{BR}=1$). Figure 8 shows a comparison between this equation and a selection of flume data, for different slopes.
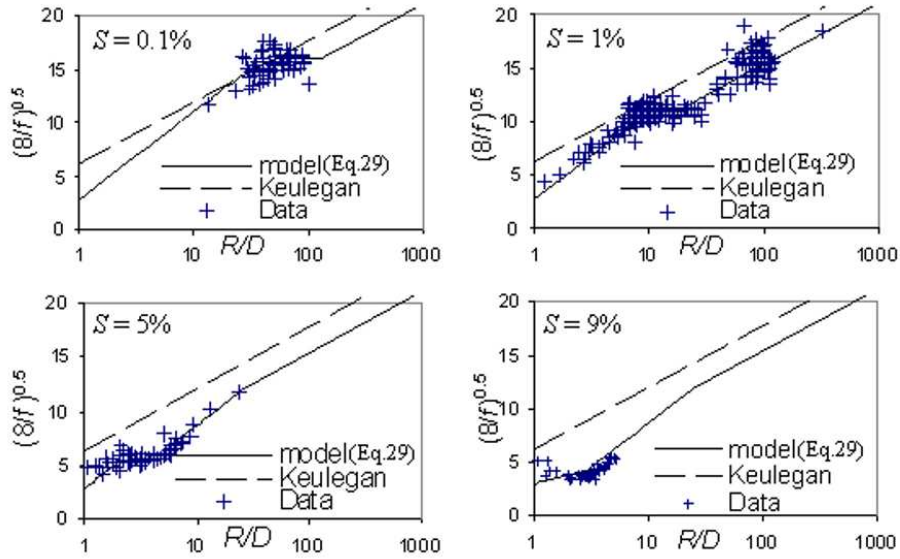
Figure 8 : Comparison between Eq.16 and a selection of flume data (Recking et al., 2008)

2.2.4. A formulation for the near-bed velocity

When the velocity profile of Figure 5 is valid (no or low bedload transport), matching the flow resistance equations Eq.15 (Aguirre-Pe and Fuentes, 1990) and Eq. 16 (Recking et al., 2008) gives an expression for the function $\alpha(R/D)$ in Eq.14:

$$\alpha = e^{2.25\kappa + \ln(\alpha_{RL}\alpha_{BR}) + \frac{\beta D}{R} - 1} \tag{19}$$

Used in Eq.14, $(u/u*)_D$ in the roughness layer can be calculated. Because we have no idea on the appropriate value for β, two possible situations are considered:

- no logarithmic part ($R/D < \beta$): $u(y)/u*$ is constant and equal to its integration over the entire flow depth $U/u*$ (Eq. 16).
- A logarithmic part is present ($R/D > \beta$): Eq. 14 is used with α defined by Eq.19.

This produces a two-part solution (with $1 < \alpha_{RL} < 3.5$ and $1 < \alpha_{BR} \leq 2.6$):

$$\begin{cases} \left(\dfrac{u}{u*}\right)_{RL} = 6.25 + \dfrac{1}{\kappa}\ln\left(\dfrac{R}{\alpha_{RL}\alpha_{BR}D}\right) & if \quad R/D < \beta \\[4mm] \left(\dfrac{u}{u*}\right)_{RL} = 6.25 + \dfrac{1}{\kappa}\ln\dfrac{\beta}{\alpha_{RL}\alpha_{BR}} - \dfrac{1}{\kappa}\left(\dfrac{\beta D}{R} - 1\right) & if \quad R/D > \beta \end{cases} \tag{20}$$

Velocity ratios $(u/u*)_{RL}$ calculated with Eq. 20 for several values of β are plotted in Figure 9 for the case $\alpha_{BR}=1$ (before or near incipient motion) as a function of the relative flow depth R/D and are compared to results obtained with the Nikuradse logarithmic profile (Eq. 2 with $y=D/2$ and $k_s=D$). Figure 9 indicates a decrease in $(u/u*)_{RL}$ with decreasing R/D, which is in accordance with experimental observations (Tsujimoto, 1991). This variation is also obtained with $\beta=0$ (logarithmic profile with $y=D/2$ and $k_s=\alpha_{RL}$), which is not surprising because most information concerning the roughness layer are supposed to be contained in flow resistance data through α_{RL}. Including a roughness layer ($\beta > 0$) only permits to modify the flow velocity distribution within the profile.
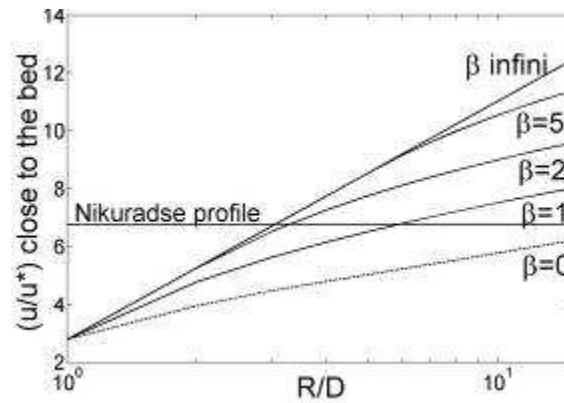

Figure 9 : Near-bed velocity ratio (u/u*) deduced from velocity profiles with and without a roughness layer of thickness βD

The above equations are supposed valid for flows with no bedload transport or where bedload effects can be considered negligible which should be the case for most natural flows (Hey, 1979).

2.3. Application to gravel, cobble and boulder bed rivers

2.3.1. Grain resistance in a large grain size distribution

The calculation of the bed shear stress depends on the definition of the grain roughness k_s, which must be representative of a flow over a flat bed, with no form resistance. But what is a flow over flat bed with no form resistance? This makes sense as long as the flow depth is high compared to the bed roughness height k_s, which was the case in Nikuradse's experiments (with sands). In that case the shear stress above a wall is transmitted entirely by the tangential shearing stress and the logarithmic profile develops. In that case the Keulegan friction equation (Eq.12) can be used with the median diameter D_{50} for k_s.

Figure 10 : Shallow flow over a uniform grain size distribution in a flume

Figure 11 : Shallow flow over a non uniform grain size distribution in a flume

Flat bed with no form resistance can still be defined for shallow flows over a uniform grain size distribution (Figure 10). This is much less evident in gravel, cobble and boulder beds where the flow depth can be small compared to the grain size and where large immobile stones are maintained at rest most of the time (Figure 11), the transported sediments being generally composed of the finer fractions (sand and gravels). In such flows a large part of the shear forces are transmitted by normal stresses (pressure) acting on protruding elements (Papanicolaou et al., 2011), which could thus be considered 'form' roughness, despite they are fully part of bed sediments (Figure 12).
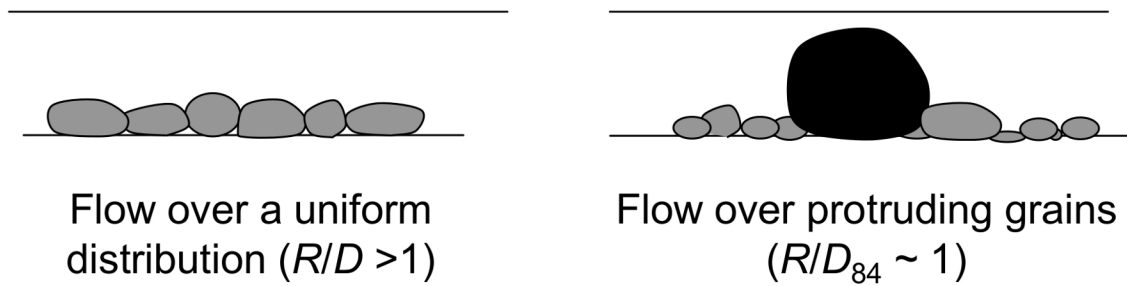
Figure 12 : Illustration of a flow over a uniform grain size distribution and a flow over protruding grains (representative of boulder streams)

Partitioning between the bed at rest and mobile bed was proposed for boulder streams (Yager et al., 2007; Yager et al., 2012), but it is an unrealistic approach for gravel and cobble beds. This is why most modern approaches compute the bed shear stress with friction equations representative of the full grain size distribution (including large immobile stones). Doing so, only channel form resistances (induced by channel curvature, gravel bars, vegetation) are excluded. In a second step, the computed bed shear stress is adapted to the mobility of each grain class with a hiding function, as discussed later (Parker et al., 1982; Wilcock and Crowe, 2003).

This has led to an ambiguity in the literature where these friction equations are often called 'flow resistance' equation for their ability to reproduce the measured mean flow velocities. This is certainly because most data sets used to evaluate the equations are restricted to flows over flat beds, in nearly uniform reaches and with no obstacles. This led Hey (1979) to consider that "*For straight gravel-bed channels skin friction is probably the prominent factor affecting the flow resistance because spill resistance is only of local significance and the absence of bedforms considerably reduces the influence of internal distortion resistance. In addition, sediment transport rates are often so low, or only affect the smallest size fractions exposed on the bed, that it is possible to assume that rigid bed conditions prevail. In these circumstances the flow resistance is basically dependent on the geometry, the cross-sectionnal variation in roughness heights, and the roughness height of graded gravel-bed sediment*". Consequently what is called 'friction' equation here can be encountered as 'flow resistance' equations in other publications.

2.3.2. Friction equations

Defining a friction equation for a natural river bed is still very challenging, especially for the large and intermediate scale roughness. Figure 6 plots a selection of field data

collected over nearly flat bed and uniform river reach (Recking et al., 2008). These data collapse with the flume data when R is scaled with D_{84}. Actually in the presence of a non-uniform roughness height, the development of the roughness layer was found to be controlled essentially by larger elements protruding from the bed (White, 1940; Nowell and Church, 1979; Wiberg and Smith, 1991), explaining why these elements would be the best grain size to scale the hydraulic radius or flow depth in such turbulent flows. As a consequence, most friction equations used in the field usually differ from flume derived equations simply by the uniform sediments diameter D replaced by D_{84} or D_{90}. For instance, Parker (1990) used Eq.4 with $k_s=2D_{90}$. By considering field measurements, Hey (1979) proposed:

$$\frac{U}{\sqrt{gRS}} = 6.25 + 5.75 \log\left(\frac{R}{3.5D_{84}}\right) \tag{21}$$

This equation is compared to Eq.16 (used with D_{84}) and a selection of field data in Figure 13. The scatter associated with the field data is very large, probably because of the difficulty to measure flow resistance during high flows capable to produce bedload, but the Hey equation actually corresponds to a best fit when no distinction is made between flows with and without bedload. Despite Eqs. 16 and 21 were obtained independently and with very different approaches (Eq.16 is a friction equation obtained with flume data and nearly uniform sediments) both equations are nearly identical. This militates for the above hypothesis that flow resistance and friction law are nearly identical in a straight uniform gravel bed river reach.
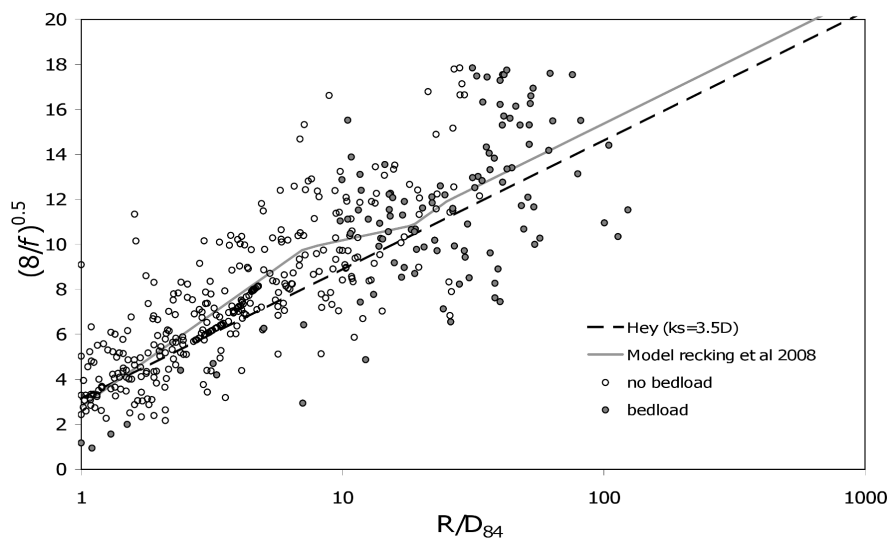

Figure 13 : Comparison between Eq.16 and a selection of field data (Recking et al., 2008)

Large diameters are also used in the Strickler equations given in the form $n=D^{1/6}/C$, where C is a constant which value is usually equal to 26 when D_{90} is considered and 21.1 when D_{50} or a uniform grain size D is considered. Used with Eq. 8 it gives:

$$\frac{U}{\sqrt{gRS}} = a_1 \left(\frac{R}{D}\right)^{1/6} \tag{22}$$

Where a_1 is a constant which value is 6.7 for $C=21.1$ and 8.3 for $C=26$. Equations were also sought specifically for the intermediate and large scale roughness. A linear function of R/D_{84} was found to be more representative for very shallow flows (Rickenmann, 1991; Lawrence, 1997; Nikora et al., 2001; Aberle and Smart, 2003; Gimenez-Curto and Cornerio, 2006):

$$\sqrt{\frac{8}{f}} = a_2 \frac{R}{D_{84}} \tag{23}$$

where $1 < a_2 < 4$. In order to cover all flow ranges Ferguson (2007) combined this equation (with a constant $a_2=2.5$) with the Manning-Strickler equation (Eq. 22 used with D_{84} and a constant $a_1=6.5$), and proposed a Variable Power Exponent (VPE) equation:

$$\frac{U}{\sqrt{gRS}} = \frac{a_1 a_2 \, (R/D_{84})}{\sqrt{a_1^2 + a_2^2 (R/D_{84})^{5/3}}} = \frac{2.5(R/D_{84})}{\sqrt{1+0.15(R/D_{84})^{5/3}}} \tag{24}$$

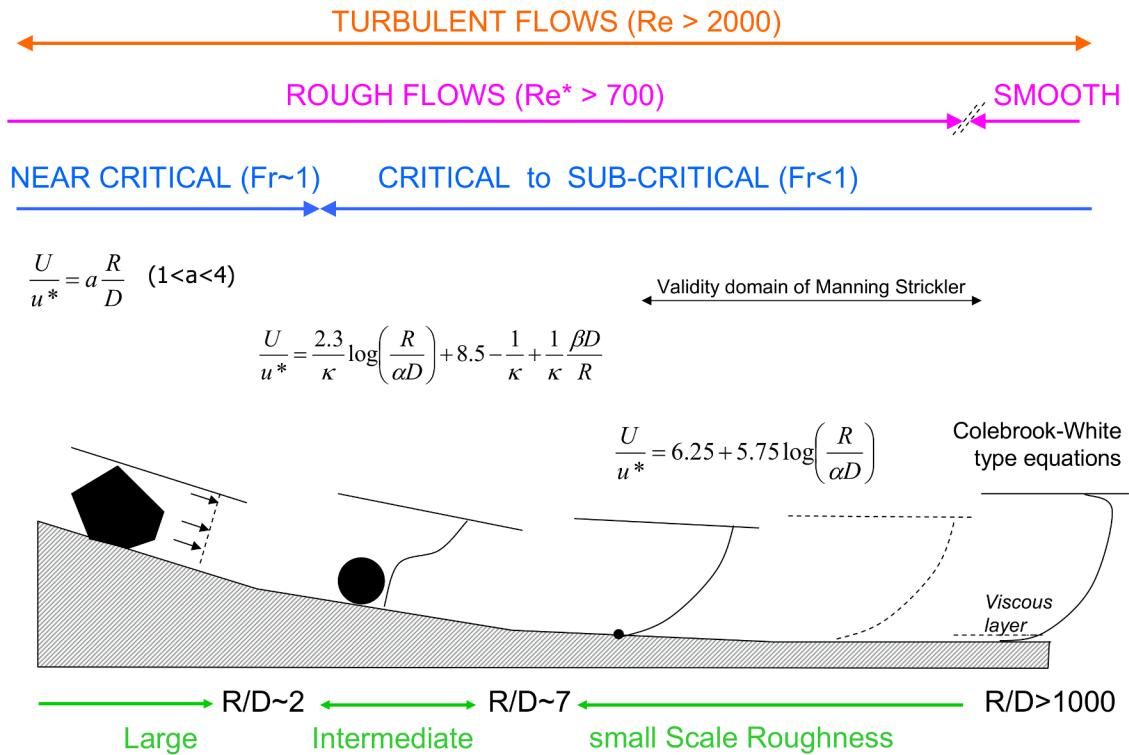Changes in friction equations with relative depths are illustrated in Figure 14.

Figure 14 : Evolution of friction equations from lowland rivers to steep mountain streams

2.3.3. Hydraulic geometry equations

In many field applications, only the discharge is known. Equations such as Eqs.10, 12 and 24 can still be used considering the mass conservation *Q=UWd* (for a rectangular section), and eventually with an additional equation linking *d* and *R* (Rickenmann and Recking, 2011). The disadvantage of this approach is that it usually requires iterations, which can be a problem for practical purposes. An alternative has consisted in using equations fitted with dimensionless hydraulic geometry parameters. These equations, which are equivalent to the Chezy equation adjusted by a measure of relative roughness (Church and Zimmerman, 2007), have proved to perform as well as more complicated equations for estimating the mean flow characteristics (Kellerhalls, 1970, 1973; Rickenmann, 1990, 1994; Aberle and Smart, 2003; Church and Zimmerman, 2007; Comiti et al., 2007; Ferguson, 2007; Zimmermann, 2010).

Using two new dimensionless terms $U^*=U/(gSD_{84})^{0.5}$ and $q^*=q/(gSD_{84}{}^3)^{0.5}$ (where *q=Q/W* and *W* is the river width) Rickenmann and Recking (2011) proposed an explicit version of the VPE equation (Eq.24) for the case of given discharge *q*:

$$\frac{U}{\sqrt{gSD_{84}}} = 1.44 q^{*0.6}\left[1+\left(\frac{q^*}{43.8}\right)^{0.82}\right]^{-0.24} \tag{25}$$

Assuming this equation is representative of the bed surface roughness as discussed above, the mean velocity computed with this equation can be used for calculating the bed shear stress. From their field data set, Rickenmann and Recking (2011) also fitted relations such as:

$$U^* = k q^{*m} \tag{26}$$

The non-linearity between the small and intermediate scale roughness (Bathurst et al., 1981) imposes equations with several parts: *k*=1.55, *m*=0.706 when $q/\sqrt{gSD_{84}^3} < 1$, *k*=1.6, *m*=0.545 when $1 < q/\sqrt{gSD_{84}^3} < 100$, and *k*=3.2, *m*=0.395 when $q/\sqrt{gSD_{84}^3} > 100$. The first set of coefficients ($q/\sqrt{gSD_{84}^3} < 1$) corresponds to the large-scale roughness (*R/D* < 2) and concerns very low-flow conditions generally not associated with transport.

2.4. Equations evaluation and concluding remarks

Figure 15 compares the Manning-Strickler (Eq.10 used with n=$D^{1/6}$/21.1), the Keulegan (Eq.12 with k_s=D) and the Recking et al (Eq. 16) equations with a data set (Recking et al., 2008) comprising 1532 runs measured in a flume over nearly-uniform sediments and covering a large range of flow conditions (0.001 < *S* < 0.2, 1 < *R/D* < 357, 0.2 < *D* (mm) < 44, 0.05 < *W* (m) < 2). All the runs were corrected for side-wall effects with the procedure proposed by

Johnson (1942) and modified by Vanoni and Brooks (1957). The Keulegan equation gives very satisfactory results, except for R/D <3 (large scale roughness) where the predicted velocities are slightly higher (about 1.5 times higher) than the measured velocities. The Manning-Strickler equation gives good results for the intermediate scale roughness ($3 < R/D < 7$), but slightly underestimate velocities for the small scale roughness (results are identical to the Keulegan equation when $n = D^{1/6}/26$ is used instead of $n = D^{1/6}/21.1$). The Recking et al equation (partly obtained with these data) gives no under or over prediction. Overall, the results obtained with the 3 equations can be considered satisfactory with most $U_{calculated} / U_{measured}$ ratios within the range [0.8-1.2].
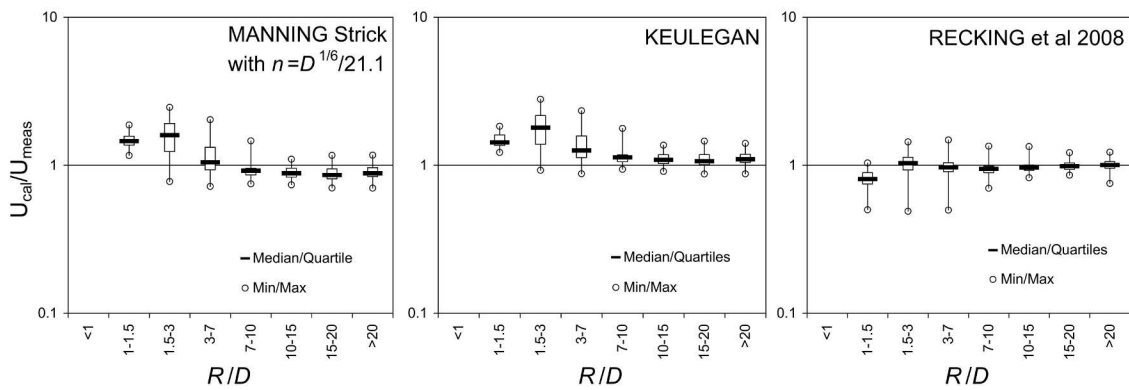
Figure 15 : Comparison of the Manning-Strickler, the Keulegan and the Recking et al equations with a selection of fume data measured with uniform sediments

Flows over nearly-uniform sediments, sketched in Figure 12a, are characterized by relative depths higher than 1.5 (no values below R/D=1 and only a few values in the range $1 < R/D < 1.5$) despite the wide range of slope considered. Thinks are different in cobble and boulder streams where flows are often near $R/D_{84} \approx 1$ or below (Figure 12b). Rickenmann and Recking (2011) recently evaluated several equations (Strickler, 1923; Keulegan, 1938; Hey, 1979; Smart and Jaeggi, 1983; Bathurst, 1985; Ferguson, 2007) with a field data set comprising 2890 values covering a wide range of flow conditions ($0.00004 < S < 0.24$, $0.0003 < D_{84}$ (m) < 1.35, $0.2 < R/D_{84} < 100$). The data set was restricted to flows over flat beds, in nearly uniform reaches and with no obstacles (flows over dunes were excluded), and is assumed representative of the bed roughness at the reach scale. Whatever approach was used, the equations proved to be more reliable for the small scale roughness (Figure 16).
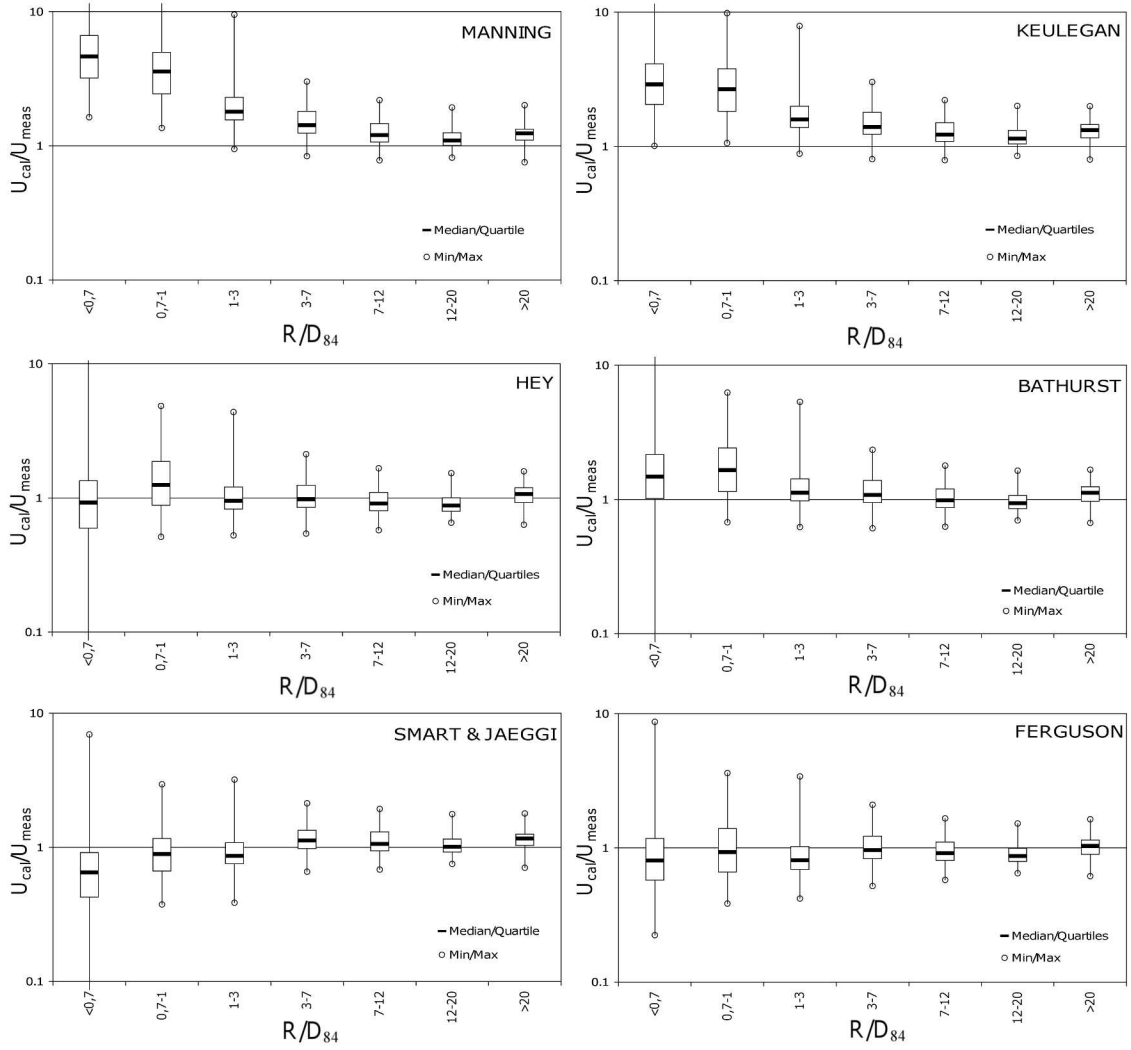
Figure 16 : Comparison of several friction equations with a large field data set (Rickenmann and Recking, 2011)

The results show that the Manning-Strickler (used here with $n=D_{84}^{1/6}/26$) and the Keulegan equations are no longer valid for the intermediate and the large scale roughness (when $R/D_{84} < 7$ approximately). The Hey (1979) equation (Eq.12 with $k_s=3.5D_{84}$) is representative of a large flow range. The best overall performance was obtained with the equation proposed by Ferguson (2007) (Eq.24). Results were improved when the hydraulic geometry approximation of the equation (Eq. 25) was used, as shown in Figure 17.
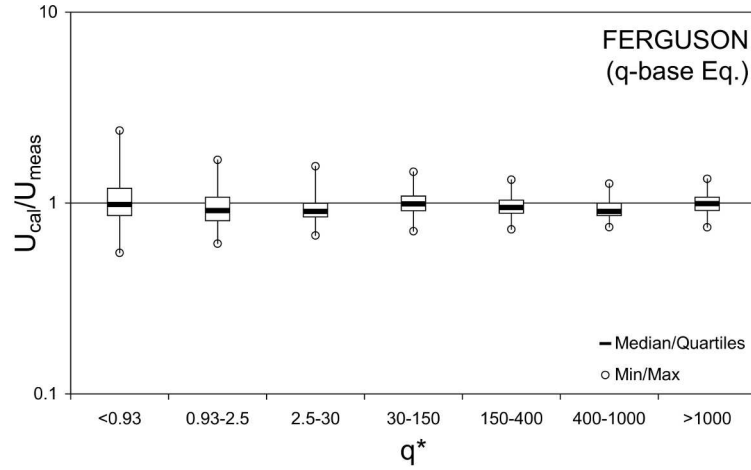
Figure 17 : Comparison of the q-base version of the Ferguson (2007) equation with a large field data set (Rickenmann and Recking, 2011)

Actually the results were improved for all equations when the discharge was used as input parameter instead of the flow depth. This can be explained by the fact that discharge measured at a controlled gauging section is a more reliable measure of the flow condition, especially in shallow flows (Rickenmann and Recking, 2011). In addition, if there is no lateral input, discharge is constant for the river reach, contrary to the velocity U and depth d couple, which should be reconsidered for each section for a given specific discharge q.

It is interesting to use hydraulic geometry equations for computing the bed shear stress with Q, because they are explicit whereas using logarithmic equations necessitate an iterative approach. A direct q-base formulation can be proposed for τ. From Eq.26 we deduce:

$$d = \left[k(gS)^p q^{-2p} D_{84}^{3p-1}\right]^{-1} \tag{27}$$

with $p = (1-m)/2$. Assuming a rectangular cross section as a first approximation, $R = \left[2/W + 1/d\right]^{-1}$, and approximating the k values by $74p^{2.6}$ we obtain (Recking, in press):

$$\tau = \rho gS\left[2/W + 74p^{2.6}(gS)^p q^{-2p} D_{84}^{3p-1}\right]^{-1} \tag{28}$$

with $p = 0.23$ when $q/\sqrt{gSD_{84}^3} < 100$ and $p = 0.3$ otherwise. This equation gives results similar to shear stresses obtained with the hydraulic parameters computed with Eq.25. It is interesting because it permits a direct estimate of the bed shear stress with the flow discharge. In addition, Eq. 28 indicates that $\tau \propto q^{0.5}$ whereas $\tau \propto R$ in $\tau=\rho gRS$, and consequently τ is less impacted by an error in discharge.

30

The boundary shears stress $\tau = \rho g R S$ computed with the measured hydraulic radius R was compared in Figure 18 with the bed shear stress computed with several equations using the measured flow velocity (paragraph 2.1.3).
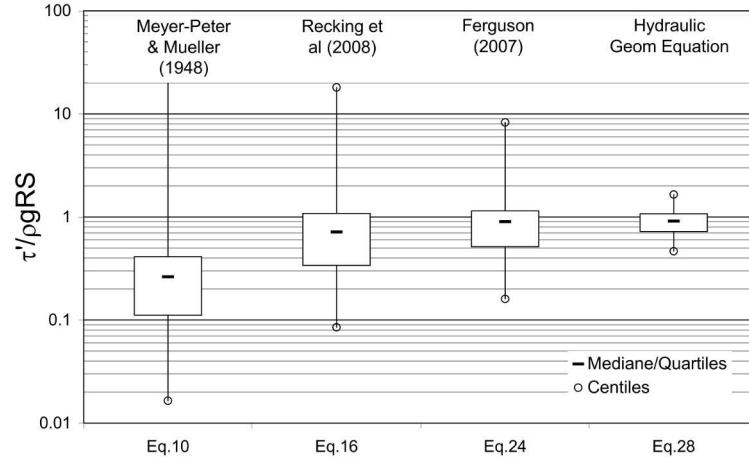
Figure 18: Comparison between the bed shear stress and the boundary shear stress computed by several methods, for a large field data set

Among all the methods tested, the Meyer-Peter and Mueller approach (Eq. 10) leads to the strongest shear stress correction. This is consistent with Figure 16 showing that the Manning-Strickler equation over-predicts the mean flow velocity for the large and intermediate scale roughness. All other methods including the Recking et al (2008) equation derived in the flume confirm that the bed shear stress is nearly identical to the boundary shear stress in straight nearly uniform natural channels.

3. INITIATION OF MOTION

3.1. The Shields curve

Using similarity principles, Shields (1936b) established a framework for bedload prediction that is still in use today. Considering the ratio between destabilizing (shear stress x surface of the exposed particle $\approx \tau D^2$) and stabilizing forces (the weight minus buoyancy $\approx g(\rho_s-\rho)D^3$) he defined the dimensionless shear stress (also called Shields stress) :

$$\tau^* = \frac{\tau}{g(\rho_s - \rho)D} = \frac{RS}{(s-1)D} \tag{29}$$

where τ is the bed shear stress as defined in the previous chapter, ρ_s is the sediment density, ρ is the water density, g is the acceleration of gravity R is the flow hydraulic radius and D is the grain diameter. Shields considered bedload a threshold phenomenon and established a diagram relating the dimensionless critical shear stress τ_c^* to the roughness Reynolds number $Re^*=u^*D/\nu$ (where $u^*=(\tau/\rho)^{1/2}$ is the shear velocity).
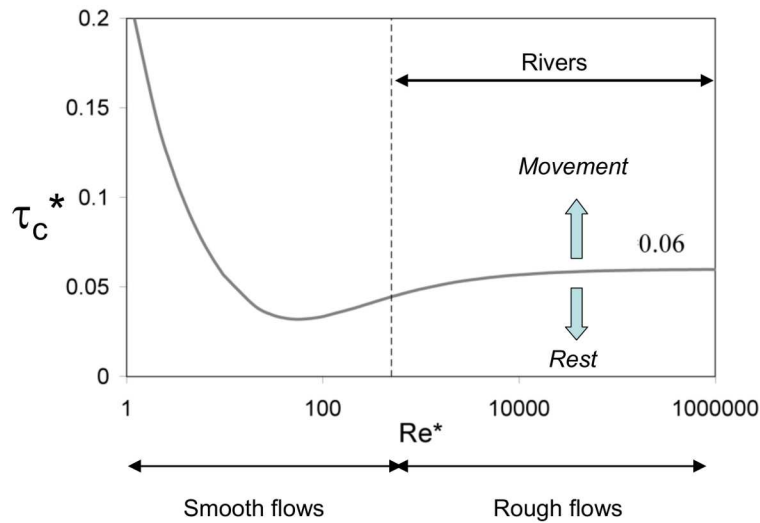
Figure 19 : The Shields curve (Shields, 1936)

Although this curve is not easy to use (because both τ_c^* and Re^* depend on the shear velocity u^*, which implies an iterative approach), one interesting practical issue is that τ_c^* was hypothesized by Shields to be constant when $Re^* > 1000$, which is the case for most natural flow conditions (rough and turbulent flows). Thus, knowing the value of this constant, the calculation of threshold flow conditions (characterized by a flow hydraulic radius R) for a given sediment (characterized by its grain-size distribution curve) and a given energy slope S should be straightforward.

However, whereas Shields proposed an asymptotic value of 0.06 for τ_c^*, the appropriate value for this constant has been widely and continuously discussed since that time. For instance, the well-known bedload transport equation proposed by Meyer-Peter and Mueller (1948) considered τ_c^* =0.047. Values as low as 0.01 were also proposed (Fenton and Abbott, 1977; Carling, 1983; Mueller et al., 2005) as well as values higher than 0.1 (Mizuyama, 1977; Church, 1978; Reid et al., 1985; Mueller et al., 2005). More generally, values were proposed in the range 0.03 (Parker et al., 2003) to 0.07 (an exhaustive review was provided by Buffington and Montgomery, 1997), with a mean value at approximately 0.045 (Gessler, 1971; Miller et al., 1977; Yalin and Karahan, 1979; Saad, 1989). Figure 20 compares critical Shields stress measured in a flume with the Shields curve. Despite these data have been obtained with nearly perfect measurement conditions (in the laboratory), the scatter is very large.
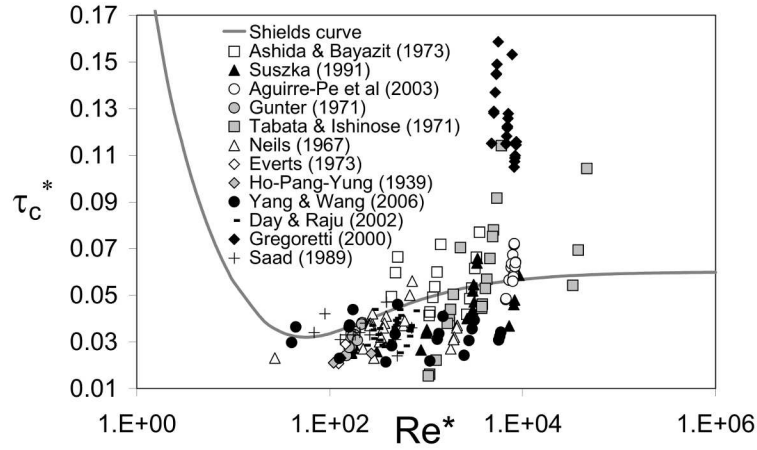
Figure 20 : Comparison between the Shields curve (Shields, 1936) and critical Shields stresses measured in a flume

The importance attached to this question can easily be understood when considering that in many natural gravel-bed rivers the Shields number τ^* barely exceeds 120% of the critical value τ_c^* (Parker, 1978; Andrews, 1983; Ryan et al., 2002; Mueller et al., 2005; Parker et al., 2007) and that for these flow conditions, transport rates increase by several orders of magnitude for very small changes in shear stress, which can lead to very large errors in bedload prediction if τ_c^* is not correct. Numerous explanations can be given for the uncertainty on τ_c^* (Buffington and Montgomery, 1997), including the definition of incipient motion itself, the shear stress definition (mean or instantaneous) and calculation (from the energy slope, the velocity profile or the Reynolds stress profile), specificities of sediments (near-uniform or nonuniform), bed clogging (Barzilai et al., 2012), and the general protocol

used (measurement techniques, time duration, side wall correction method). A subject that has received less attention is the natural dependence of τ_c^* on flow parameters. The previous chapter has discussed changes in flow hydraulics with changing relative flow depth R/D. In this chapter I present how these changes can affect the grains movement.

3.2. Variation of the critical Shields stress with slope

3.2.1. Overview

When the data of Figure 20 are plotted as a function of the mean bed slope (equal to the energy slope for the given uniform flow conditions considered) dependence can be observed, as shown in Figure 21.
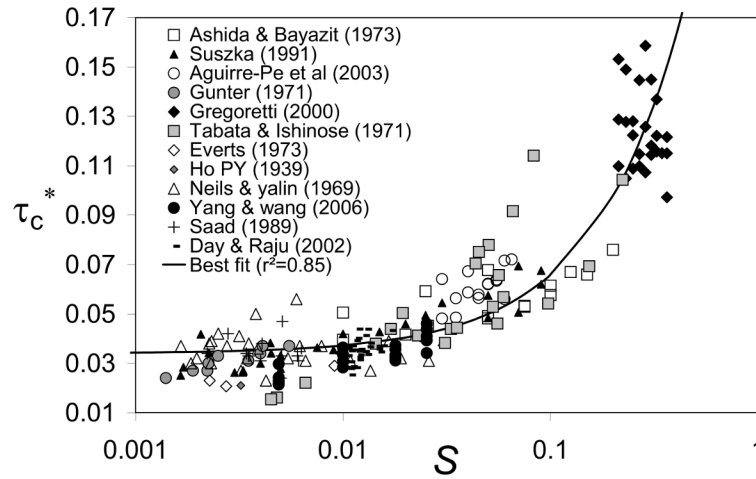
Figure 21 : Plot of the critical Shields stresses values as a function of the slope

Shields himself first recognized this dependence (pp. 16-17) and observed increasing critical Shields stress with increasing slopes. This result has been confirmed since that time by several researchers, on the basis of both flume and field experiments (Bogardi, 1970; Tabata and Ichinose, 1971; Aksoy, 1973; Bathurst et al., 1982; Bettess, 1984; Bathurst, 1987; Graf and Suszka, 1987; Tsujimoto, 1991; Shvidchenko and Pender, 2000; Shvidchenko et al., 2001; Armanini and Gregoretti, 2005; Mueller et al., 2005; Vollmer and Kleinhans, 2007; Lamb et al., 2008; Ferguson, 2012). Other researchers proposed a $\tau_c^*(R/D)$ equation (Mizuyama, 1977; Torri and Poesen, 1988; Suszka, 1991; Lenzi et al., 2006) instead of a $\tau_c^*(S)$ equation, which is equivalent, considering Eq.29. Because these observations were mostly reported for low relative depth R/D corresponding to gravel initiation of motion on steep slopes, this led Bathurst et al (1982) to hypothesize that the traditional Shields approach (which assumes a constant value of approximately 0.04–0.06 at a high Reynolds number)

could be based on the coincidence that most studies involved values of channel slope small enough that the real variation of τ_c^* with flow conditions has been too small to deserve comment. For instance, Shields himself considered the slope effects negligible for the low slopes (≤1%) examined in his analysis (Shields, 1936 , p11).

Increasing τ_c^* with increasing slope could be explained in Eq.29 only if the changing flow hydraulics (mean velocity and turbulence profiles) with increasing slopes leads to critical relative depths (i.e. *R/D* measured at incipient motion) declining slower than the rate of slope increase. This led Tsujimoto (1991) to postulate that the effect of slope on τ_c^* is composed of two parts (Eq. 30): $\Psi_1(S)$ as an effect of gravity itself and $\Psi_2(S)$ as an effect of the degeneration of velocity distribution due to small relative depth. The former would be a decreasing function of *S* while the latter would be an increasing one.

$$\tau_c^* = \psi_1(S)\psi_2(S) \tag{30}$$

However an increasing Shields stress with increasing slope has for a long time received little attention because it is an unexpected result; indeed, the inverse could have logically been expected when the channel slope becomes very steep because of increased gravity effects (Luque and Van Beek, 1976; Chiew and Parker, 1994; Dey, 2003). This led some investigators to choose to exclude low relative depth data as they were likely to represent additional effects. For instance, in their exhaustive review, Buffington and Montgomery (1997) also observed a negative correlation between τ_c^* and *R/D*, but they considered it as a consequence of shear stress calculation in presence of form drag at low relative depth and excluded all values having *R/D* < 5 from their analyses.

3.2.2. Experimental evidences

The form drag hypothesis has often been used to explain observed variations in τ_c^* (Mueller et al., 2005). This hypothesis also holds for flume results with near-uniform sediments, as most studies extrapolated to zero the bedload transport rate data despite associated flows are usually associated with the presence of small bedforms (undulating bed), whatever the initial planar bed surface considered (Recking et al., 2009a). Here experimental evidences are used to demonstrate that whereas bedforms can contribute to increasing critical Shields values in some circumstances, this does not explain the variations in τ_c^* observed with low relative depth on steep slopes.

Instead of extrapolating to zero bedload values (which flows can be suspected to be associated with bedforms), the procedure has consisted to extrapolate from zero to high flows

flow resistance values measured over flat bed with no bedload. It is the changes observed in flow resistance values, as shown in Figure 7, that were used as an evidence of bedload appearance. Using my own data (Recking, 2006) and additional data from the literature, I measured the critical relative depth R/D_c and I computed the associated critical Shields stress with Eq.29 for different slopes considered in the range $0.001 < S < 0.1$ (Recking, 2007). The results are plotted in Figure 22 and confirm that even when considering only flows over flat beds, the critical Shields stress increases with increasing slope.
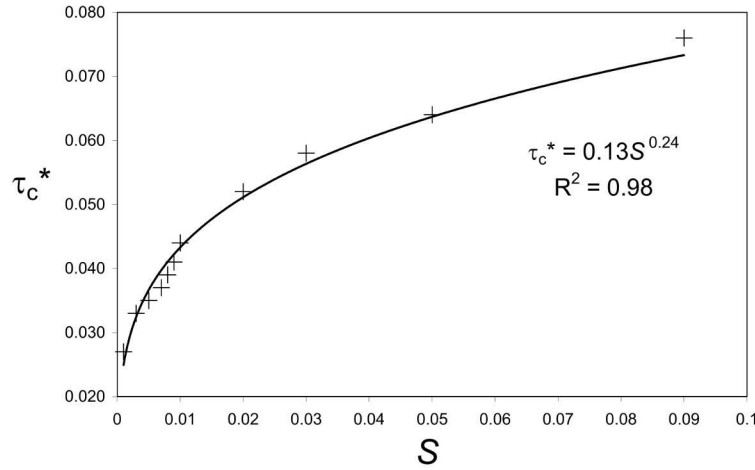
Figure 22 : Changes in critical Shields stress with slope deduced from flow resistance measured over flat beds (from Recking, 2007)

Finally, a cross-analysis between flow resistance and bedload transport rates led to the following critical Shields stress function for sediments of nearly uniform grain size distribution (Recking et al., 2008):

$$\tau_c^* = 0.15S^{0.275} \tag{31}$$

The strength of this equation stems from its having been obtained by two other independent studies using different methods: Shvidchenko et al. (2001) obtained the same equation (coefficient 0.11–0.2 varying with grain diameter and exponent 0.278) using their own flume measurements and Lamb et al. (2008) obtained a very close equation (coefficient 0.15, exponent 0.25) by fitting critical Shields stress data from the literature.

3.2.3. Theoretical development

Grain movements are governed by the association of the drag and lift forces, these latter being dependent, respectively, on the mean velocity and on the velocity gradient in the vicinity of the grain. If the mean velocity and the velocity gradient are affected by low relative depths on steep slopes, as suggested in the previous chapter, it would have direct

consequences on the force balance and τ_c^*. There has been several attempts for demonstrating these effects using an analytical model based on a force balance, (Tsujimoto, 1991; Armanini and Gregoretti, 2005; Vollmer and Kleinhans, 2007; Lamb et al., 2008), but whatever the approach used, one major difficulty consists in evaluating the model's ability to reproduce the roughness layer velocities and its variations with relative depth because available roughness layer velocity measurements are scarce. An alternative presented here consists in using the near-bed velocity profile deduced from flow resistance measurements in paragraph 2.2.4 (Eq.20).

The forces acting on a cohesionless particle are lift (F_L), drag (F_D), buoyancy and gravity (W). At the threshold of motion, forces acting tangential (F_t) and normal (F_n) to a particle must satisfy the relation:

$$\frac{F_t}{F_n} = \tan\phi \tag{32}$$

where ϕ is the intergranular friction angle. Considering the angle a of the channel bed slope S ($S=\tan a$), when rearranged with forces this yields:

$$\frac{W\sin a + F_D}{W\cos a - F_L} = \tan\phi \tag{33}$$

The forces can be expressed as:

$$F_D = \frac{1}{2}\rho C_D A_x u_D^2 \tag{34}$$

$$F_L = \frac{1}{2}\rho C_L A_x u_D^2 \tag{35}$$

$$W = \rho_s g V_p - \rho g V_{ps} \tag{36}$$

where C_D and C_L are drag and lift coefficients, D is the grain diameter, A_x is the cross-sectional area of the particle, which is perpendicular to and exposed to the flow, V_p is the volume of the particle (used to calculate the gravity force $\rho_s g V_p$), V_{ps} is the submerged volume of the particle (used to calculate the buoyancy force $\rho g V_{ps}$) and u_D is an integration of the velocity profile over the exposed height of the grain. We will approximate u_D by the fluid velocity calculated at the center height of the particle $y=D/2$ (Ikeda, 1982). Very sophisticated models have been proposed in the past (Wiberg and Smith, 1987; Bridge and Bennett, 1992) by integrating the grain position and its protrusion into the bed. As the purpose here is to test the adequacy between measured flow resistance and critical Shields variations, a simpler model was considered. For simplicity particles are assumed to be spherical and fully exposed,

with the location of the virtual origin of the velocity profile located in the vicinity of the bottom of the considered grain particles (see discussion by Ikeda, 1982 for an explanation of this choice). Combining Eqs. 33-36 yields the following expression for the critical Shields number:

$$\tau_c^* = \frac{4}{3} \frac{s - \xi_V}{s - 1} \frac{\tan\phi\cos a - \sin a}{\xi_A(C_D + \tan\phi C_L)} \frac{1}{\left[(u/u*)_D\right]^2} \tag{37}$$

Where ξ_A and ξ_V are additional geometrical coefficients used for correcting the grain surface and volume exposed to the flow when the flow relative depth R/D is less than 1 on very steep slopes: they are unity when $R/D>1$ and a function of R/D when $R/D<1$ (see Recking 2009 for more details).

For a given bed slope (a constant) and material (characterized by D and ϕ), τ_c^* will depend on C_D, C_L and the velocity profile. Usually this equation is solved by ignoring the lift force ($C_L=0$), but without any proper justification (Vanoni et al., 1966) because both analytical and experimental studies have confirmed its presence, with a slight effect on incipient motion (Einstein and El-Samni, 1949; Inokuchi and Takayama, 1973). The slope is also often ignored ($a=0$), which is justified for slopes less than 10%. The term $(u/u*)_D$ is usually calculated from the Nikuradse logarithmic velocity profile (Eq.2 used with $y_0=k_s/30$). In its simplest form, $S=0$, $\phi=52°$ (Buffington et al., 1992), $C_D=0.45$, $C_L=0$, $k_s=D$ and $(u/u*)$ calculated at $y=D/2$, the model produces a constant critical Shields value $\tau_c^* \approx 0.06$.

The objective here is to consider deviations from the classical logarithmic profile associated with the roughness layer development for low relative depth flows (Figure 5). This can be done by replacing $(u/u*)_D$ in Eq.37 by Eq. 20 (setting $\alpha_{BR}=1$) and by replacing R/D in Eq. 20 by $\tau_c^*(s-1)/S$ determined by rearranging Eq.29; it gives:

$$\tau_c^* = \frac{4}{3} \frac{s - \xi_V}{s - 1} \frac{\tan\phi\cos(\text{atan } S) - \sin(\text{atan } S)}{\xi_A(C_D + \tan\phi C_L)\left[6.25 + \frac{1}{\kappa}\ln\left(\frac{\tau_c^*(s-1)}{\alpha_{RL} S}\right)\right]^2} \qquad if \quad \tau_c^* < \frac{\beta S}{s - 1}$$

$$\tau_c^* = \frac{4}{3} \frac{s - \xi_V}{s - 1} \frac{\tan\phi\cos(\text{atan } S) - \sin(\text{atan } S)}{\xi_A(C_D + \tan\phi C_L)\left[6.25 + \frac{1}{\kappa}\ln\left(\frac{\beta}{\alpha_{RL}}\right) - \frac{1}{\kappa}\left(\frac{\beta S}{\tau_c^*(s-1)} - 1\right)\right]^2} \qquad if \quad \tau_c^* > \frac{\beta S}{s - 1} \tag{38}$$

With $1 < \alpha_{RL} = 4\left(\frac{\tau_c^*(s-1)}{S}\right)^{-0.43} < 3.5$

This two part expression for τ_c^* results from the two-part solution of Eq. 20 where the respective *R/D* ranges were replaced by corresponding τ_c^* ranges. τ_c^* can be solved iteratively for different slopes.

Comparison of this theoretical model with the measured critical Shields stress values of Figure 20 necessitates defining the value for the constants. Measurements with natural sediments (Buffington et al., 1992; Gregoretti, 2000) indicated that in the field a mean value of 52° would be appropriate for the intergranular friction angle ϕ (which value is much higher than the masse angle of repose value 32° usually considered for a en masse failure of a bed volume). For flows over natural sediments C_D=0.45 is usually considered. But Coleman (1967) measured a decrease in both drag and lift coefficients with increasing particle Reynolds number *Re** (in Vollmer and Kleinhans 2007) and proposed an asymptotic value of C_D=0.25 for *Re** higher than 5.10^4 whereas other measurements indicated that C_D could also increase up to 0.9 for low relative depth (these aspects are discussed in Armanini and Gregoretti, 2005 and Lamb et al. 2008). The same uncertainties exist for lift force. It is usually considered through a ratio C_L/C_D=0.85 (Chepil, 1958; Wiberg and Smith, 1987; Seminara et al., 2002; Armanini and Gregoretti, 2005; Lamb et al., 2008). Lift force corresponds to a pressure gradient generated by the mean flow velocity gradient near the bed and could be reduced when the flow velocity profile becomes uniform close to the bed. Patnaik et al.(1994) measured a decreasing lift coefficient C_L with decreasing relative submergence δ/D (where δ is the boundary layer thickness) in wind tunnel experiments. However, to the best of my knowledge there was no flume investigation of the lift coefficient at low relative depths and the relation C_L/C_D=0.85 was maintained. A sensitivity analysis was considered for all parameters in Recking (2009), especially for the roughness layer thickness β which was set to one.

The results plotted in Figure 23 shows that when the velocity profile is modified for taking into account the roughness layer, the force balance model adequately reproduces the increase in critical Shields stress with increasing slope. Figure 23 also shows that the same force balance used with Nikuradse's law (Eq.2) can not reproduce the variations in τ_c^*, even when considering a reduced drag force resulting from reduced grain submergence (when *R/D*<1, through ξ_A and ξ_V).
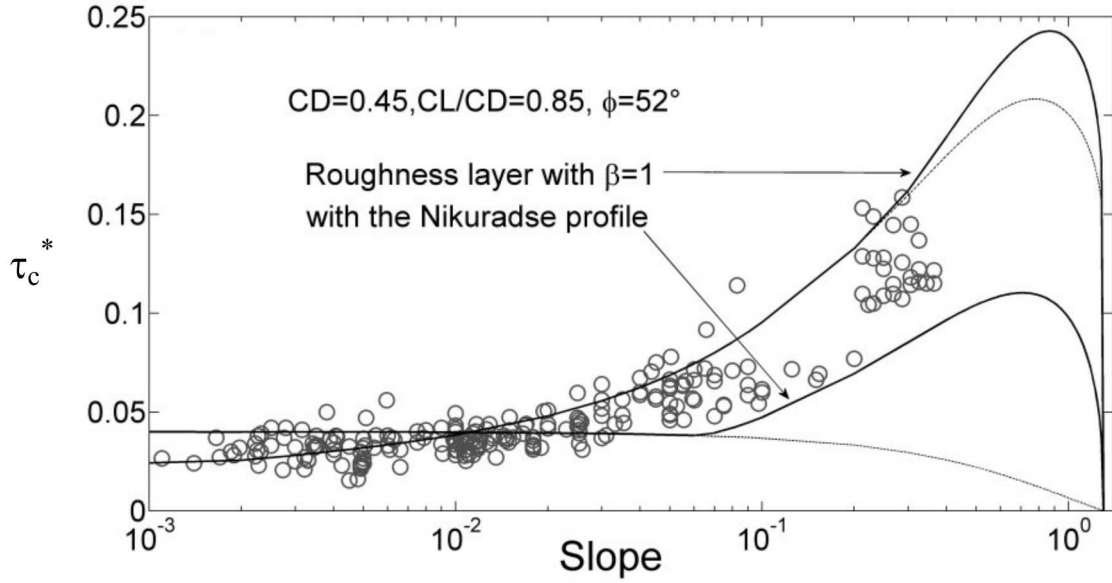
Figure 23 : Comparison between the theoretical model and the near-uniform sediment data set (dashed lines correspond to $\xi_A = \xi_V = 1$, i.e. no grain surface and volume correction)

3.3. Field implications

A variation of the critical Shields stress with the slope has strong implications. However, as observed for friction laws, flume observations (especially when obtained with nearly uniform sediments) may not match exactly what is observed in the field.

3.3.1. Hiding effects

Defining incipient motion conditions for poorly sorted sediments can be difficult because all individual size fractions in a mixture may not behave identically for a given bed shear stress τ. More particularly, two effects, one absolute and one relative (Wilcock and Southard, 1988), complicate the phenomenon. The absolute size effect (ratio of driving to resisting forces) makes the smaller grains easier to move, whereas the relative size effect (hiding fine sediments and overexposure of coarser sediments) produces the opposite effect. Based on flume and field measurements or theoretical analysis, some researchers (Parker and Klingeman, 1982; Andrews, 1983; Wiberg and Smith, 1987; Kuhnle, 1992; Wilcock, 1993) considered that both effects nearly compensate each other (relative protrusion of bed particles into the flow compensates for the differences in particle weight) and that consequently particles of various sizes have equal mobility, i.e., are entrained at about the same mean bed shear stress (or the same flow discharge). Others observed a selective size entrainment with

40

increasing shear stress (Komar, 1987; Ashworth and Ferguson, 1989; Lisle, 1995; Lanzoni, 2000).

All these studies proposed a hiding function (Eq.39) giving the critical Shields number τ_{ci}^* associated with diameter D_i from the critical Shield τ_{c50}^* associated with median diameter D_{50}:

$$\tau_{ci}^* = \tau_{c50}^* \left(\frac{D_i}{D_{50}} \right)^b \tag{39}$$

where b is a coefficient whose value is 0 if the critical shear stress is simply proportional to individual particle size (constant critical Shields value) or –1 in case of complete equal mobility (values were generally proposed between –0.6 and –1). Subscript 'c' is commonly replace by 'r' when authors referred to a non zero reference bedload transport (Parker and Klingeman, 1982) instead of a critical Shields value (zero transport).

3.3.2. Comparison with field measurements

A data set comprising 92 critical Shields stress measured in the field was built with data from the literature (Recking, 2009). Values of τ_{c50}^* (considered for the median diameter D_{50}) are compared in Figure 24 with the theoretical model (Eq.38) and with near-uniform sediments data of Figure 20. All data confirm a variation with the slope, however the field data plot above the near-uniform sediment data
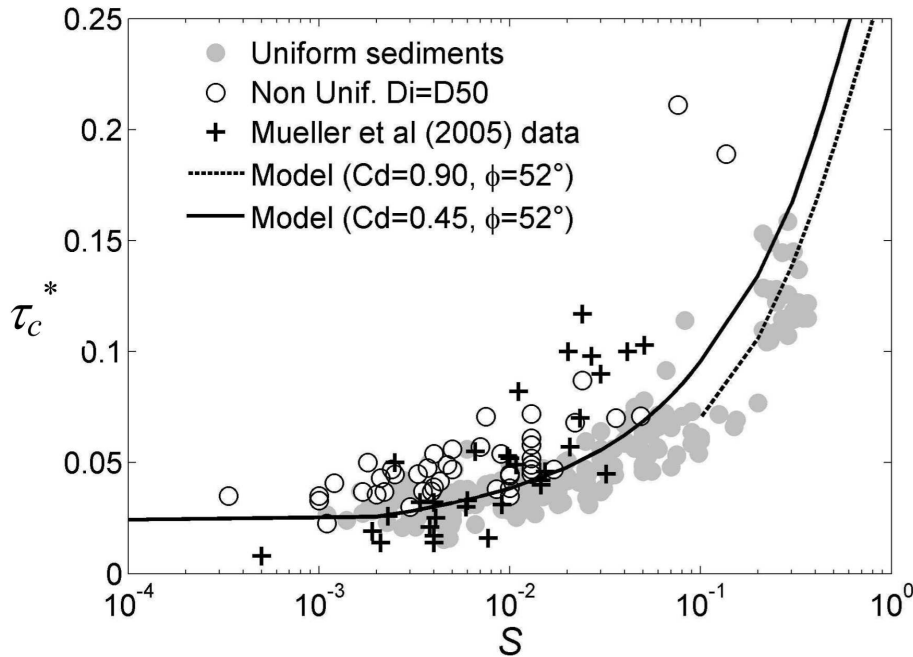

Figure 24 : Comparison between field values, near-uniform sediment data, and the theoretical model

41

Differences between field and flume values can be explained from the flow properties. Incipient motion of a grain depends on the resistance this grain exerts to the flow. One important feature that characterizes flows over near-uniform sediments is that the grain diameter D used to scale the critical shear stress in the Shields number is the one responsible for the total flow resistance (assuming the idealized case where no additional flow resistance is to be considered, which is the case in flume experiments). With poorly sorted sediments, only protruding elements are responsible for the roughness layer development and the flow resistance equation was observed to behave like near-uniform sediments when the flow depth was scaled with D_{84} (see paragraph 2.3.2). Thus, for comparison with near-uniform sediments, D_{84} should also logically be used to scale the shear stress in the Shields number. This hypothesis is supported by comparing τ_{c84}^{*} values and the near-uniform sediment data set in Figure 25.
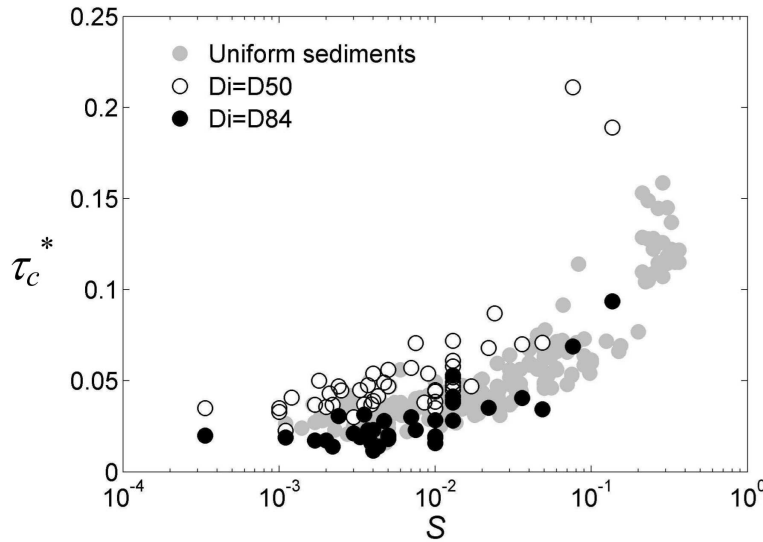
Figure 25: Comparison between τ_{c50}^{*}, τ_{c84}^{*} and near-uniform sediment data

Figure 26 plots τ_{c16}^{*}, τ_{c50}^{*} and τ_{c84}^{*}. All fractions can be approximated by a linear function of the slope. There is more scatter for τ_{c16}^{*} and τ_{c84}^{*} because corresponding grain diameters are generally not defined or poorly defined (moreover, D_{90} is often used instead of D_{84}).
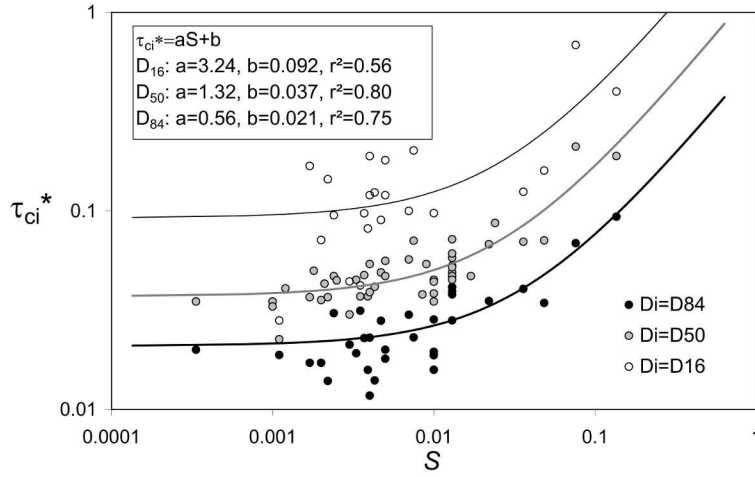
Figure 26: τ_{ci}^{*} values versus the slope. All fraction sizes can be approximated by a linear function $\tau_{ci}^{*}=aS+b$.

The best fit was obtained for τ_{c50}^{*} and was used with Eq. 39 to produce a general function:

$$\tau_{ci}^{*} = (1.32S + 0.037)\left(\frac{D_i}{D_{50}}\right)^{-0.93} \tag{40}$$

The value for $b=-0.93$ permits to reproduce all τ_{ci}^{*} values within $\pm 50\%$. However this b-value is uncertain as values reported in the field data set vary between -0.5 and -1. Improving this result would require a better understanding of the physical processes controlling b. For instance the slope effect described for τ_{ci}^{*} may also contribute to the scatter observed in b (see Recking, 2009 for discussion).

3.4. Shields versus Isbach

3.4.1. The Isbash equation

Interest in threshold conditions for transport originated from practical concerns over the effects that river channel instabilities may have on infrastructure, such as low-head diversion dams, roads, bridges, and levees. The basis for many of the techniques used today to specify rock sizes in engineered channels can be traced back to the classic work of Shields (1936) presented in the above paragraphs, but also to Isbash (1936), who presented results from a separate set of experiments in which he assessed the stability of blocks and rocks dropped into running water. The main equation was formulated in terms of a critical flow velocity U_c [m/s] that will move a rock of diameter D, and is written:

$$U_c = E\sqrt{2g(s-1)D} \tag{41}$$

where E is a dimensionless velocity. In theory, the velocity used in Eq.41 should be the velocity in the vicinity of the stone, however, in practice, the equation is usually used with the

depth averaged velocity computed with standard equations (CIRIA/CUR/CETMEF, 2007). The initial objective of the experiments was to develop criteria for the stability of dams, however, the equation was subsequently used by engineers in the design of riprap (USACE, 1991; Peirson and Cameron, 2006; CIRIA/CUR/CETMEF, 2007), and also in the assessment of environmental problems (Saldi-Caromile et al., 2004).

Despite differences in the methods used in the experiments (Shields extrapolated bedload transport rates to a zero value whereas Isbash measured the stability of blocks dropped into running water) the Shields and the Isbach equations were developed for the same objective: prediction of the stability of a rock exposed to a flow, and thus should be equivalent.

3.4.2. Linking the equations

In the Isbash equation, the dimensionless parameter E is assigned a value of 0.86 when the stone is exposed to the flow, and 1.2 when the stone is protected by other stones. The two situations are sketched in Figure 1.
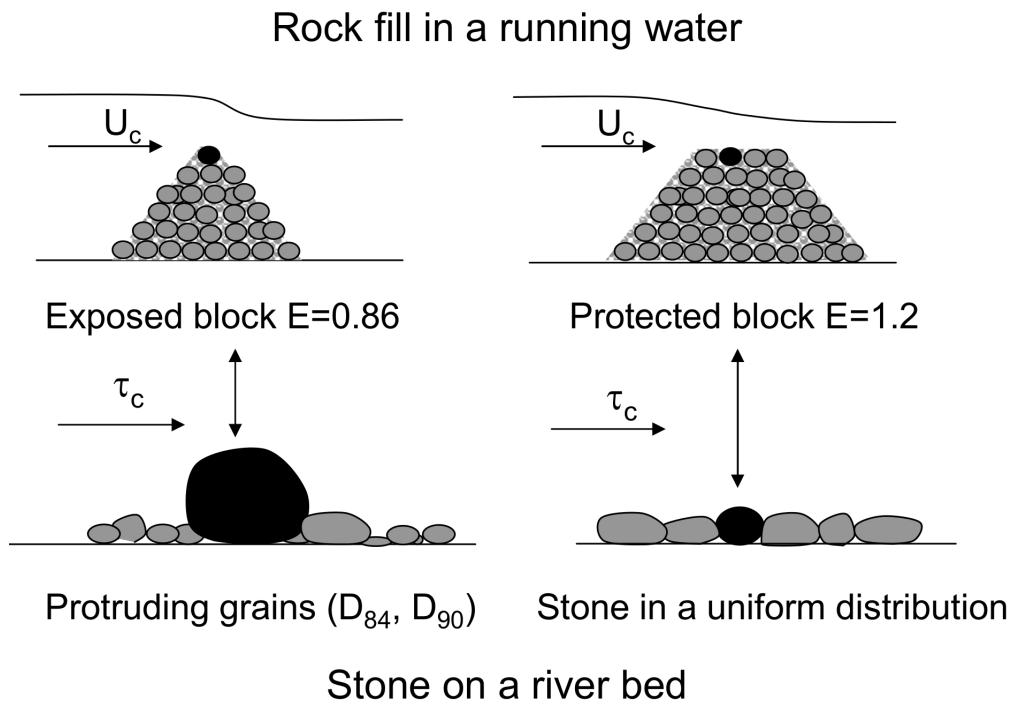

Figure 27 : Illustration of protected and exposed blocks, in a dam and in a natural river bed (Recking and Pitlick, in Press)

The upper panel shows conditions similar to Isbash's experiments where stones dropped into the water accumulated over time to form a triangular- or trapezoidal-shaped deposit. The stone perched atop the triangular-shaped deposit would be relatively exposed,

whereas the stone nestled among other stones in the trapezoidal-shaped deposit would be protected by other stones. The critical velocity for entrainment of exposed or protected rocks was deduced from this situation. The lower panel shows analogous conditions for individual rocks resting on the bed of a natural channel. In this case, the rock may be considered exposed or protected depending on the size in relation to neighbouring rocks. For the conditions shown, the critical Shields stress of the exposed rock (left) is less than the protected rock (right), similar to the difference in the value of E in Isbash's equation.

Eqs. 29 and 41 can be combined to give the minimum grain diameter D_{min} that is stable in a flow of given velocity or depth :

$$D_{min} = \frac{R_c S}{(s-1)\tau_c^*} = \frac{U_c{}^2}{2g(s-1)E^2} \tag{42}$$

from which we obtain:

$$\tau_c^* = 2\frac{gR_c S}{U_c^2}E^2 \tag{43}$$

Eq. 43 can be simplified further using the Darcy-Weisbash equation (see § 2.1.2):

$$\frac{U}{u*} = \frac{U}{\sqrt{gRS}} = \sqrt{\frac{8}{f}} \tag{44}$$

Leading to:

$$\tau_c^* = \frac{f}{4}E^2 \tag{45}$$

A friction equation is needed for comparing the two approaches.

3.4.3. The protected stone (E=1.2) as an individual stone in a uniform distribution

To compare the mobility of a protected stone in a rock embankment with that of uniform-sized stones in natural channels (Figure 27b), we estimate flow resistance using the Manning-Strickler equation used with the manning coefficient $n=D^{1/6}/21.1$, and the Recking et al equation (Eq.16). The Manning-Strickler equation is interesting because by its simplicity, it permits an explicit solution of Eq. 45. It is written:

$$\sqrt{\frac{8}{f}} = 6.7\left(\frac{R}{D}\right)^{1/6} \tag{46}$$

For the threshold conditions, we can rewrite Eq. 29 as:

$$\left(\frac{R}{D}\right)_c = (s-1)\frac{\tau_c^*}{S} \tag{47}$$

Substituting Eq.47 into Eq. 46, and combining with Eq. 45, gives:

$$\tau_c^* = 0.085 S^{1/4} E^{3/2} \tag{48}$$

The Recking et al equation necessitates replacing R/D by $(s-1)\tau_c^*/S$ (Eq.47) and implies an iterative approach for τ_c^*. Figure 28 indicates that both flow resistance equations used with E=1.2 reproduces well the threshold for motion of uniform sediments measured in flume experiments.

Figure 28 : Comparison of the Isbash equation for the case of protected grains (E=1.2) with the measured critical shear stress for uniform sediments

The result obtained with Manning Strickler (red curve) can be approximated by:

$$\tau_c^* = 0.11 S^{0.25} \tag{49}$$

which is very close to the equation presented in Figure 22 and to $\tau_c^* = 0.15 S^{0.25}$ proposed by Lamb et al. (2008) for uniform materials:

3.4.4. The exposed stone (E=0.86) as a protruding stone in a natural distribution

The Ferguson (2007) equation (Eq.24) was used to estimate flow resistance in cases where grains are fully exposed to the flow (Figure 27a). Replacing R_c/D_{84} by $(s-1)\tau_c^*/S$ (Eq.47) for threshold conditions, and replacing f in Eq.45 gives:

$$\tau_c^* = 2 \frac{a_1^2 + a_2^2 \left[(s-1)\tau_c^*/S\right]^{5/3}}{a_1^2 a_2^2 \left[(s-1)\tau_c^*/S\right]^2} E^2 \tag{50}$$

This equation can be solved iteratively by calculating the values of τ_c^* associated with E=0.86 for different slopes. The results are plotted in Figure 29 with a compilation of critical Shields stress values measured in the field for the three characteristic grain sizes D_{16}, D_{50} and D_{84}

(presented in Recking 2009). The Isbash equation for exposed grains (E=0.86) coincides with the critical Shields stress of protruding grains in a natural sediment mixture. The same relation shown in Figure 29 can be approximated by a power law:

$$\tau_c^* = 0.27 S^{0.46} \tag{51}$$

which is very close (same exponent) to $\tau_c^*=0.36S^{0.46}$ Pitlick et al. (2008) proposed from field measurements.
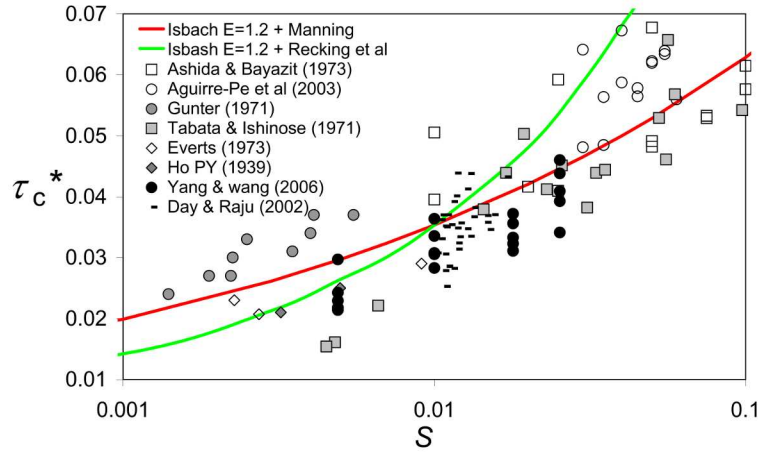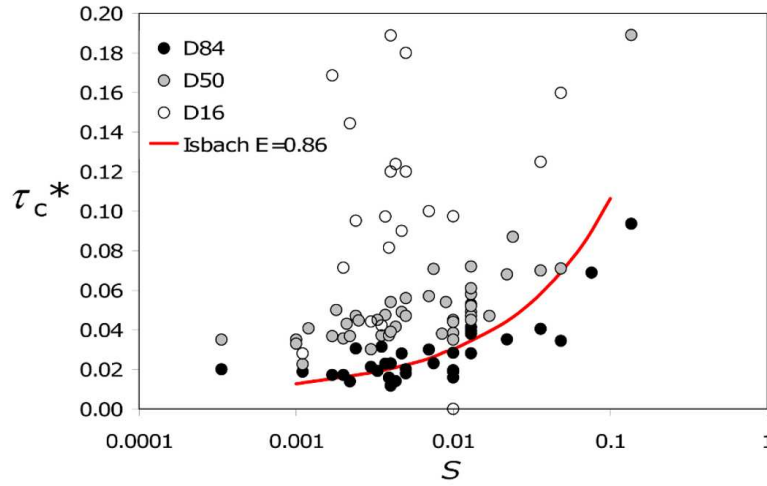

Figure 29 : Comparison of the Isbash equation for the case of exposed grains (E=0.86) with the measured critical shear stress for non-uniform sediments (measured for D_{16}, D_{50} and D_{84}) (from Recking and Pitlick, in Press)

3.4.5. Consequences for riprap design

For riprap design the Isbash equation is usually used with E=0.86 and the Manning-Strickler equation for flow resistance. This is equivalent to using Eq. 48 with E=0.86, which gives values of τ_c^* in the range of 0.01-0.03 when varying the slope. The criterion for entrainment presented in the Rock Manual (CIRIA/CUR/CETMEF, 2007) is $\tau_c^*=0.03$, which is consistent with values reported for natural channels with slopes less than about 0.005. However, if a critical Shields stress of 0.03 is used in the design of riprap in mountain streams with steep slopes, it can lead to large oversizing. Figure 30 shows three separate relations for estimating the minimum block size D_{min} for a given flow depth d, plotted as functions of reach-average slope.
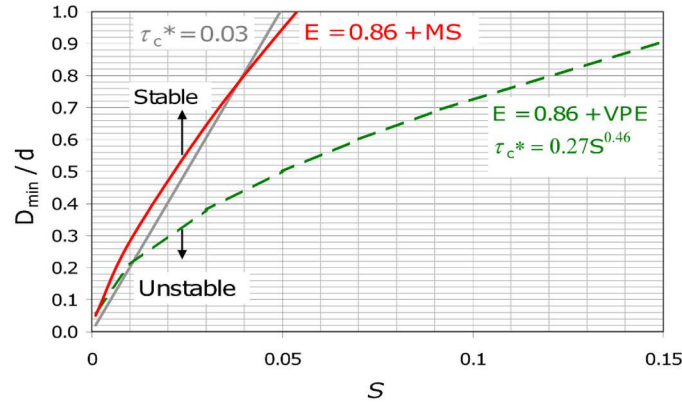
Figure 30 : Relations for estimating the minimum size of blocks, D_{min}/d for a range of channel slopes. The lines labelled E=0.86 +Manning Strickler (MS) and $\tau_c^*=0.03$ represents the standard design criteria based on equations of Isbash and Shields; the line labelled $\tau_c^*=0.27S^{0.46}$ represents an approximation of Eq.50.

The first two relations are formulated using standard design criteria, where the threshold for motion is estimated by assuming $\tau_c^*=0.03$ or E=0.86, and flow resistance is estimated with the Manning-Strickler equation (Eq. 46); these two relations plot essentially on top of each other. The third relation is formulated using Eq.51. The difference between this relation and the two standard relations shows that the standard approach quickly leads to unrealistic values in mountain streams, an effect which is well known by practitioners. While this acts to increase project security, it can strongly impact project costs. In addition, the stability of riprap in mountain streams is more related to the quality of the protections against scouring effects than to the size of the stone itself.

4. BEDLOAD PREDICTION

This part recalls the state of the art and the results of my research on this topic. It can not be disconnected from chapters 1 and 2 because computing bedload necessitates first to know the bed shear stress and the thresholds conditions for transport.

4.1. Flume and field bedload transport

4.1.1. Overview

Bedload transport is the transport of material in contact with the bed, by rolling or saltation. It differs from the transport by suspension (not considered here) where sediments are transported over long distances by the flow turbulence, with almost no contact with the bed. Because of the difficulties to study bedload in the field (Liebault and Laronne, 2008), it has widely been studied in the flume, at the laboratory. This has led to several simplifications which have strong implications:

-   flume transport is one dimensional whereas in the field transport is two dimensional: this can lead to large differences because of nonlinear bedload transport response to the variance in shear stress and bed material over a natural section (Ferguson, 2003).

-   In flume experiments, bedload is usually measured for a given steady and uniform flow condition, at dynamic equilibrium (all parameters are maintained nearly constant), and after several hours experiments for a given run. In the field bedload consists essentially in nearly instantaneous cross-section averaged data measured for the given flow condition.

-   Most flume experiments were performed with uniform or nearly uniform grain size distribution (Figure 10) whereas almost all rivers, including sand bed rivers, have poorly sorted sediments (Figure 11). Consequently, flume experiments do not reproduce the effects associated with grain to grain interactions (Recking et al., 2009b).

-   In gravel, boulder and cobble bed rivers, transport is generally associated with a very low Shields stress ratio, with $\tau^*/\tau_c^* \approx 1$ or below (Figure 11). On the other hand most flume experiments were performed with a high Shield stress ratio ($\tau^*/\tau_c^* \approx 2$ or higher) in order to avoid bed meandering: consequently they are more likely to reproduce field bedload transport observed during high flows only, or in sand bed rivers (where usually $\tau^*/\tau_c^* > 2$).

Figure 31 : Vertical and longitudinal sorting in a gravel bed river: grains are dispatched into distinct patches of similar grain size and sorting

The two last field properties have strong consequences on bedload transport that should be considered in bedload modeling. In many rivers with coarse bed material, grains are dispatched into distinct patches of similar grain size and sorting and the sediment supplied is stored vertically in a coarse fraction that is retained on the bed surface (Figure 31), i.e., the armor layer, and a fine fraction that goes into temporary storage in the bed, i.e., the substrate (Pitlick et al., 2008). A different transport phase can be considered regarding the armor mobility (Jackson and Beschta, 1982; Ashworth and Ferguson, 1989; Ryan et al., 2002; Bathurst, 2007): as long as the threshold for break-up of the armor layer is not attained, phase 1 is considered, with bedload composed of fine sediments supplied from upstream or from patches of fine materials and passing over the immobile armor layer. When the flow condition permits the break-up of the armor, phase 2 is considered where coarse grains can participate in transport and the availability of fine sediments from the subsurface is increased (Parker et al., 1982). To finish, a phase 3 can also be considered once all sizes are in motion (Parker et al., 1982; Wilcock and McArdell, 1993). Phases of transport are sketched in Figure 32 with the mobility of the bed pavement considered through the threshold mobility of the bed surface D_{84}.
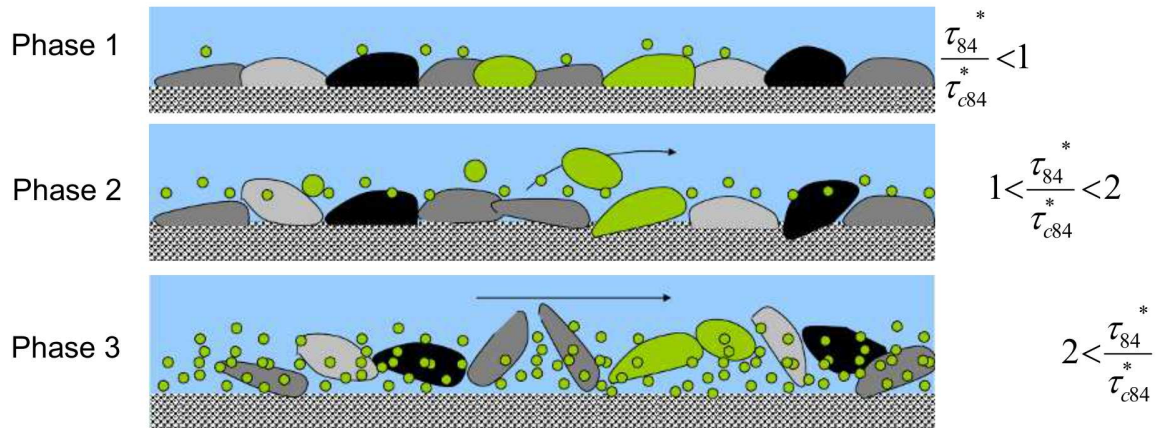
Figure 32 : Sketch of the 3 phases of transport, with the mobility of the bed pavement considered through the threshold mobility of the bed surface D_{84}.

4.1.2. Comparing the data produced in the flume and in the field

For comparing the flume and the field approaches, two data sets were built with data from the literature. The flume data set comprises 1,317 values produced in flume experiments by 17 different authors. The data are described in Recking et al. (2008) and are available (as supplementary material) in a later publication (Recking, 2010). They correspond to a large range of flow and transport conditions presented in Table 1.

Parameter	Range
Slope [-]	0.001–0.2
Diameter [mm]	0.3–44.3
Shields number τ^* [-]	0.014–3.43
Einstein parameter Φ [-]	3.8E–9–264

Table 1: Main characteristics of flume data

Parameter	Range
Slope (m/m)	0.0002–0.08
Diameter D_{50} (mm)	0.4–220
Diameter D_{84} (mm)	0.9–558
Discharge (m3/s)	0.012 -7104
Bankfull depth (m)	0.06–6.2
Bankfull width (m)	0.3–200
Einstein parameter Φ [-]	2E–11–215

Table 2: Main characteristics of field data

The field data set comprises 8,940 bedload values collected over 109 river reaches with various methods, such as Helley-Smith samplers (Emmett, 1980) or sediment traps (Reid and

Laronne, 1995). The complete data sets is available (on-line as supplementary material) in recent publications (Recking, 2010, sub.) and the corresponding ranges of field conditions are presented in Table 2.

Figure 33 compares the flume and the field data sets (10,257 values). The x-axes plots the Shields stress τ^* and the y-axes plots the dimensionless bedload transport (Einstein, 1950) defined by:

$$\Phi = \frac{q_v}{\sqrt{g(s-1)D}} \tag{52}$$

where q_v [m^3/s/m] is the volumetric transport rate per unit width, $s = \rho_s/\rho$ is the ratio between sediment and water density, and D is the grain diameter. For the field data τ^* and Φ were computed with the median diameter D_{50}.
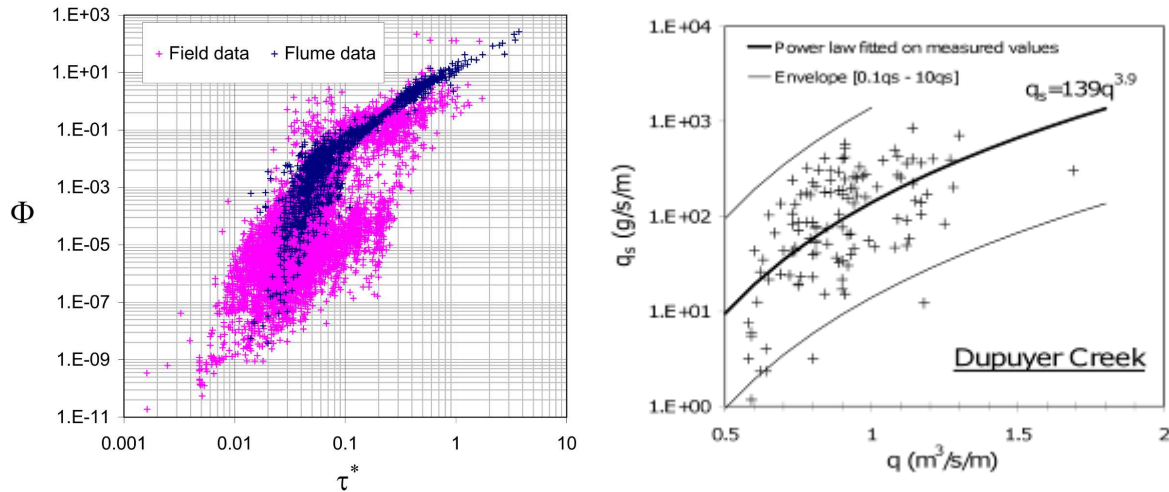
Figure 33 : (a) Comparison between bedload measured in the flume and in the field (the median diameter D_{50} was considered for τ^* and Φ) (b) Bed load measured in Dupuyer Creek as a function of water discharge [data from Whitaker and Potts, 2007b]

The first observation is that most transport rates measured in the field are weaker than values investigated in flume experiments. One can deduce from this figure that the scatter is quite substantial, and that a single Shields number can be associated with bedload transport values covering almost seven orders of magnitude (τ^*=0.03 is associated with 1E−9< Φ < 1E−2). Actually the scatter also exists inside each individual data set, and corresponds to large fluctuations of bedload discharge for a given flow condition, as illustrated with the Dupuyer Creek measurements (Whitaker and Potts, 2007) shown in Figure 33b: many measured bedload transport values correspond to a given flow discharge within plus or minus one order of magnitude.

Differences in sampler efficiency may explain some of the scatter observed in and between the data sets. For instance, the small width of the Helley-Smith sampler orifice (76 or 152 mm) may cause underestimation of measured grain size and bedload transport rates, especially for high transport rates, with large pebbles moving only at this time. These uncertainties are very difficult to evaluate because the various investigations of Helley-Smith sampler efficiency have produced somewhat contradictory results (Emmett, 1980; Hubbell and Stevens, 1986; Childers, 1999; Ryan and Porth, 1999; Sterling and Church, 2002; Bunte and Abt, 2005; Ryan et al., 2005; Vericat et al., 2006). The sampling strategy can also affect the quality of the measured data (Ergenzinger et al., 1994; Bunte and Abt, 2005; Singh et al., 2009; Fienberg et al., 2010).

Measurement errors may contribute to, but are not the only explanation for the fluctuations observed. Natural bedload fluctuations also exist and have been identified in nearly all field investigations (Bunte, 1992; Madej and Ozaki, 1996; Garcia et al., 2000; Paige and Hickin, 2000; Habersack et al., 2001; Cudden and Hoey, 2003): they are explained by bedforms migration (Gomez et al., 1989), grain sorting (Gomez, 1983; Whiting et al., 1988; Recking et al., 2009b) or nonlinearity effects (Ferguson, 2003; Recking, sub.).

4.1.3. Modelling bedload transport

Dozens bedload transport equations have been derived over the years, most of them partly if not totally calibrated with flume experiments. These equations are based on bed shear stress (DuBoys, 1879), stream discharge (Schoklitsch, 1962), stream power (Bagnold, 1977), or a stochastic approach (Einstein, 1950), and most of them are threshold equations. The most famous and probably widely used equation is the Meyer-Peter and Mueller (1948) equation written:

$$\Phi = 8(\tau^* - \tau_c^*)^{3/2} \tag{53}$$

Where $\tau_c^* = 0.047$. Meyer-Peter and Mueller proposed to compute the Shields stress τ^* with a flow depth correction given by Eq.11. This equation is compared to the flume data in Figure 34, and two comments can be made:

- the threshold condition is not satisfied as a lot of bedload values correspond to $\tau^* < \tau_c^*$;
- the 3/2 asymptotic trend of the power equation is not confirmed.

The threshold condition definition becomes a real problem when considering the field data (Figure 33a).
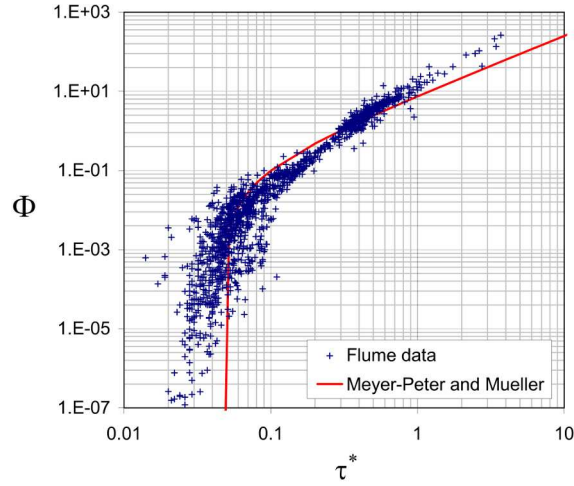
Figure 34 : Comparison between the Meyer-Peter and Mueller equation and the flume bedload transport data set

The threshold limitation is not surprising when considering that the critical Shields stress is not constant but vary with the hydraulics associated with different slopes (§3.2). In order to overcome the threshold problem, non-threshold equations have been proposed, considering that in turbulent flows, even the lowest discharge can produce a very low transport of fine sands (Paintal, 1971; Parker, 1990). Modern non-threshold equations (Parker et al., 1982; Wilcock, 2001) better consider the shape of the function by adjusting the low transport rates with a transport stage parameter defined by τ/τ_r, where τ_r is a reference shear stress associated with a very low predetermined transport rate. These functions refer to a dimensionless transport rate $W^*=(s-1)gq_v/(\rho_s u^{*3})$ (where q_v is the volumetric bedload transport per unit width, and $u^*=(gRS)^{0.5}$ is the shear velocity), which presents the advantage of not being dependent on the sediment diameters, as is the case for the more conventional Einstein parameter (Eq.52).

In their more sophisticated versions, these equations also incorporate a hiding function, allowing a fractional-based calculation, i.e., the calculation is made size by size (Parker and Klingeman, 1982; Wilcock and Crowe, 2003). Considering a bedload equation established for a characteristic grain size D and given as a function ζ of the shear stress and the reference shear stress:

$$q_v = \zeta(D,\tau,\tau_r) \tag{54}$$

the fractional-based calculation consists in assuming that the functional relation ζ holds for each size fraction D_i of the sediment mixture to calculate:

$$q_{vi} = f_i\zeta(D_i,\tau,\tau_{r_i}) \tag{55}$$

54

where f_i is the proportion of material in the ith size class, τ_{ri} is the associated reference shear stress for diameter D_i, and q_{vi} is the bedload transport rate associated with diameter D_i. The value for τ_{ri} is usually expressed as a function of τ_{r50} calculated for the median grain size D_{50} (of the surface or subsurface mixture) with a hiding function taking the form given by Eq.39. The total bedload transport rate is thus given by:

$$q_v = \Sigma q_{vi} \tag{56}$$

The more recent surface-based equation from Wilcock and Crowe (2003) improved the hiding function by more accurately considering the relation between the transport stages and the associated bed surface grain size distributions:

$$W_i^* = \frac{(s-1)g q_{vi}}{f_i u_*^3} = \begin{cases} 0.002\phi^{7.5} & \text{for} \quad \phi < 1.35 \\ 14\left(1 - \dfrac{0.894}{\phi^{0.5}}\right)^{4.5} & \text{for} \quad \phi \geq 1.35 \end{cases} \tag{57}$$

With $\quad \phi = \dfrac{\tau_{Dm}^*}{\tau_r^*}\left(\dfrac{D_i}{D_m}\right)^{-b}$, $\tau_r^* = 0.021 + 0.015 \exp[-20 F_s]$, $\quad b = \dfrac{0.67}{1 + \exp\left(1.5 - \dfrac{D_i}{D_m}\right)}$

Where D_m is the mean grain size of the bed surface and F_s denotes the fraction of the material of the surface layer that is sand. The grain size distributions must be sampled (at 1-ψ intervals or more) and the grain shear stress can be calculated with $\tau = \rho g (S D_{65})^{1/4} U^{3/2}$ (Wilcock et al., 2009).

4.2. Equations evaluation

Eighteen standard bedload transport formulas (Meyer-Peter and Mueller, 1948; Brown, 1950; Einstein, 1950; Schoklitsch, 1962; Yalin, 1963; Engelund and Hansen, 1967; Ackers and White, 1973; Mizuyama, 1977; Parker, 1979; Bagnold, 1980; Smart and Jaeggi, 1983; Van Rijn, 1984; Yang, 1984; Karim and Kennedy, 1990; Rickenmann, 1990; Abrahams and Gao, 2006; Wong and Parker, 2006) were compared to the flume and the field data sets (see Recking et al, 2012 for more a complete presentation of these equations). All equations were chosen because they permit a surface-based calculation with limited knowledge of sediment characteristics and they are widely used.

To test the formulas, we calculated the percentage of the ratio r = [calculated transport rate] / [measured transport rate] included in a given interval. For example, a score of 40% obtained for the interval [0.1–10] means that 40% of the predictions are correct within plus or minus one order of magnitude. Because this precision interval was present in almost all the

measured signals (as shown in Figure 33b), a bedload function working with mean parameters will at best reproduce the median value for a given discharge, but will not reproduce the measured dispersion. In other words, a given flow condition will be associated with a single calculated value, but also with several measured values covering more or less one order of magnitude around the median. Consequently, the interval [0.1–10] was used for the tests. Because the objective was to evaluate the prediction accuracy in a general sense, scores are not given for each equation individually but presented by a median associated with the quartiles, a maximum, and a minimum.

Because all the equation considered here are one-dimensional (derived in a flume), and because they are used with section averaged data (shear stress, grain size distribution), underestimation is expected as a consequence of nonlinearity. This was demonstrated by Ferguson (2003): using a probability function describing the shear stress variation around its mean value, he showed that additional flux locally induced by high shear stress outweighs the lower flux induced by low shear stress and that, consequently, the total flux (the sum of all local fluxes) should be higher than the flux computed with the averaged shear stress.

4.2.1. Comparison with flume measurements

All equations were used exactly as they were proposed by the authors. The results are plotted in Figure 35 and Figure 36. Equation 31 (for τ_c^*) was used for splitting the results into different flow ranges in the figure (but the calculations were made with the original τ_c^* values specified by the authors). Figure 35a plots the scores as a function of τ^*/τ_c^* and shows that equations are valid only when $\tau^*/\tau_c^* > 1.2\text{-}1.4$. The decrease in efficiency near incipient motion corresponds to zero prediction (Figure 35 b) and/or overestimation (Figure 35 c).

Figure 36 plots the scores as a function of the grain diameter D and the slope. No clear trend can be observed with the grain diameter and a small trend is observed with the slope. Actually, these generally high scores must be related to the fact that more than 65% of the runs were performed with a Shields ratio $\tau^*/\tau_c^* > 1.5$. This appears clearly in Figure 36b where the scores are directly proportional to the percentage of runs verifying $\tau^*/\tau_c^* > 2$ (a similar correlation was obtained when considering $\tau^*/\tau_c^* > 1.5$).
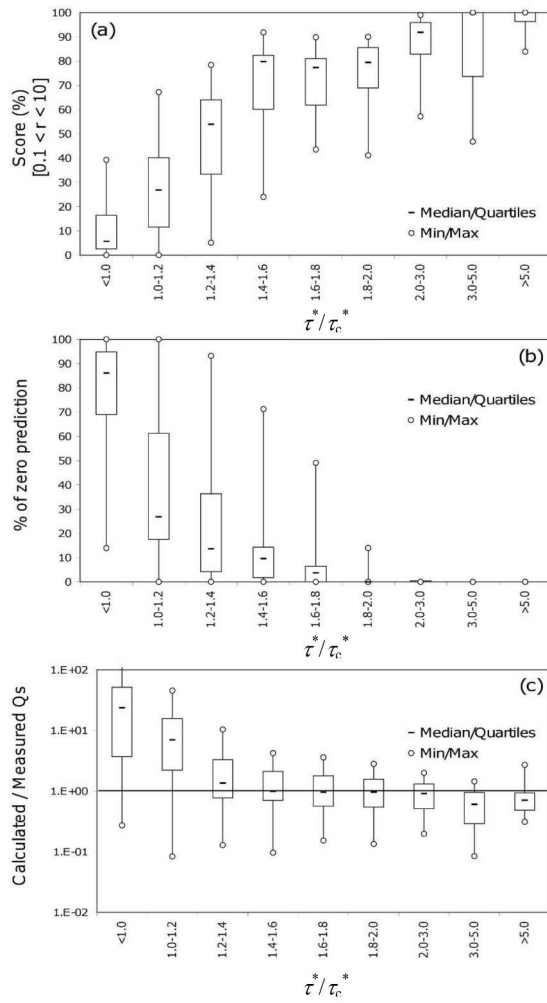
Figure 35: Test of models efficiency with the flume data, as a function of τ^*/τ_c^*. (a) Score (%) of r within the range [0.1–10]; (b) percentage of zero prediction (thresholds formulas); and (c) ratio between calculated and measured bedload transport
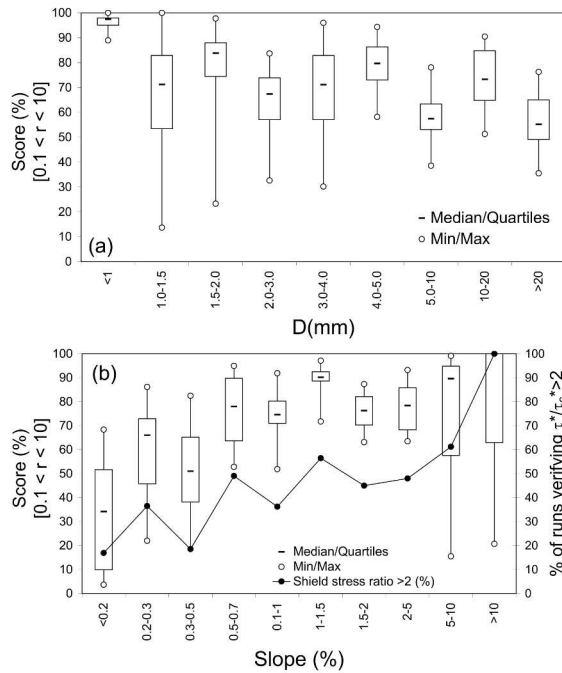

Figure 36: Results of the tests with the flume data as a function of (a) D and (b) slope

4.2.2. Comparison with field measurements

All equations were used exactly as they were proposed by their authors. The results of the tests are presented in Figure 37 and Figure 38. In Figure 37, results were plotted as a function of the mobility of the coarser elements of the bed surface, considered through the τ_{84}^*/τ_{c84}^* ratio, where τ_{84}^* is the Shields number calculated for diameter D_{84} and τ_{c84}^* is the critical Shields stress for D_{84} estimated with Eq. 40. Figure 37a indicates that only at high transport stages are all formulas effective. The efficiency is moderate when $1 < \tau_{84}^*/\tau_{c84}^* < 2$ and close to zero when $\tau_{84}^*/\tau_{c84}^* < 1$. This decreased efficiency with decreasing Shields stress is associated with (i) zero predictions when $\tau_{84}^* < \tau_{c84}^*$ (Figure 37b) and (ii) overprediction (by up to several orders of magnitude) when the calculated transport is non-zero (Figure 37c plots the statistical quantities calculated from the median value of qs_{cal}/qs_{meas} obtained with each formula within the flow range considered). Overprediction is an unexpected result as discussed in the introductive part. It could be explained by hiding effects (not included in formulas) reducing the mobility of particles for a given shear stress.

These scores were also plotted as a function of diameter D_{84} in Figure 38a. Sharply decreased efficiency is evident when D_{84} is higher than 50 mm, and the scores are nearly zero when D_{84} is higher than 100 mm. This means that either using formulas established in a flume with fine and almost uniform gravels cannot be extended to coarse gravels and cobbles in the field or that the equations are correct but the field measurements are not. The two hypotheses are plausible depending on the flow condition considered:

(i) At low flows, bedload in many gravel and cobble bed rivers essentially consists of partial transport (fine gravels move whereas the largest gravels are maintained at rest); grains sorting and the variance in shear stress and bed surface grain size are maximum.

(ii) The second hypothesis must be considered for high transport rates because the threshold diameter $D=50$ mm roughly corresponds to the width of the standard portable Helley-Smith samplers (76.2 mm) used for most measurements. However, additional analysis presented in Recking et al (2012a) suggest that the measurement technique only partly explain this result.

Figure 38b plots the scores with the slope *S*. The results are good only for very mild slopes ($S < 0.1\%$), which, considering the previous discussion, stem from these slopes being associated with sand and fine gravels only. These results are also likely related to the effects due to changing flow hydraulics with increasing slope (Shvidchenko et al., 2001; Mueller et al., 2005; Vollmer and Kleinhans, 2007; Lamb et al., 2008; Recking, 2009), which are not taken into account by most formulas
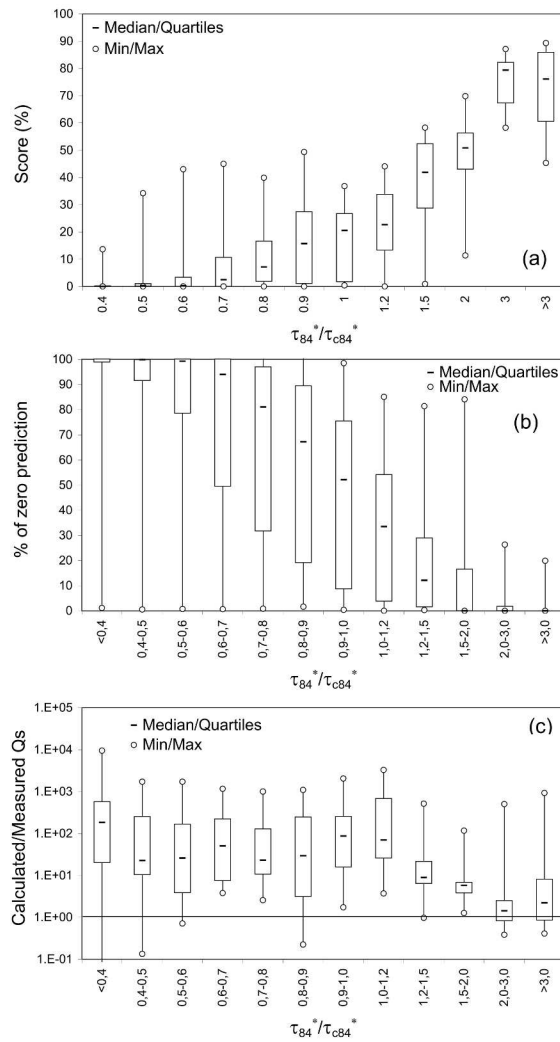
Figure 37: Analysis of the model's effectiveness when tested on instantaneous field measurements. (a) Score (%) of r within the range [0.1–10]; (b) percentage of zero prediction (thresholds formulas); and (c) ratio between calculated and measured bedload transport. The results are plotted as a function of τ_{84}^*/τ_{c84}^*.
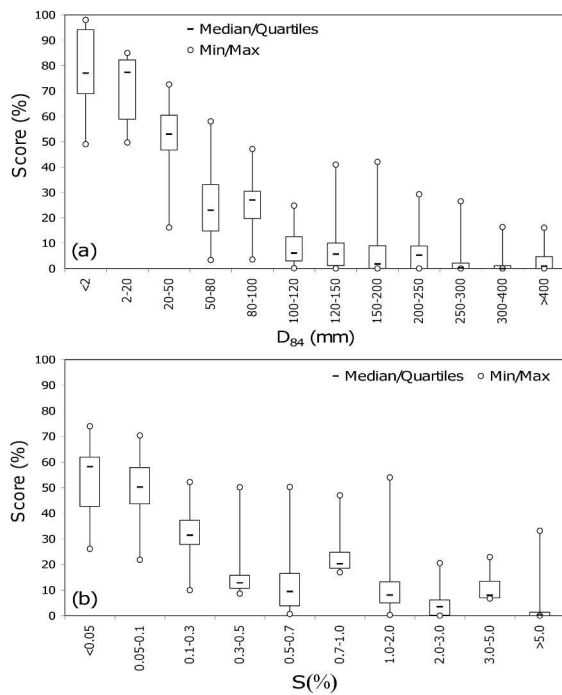
Figure 38: Results of the test with the field data as a function of (a) D_{84} and (b) slope

4.2.3. Taking into account critical Shields stress variations

One limitation suggested in the above tests is that equations were built for a limited flow range, and incorporate a constant threshold value. This is why a new equation was proposed (Recking et al., 2008) taking into account a variation of the critical Shields stress with the slope, and more generally flow resistance and bedload interactions.
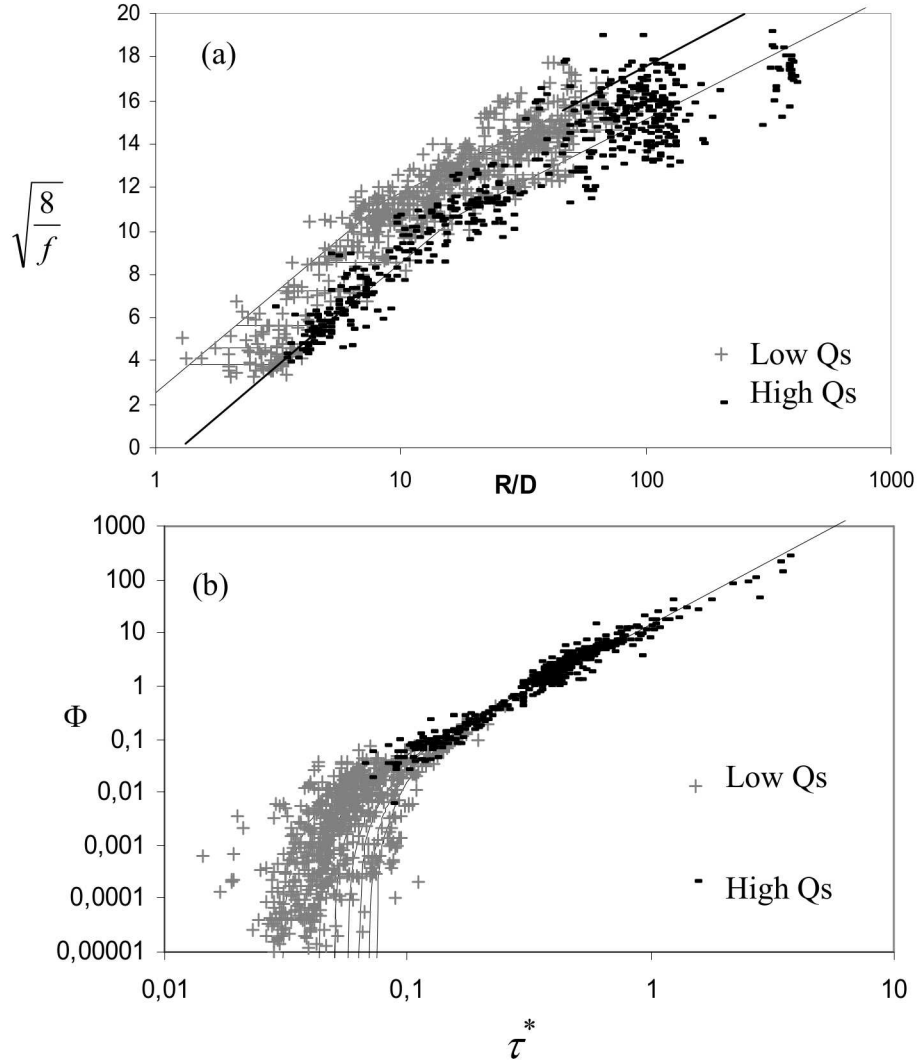
Figure 39: Plot of 1270 flume values in (a) a flow resistance (R/D,$(8/f)^{0.5}$) and (b) a transport rate (τ^*,Φ) diagram considering points belonging to regimes 2 and 3 as defined by the flow resistance model (Eq.16, Figure 7)

The [uniform sediment] flow resistance and bedload data plotted in Figure 39 suggest that the changes observed in grain motion and flow resistance (as presented in §2.2.2) also correspond to a change in the bedload transport rate. Two groups, characterized by a change in the $\Phi(\tau^*)$ relation shape, can be isolated. The first group (in grey in the figure) largely contributes to

data dispersion. The second group (in black in the figure), corresponds to high bedloads and is less scattered. A detailed analysis of the first group shows that the scatter is reduced after stratification by the slope. This corresponds to a change in the critical Shields stress with the slope describes in paragraph 3.2.
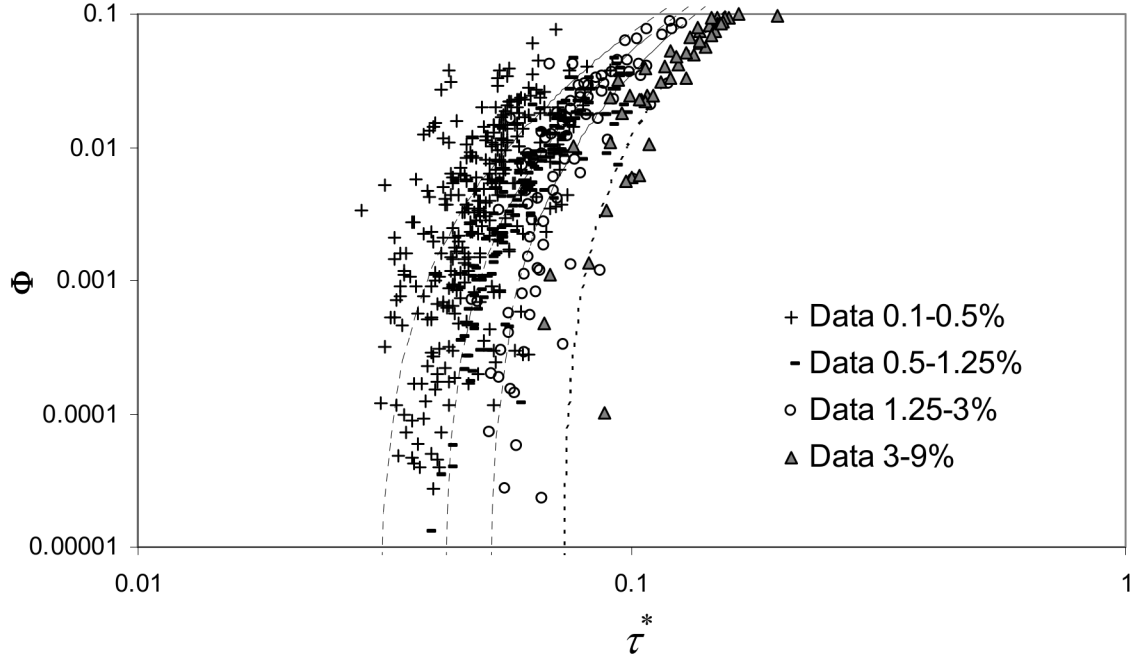
Figure 40: Low transport flume data plotted with consideration of the slope *S*

A semi-empirical relationship based on the tractive force concept was fitted to the data, which gave a two part model:

$$\Phi = 15.6(\tau^* - \tau_c^*)^2 \quad \text{when } \tau^* < 0.65S^{0.41} \tag{58}$$

and

$$\Phi = 14\tau^{*2.5} \qquad \text{when } \tau^* > 0.65S^{0.41} \tag{59}$$

A test with independent flume data has shown that taking into account the critical Shield stress variation improves predictions when compared to other standard approaches (Recking et al., 2008) (Table 3, Figure 41). However, the comparison with the field data set gave very bad results, with only 50% of the runs predicted with a non-zero transport, and for the other runs, large overprediction (Figure 42).

Model	0.8 < r < 1.2	0.6 < r < 1.4	0.5 < r < 2
MPM /Manning (1948)	10-17	25-32	41-46
Smart & Jaeggi (1983)	14-16	26-29	37-40
Engelund & Hansen (1967)	9-11	25-27	39-41
Graf & Suszka (1987)	14-/	34-/	47-/
Schoklitsch (1962)	/-13	/-24	/-34
Rickenmann (with q, 2001)	/-13	/-28	/-36
Abrahams et Gao (2006)	22-/	36-/	51-/
Parker (1979)	19-/	34-/	53-/
Eq.16+58	**30-37**	**54-58**	**68-70**

Two values are associated with each case: the left value is the score obtained by calculating $\Phi(\tau^*)$ and the right value is the score obtained by calculating $\Phi(Q, S, D)$ when a friction law is proposed by the author.

Table 3: Scores (%) for each model in the ranges [0.8<*r*<1.2], [0.6<*r*<1.4] and [0.5<*r*<2]

Figure 41 : Comparison between flume measurements and results of calculations with consideration of Shields stress variations with slope (Eq.16+58)
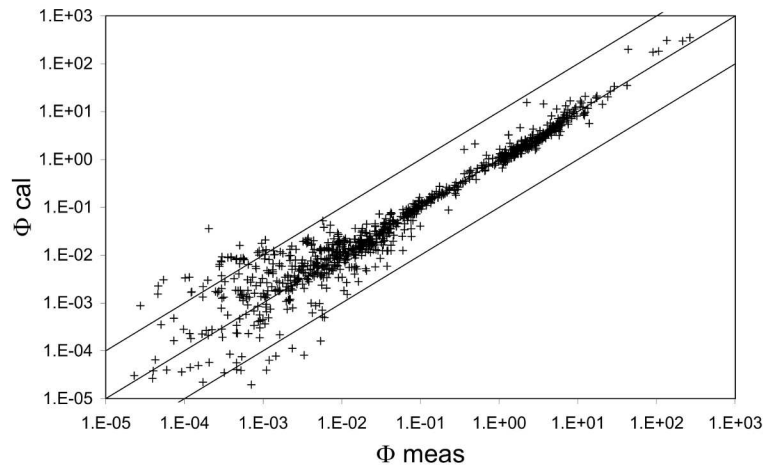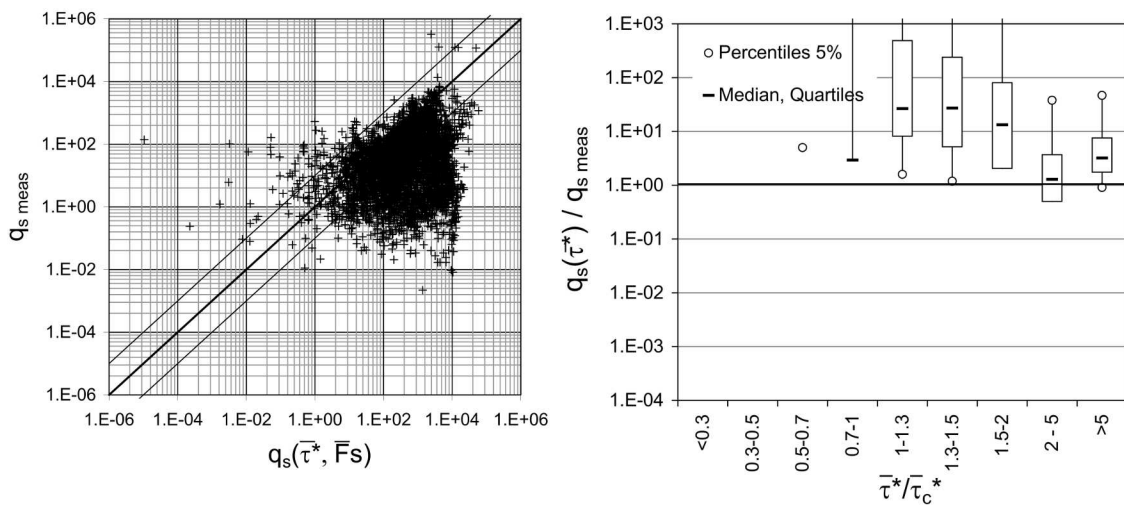

Figure 42 : Comparison between field measurements and results of calculations with consideration of Shields stress variations with slope (Eq.16+58)

4.2.4. Fractional calculation

In the previous paragraph, it was hypothesized that equations derived in a flume with fine and nearly uniform gravels, could not reproduce the field partial transport. This is why additional tests were performed with the recent surface-based Wilcock and Crowe (2003) equation (Eq.57), which was specially derived for partial transport conditions (Eq.57). This equation improved the hiding function by more accurately considering the relation between the transport stages and the associated bed surface grain size distribution, and is particularly recommended for partial transport. The grain size distribution of each individual data set was sampled at 1-ψ intervals and the shear stress was computed with the procedure given in Wilcock et al. (2009). The results are presented in Figure 43.
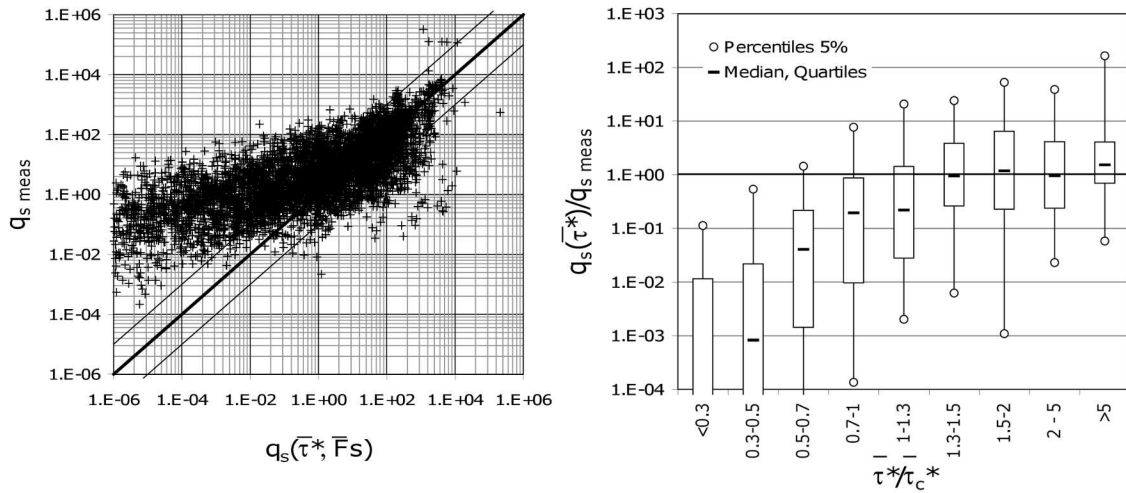
Figure 43: Comparison between field measurements and results of calculations with the Wilcock and Crowe (2003) equation used with the mean flow parameters

As for Figure 37, results of computations were plotted as a function of $\tau_{84}{}^*/\tau_{c84}{}^*$ with $\tau_{c84}{}^*$ calculated with Eq. 40 (but the equation was used exactly as it was proposed by their authors). Figure 43 indicates that results are very good when the Shields stress ratio is higher than 1.3, which is much better than what was obtained with standard equations (Figure 37). It corresponds to large floods as in gravel and cobble bed rivers, most transport are associated with $\tau_{84}{}^*/\tau_{c84}{}^* < 1.3$. However, contrarily to other standard equations, the Wilcock and Crowe equation reproduces adequately the expected bedload underestimation for the low Shields stress values, as discussed in the introductive part of this section. Prediction with 1D equations should be improved either by computing the local shear stresses (Ferguson and Church, 2009; Camenen et al., 2011) or by introducing a probability function describing the variance in shear stress when calculation are made with section-averaged input data (Bertoldi et al., 2009).

4.2.5. Conclusion of the equations evaluation

The evaluation with large flume and field data sets has shown that:

(1) even with perfectly controlled data obtained in the flume, equations are not valid close to incipient motion conditions. A prediction factor of 2 (prediction within the interval [0.5–2]) was the minimum that could be expected when testing equations with time-integrated flume measurements;

(2) equations derived in flumes with nearly uniform sediments poorly reproduce the field measurements. These equations were developed with no consideration for partial transport of a poorly sorted sediment and are not able to take into account the reduced mobility of fine materials when protected by larger ones (i.e. supply limitation), leading to overprediction;

(3) fractional calculation with the Wilcock and Crowe equation reproduces partial transport but underpredict the fields measurements when used with width-averaged parameters because of nonlinearity.

4.3. Improving the methods

4.3.1. A field derived equation

In order to overcome the nonlinearity effects induced by using a 1D flume equation with section-averaged data, a field derived equation was proposed. The central idea leading the development of the new equation was:

- (i) it should be non-threshold and expressed by a Shields stress ratio instead of an excess Shields stress

- (ii) all parameters (shear stress and bedload transport) are made dimensionless with the diameter D_{84} of the bed surface because these large diameters scale the hydraulics (§2.3), they scale incipient motion (§3.3), and by contributing to bed surface armouring, they control the availability of fine sediments for transport (Parker and Klingeman, 1982),

- (iii) mobility of the bed surface D_{84} is well described by the ratio $\tau_{84}^{*}/\tau_{c84}^{*}$ where τ_{c84}^{*} is given by Eq.40 (replacing D_i by D_{84}), and τ_{84}^{*} is calculated with Eq. 28;

- (iv) the transport of finer fractions is considered in an implicit manner, as a function of the mobility of diameters D_{84};

- (v) full mobility in the field (intense transport) is similar to full mobility in the flume and Eq.59 can be used with D_{84}; this hypothesis was necessary as intense transport was poorly documented in the field (Laronne and Reid, 1993).

A set of equations was developed with respect to the above conditions and validated (blind test) with a large field data set comprising 3000+ values (Recking, 2010, in press):

$$\Phi = 14\tau_{84}^{*2.5}/[1+(\tau_m^*/\tau_{84}^*)^4] \tag{60}$$

$$\tau_m^* = (5S+0.06)\left(D_{84}/D_{50}\right)^{4.4\sqrt{S}-1.5} \tag{61}$$

$$\tau_{84}^* = \frac{SR}{(s-1)D_{84}} = \frac{S}{(s-1)D_{84}[2/W+74p^{2.6}(gS)^p q^{-2p} D_{84}^{3p-1}]} \tag{62}$$

where $p = 0.23$ when $q/\sqrt{gSD_{84}^3} < 100$ and $p = 0.3$ otherwise. τ_m^* is by model construction, the transition between full mobility and partial transport. This equation was constructed by considering the mobility of the bed surface D_{84} (which must be measured with the nontruncated pebble count technique; Wolman, 1954), and its originality is illustrated in Figure 44 compared with the well-known threshold equation proposed by Meyer-Peter and Mueller (1948), considering $\tau_c^* = \tau_m^* = 0.047$ (where τ_c^* is the critical Shields stress). Whereas the Meyer-Peter and Mueller equation considers a zero transport for the whole mixture when $\tau^* < 0.047$ (calculated for D_{50}), the new equation considers only the end of full mobility (end of transport for the largest elements) and a progressive decrease to near-zero transport when τ^* (calculated for D_{84}) tends to zero.
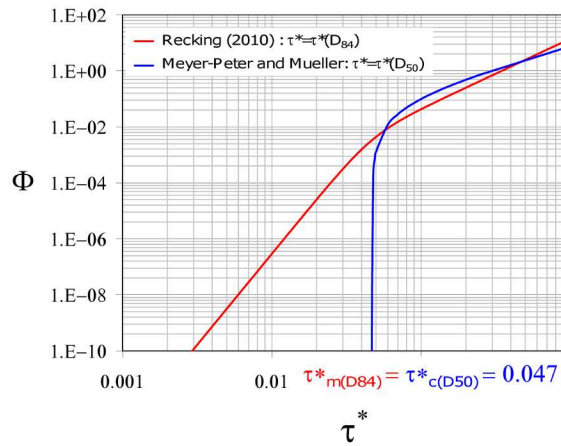
Figure 44: Comparison of the nonthreshold model from Recking (2010) and the Meyer-Peter and Mueller (1948) model for $\tau_c^* = \tau_m^* = 0.047$.

In Eq.61, the -1.5 exponent comes from Eq.40 and refers to changing flow hydraulics with slope, whereas the slope exponent $4.4\sqrt{S}$ comes from the field adjustment and was introduced for taking into account changing sediment mobility (due to grain arrangement) with slope. One important property of τ_m^* is that it acts by reducing transport with increasing slope for a

given shields stress τ^*. No field data were available for fitting the value of τ_m^* for the case of sand bed rivers, but available flume data (Recking et al., 2008) suggest that a constant value $\tau_m^* = 0.045$ is adapted.

The model was tested on the large field data set comprising 8000+ values (3000 of which has served in the model construction) and results plotted in Figure 45 and Figure 46 are satisfactory, with no under or over prediction.
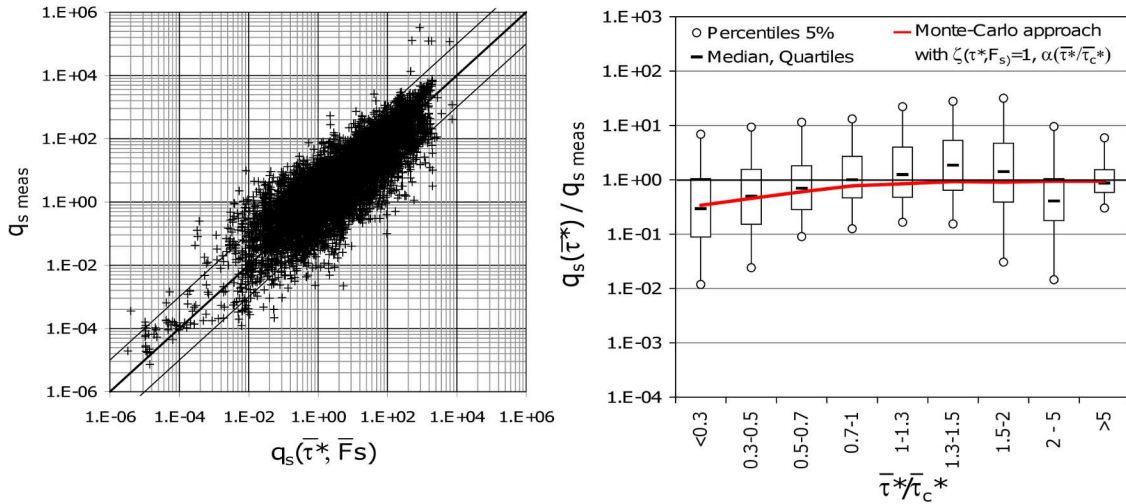
Figure 45: Comparison between field measurements and results obtained with Eqs. 60-62 used with the mean flow parameters.
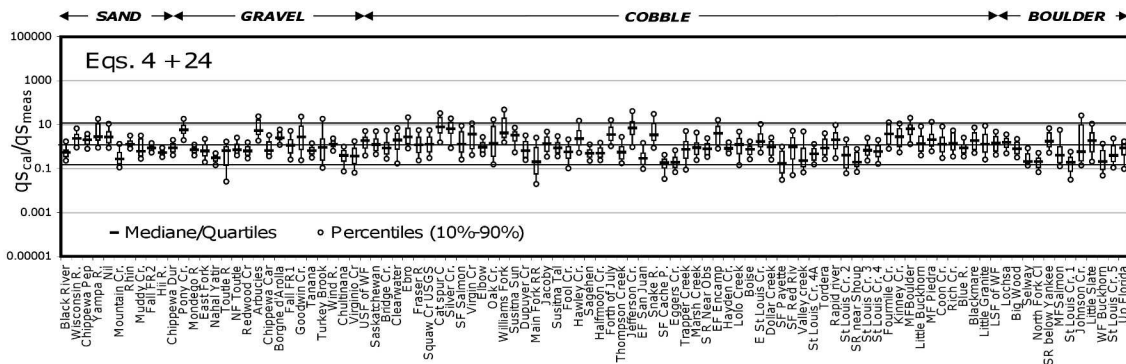
Figure 46: Comparison of the bedload transport model (Eqs. 60-62) and bedload collected over 100 river reaches

Because it was derived on the basis of reach-averaged data this model has a built-in allowance for the effects of spatial variability, which considerably improves the computation of bedload transport when compared to standard 1-dimensional (usually flume derived) equations. Its robustness is also partly explained because D_{84} is easier to define than the finer diameters and overall may be persistent during flooding (Wilcock and DeTemple, 2005; Clayton and Pitlick, 2008).

4.3.2. Back to the flume

It was not possible to reproduce the 2D field data with 1D flume-derived equations. Is the inverse true? Logically, nonlinearity effects should lead to overprediction when 2D field derived equations are used with 1D flume bedload measurements. This was tested by comparing Eqs. 60-62 to the flume data set from Wilcock et al. (2001), which is (to the best of my knowledge) the only published flume data obtained with partial transport conditions (Wilcock and McArdell, 1993). Five runs were produced in a 0.6 m wide and 8 m long tilting flume, with recirculation of poorly sorted sediment mixtures with different sand contents, and the data are available online in Wilcock et al. (2001).

A plot of the calculated versus measured values in Figure 47a indicates that the model overpredicts the flume data as expected. Actually, efficiency is reduced when the fraction of sand F_s on the bed surface is small (J06 and J14). The effect of F_s is not very surprising since Eq. 60 considers the transportation of the finer fractions in an implicit manner, as a function of the mobility of the coarser fraction. This assumes that this finer fraction is present at the bed surface, which was not the case for runs J06 and J14 and Figure 47a illustrates a case of supply limitation.
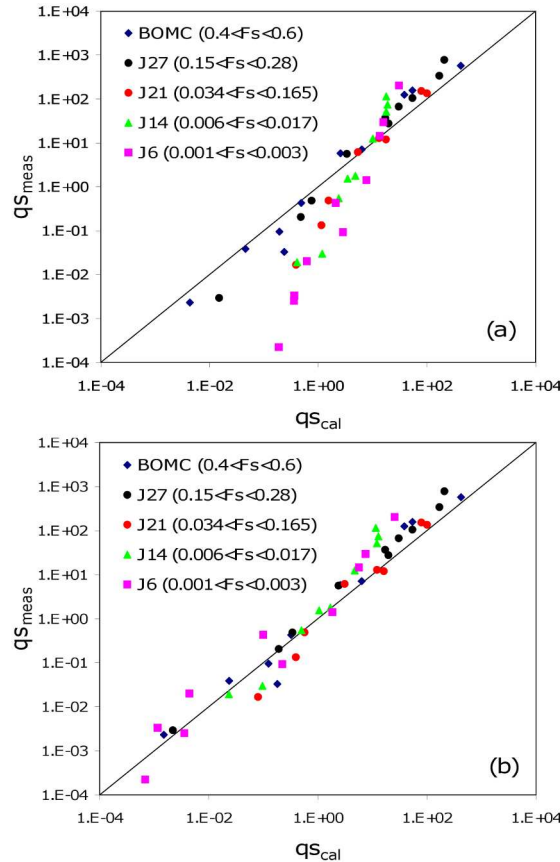
Figure 47: Comparison between the flume measurements of Wilcock et al. (2001) and bedload computed with (a) Eq. 60-62 (b) with Eq.64

The model was adapted for these situations by introducing a coefficient ζ which converges to 1 when the sand fraction F_s converges to 1 or when the transport is important (Recking, sub.); it gives:

$$\Phi(\tau^*, F_s) = \zeta(\tau^*, F_s)\Phi(\tau^*) \tag{63}$$

Where $\Phi(\tau^*)$ is given by Eq.60 and

$$\zeta(\tau^*, F_s) = \left[1 + (0.15\sqrt{\frac{\tau_c^*}{\tau^*}} - 0.12)\ln(F_s)\right]^{10} \qquad \text{for } \tau^*/\tau_c^* < 1.5 \tag{64}$$

$$\zeta(\tau^*, F_s) = 1 \qquad \text{for } \tau^*/\tau_c^* > 1.5$$

Where τ_c^* is the threshold Shields stress for mobility of D_{84} (given by Eq.40).This function fits the flume data well for each run (Figure 47b). It calculates the bulk bedload transport and performs as well as the fractional equation proposed by Wilcock and Crowe (2003); like this equation, it under-predicts the field measurements (Figure 48).
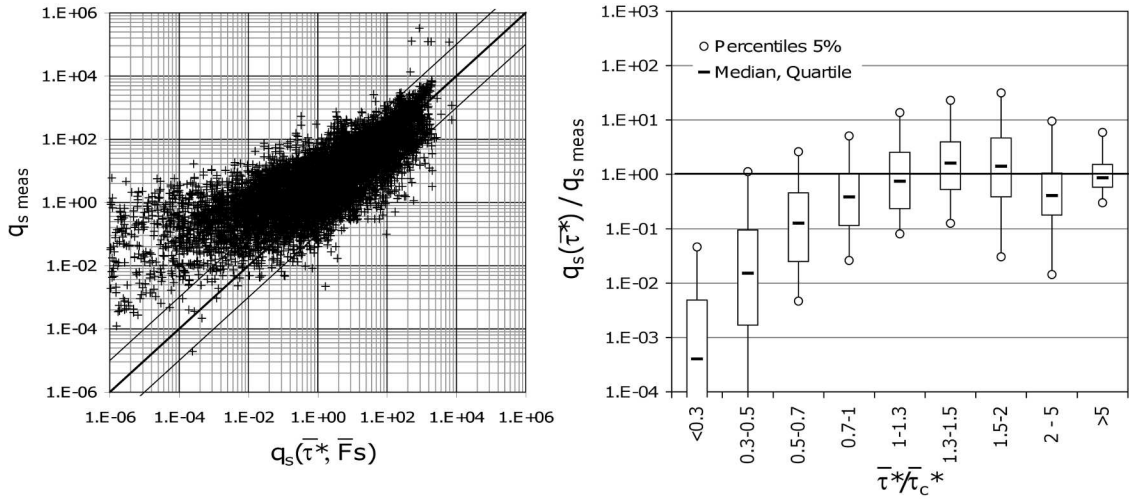
Figure 48 : Comparison between Eq.63 and the field data

4.3.3. Linking the flume and the field, surface and subsurface

Surprisingly, supply limitations observed in the flume (and described above) were not observed with the field data sets, and in many circumstances the sand fraction is abundant in bedload transport despite it is almost absent at the bed surface. The commonly accepted explanation is that fine sediments are supplied by the bed subsurface, considering that in gravel bed rivers the grain size distribution of the transported sediment is usually very similar to the subsurface grain size distribution (Parker et al., 1982). However, sand supply by the bed subsurface supposes that the surface pavement is destroyed, or at least destabilized by the flow. This is an unexpected issue for most of the flows considered in the data sets, usually

associated with a very low shear stress (with $\tau_{84}{}^* / \tau_{c84}{}^* \ll 1$ for many runs). Actually the variance in shear stress across the section could explain local subsurface sediments delivery as discussed hereafter with a Monte-Carlo approach (Recking, sub.).

Hypothesizing that the equations (Eqs.63 and 64) adequately reproduce local transport, one can artificially reproduce bedload samples affected by variations in flow and bed characteristics. In the following, each parameter P designates the local value and its width-averaged value is written $\overline{P} = \frac{1}{W} \int_{y=0}^{W} P \, dy$. The Monte-Carlo approach consists, for each mean input parameters ($\overline{F}_s, \overline{D}_{84}, \overline{\tau}$), in performing a large number of random draws in their probability distributions for constructing several sets of (F_s, D_{84}, τ). In a second step, the associated Shields stress τ^* and solid discharge $q_s(\tau^*, F_s)$ were computed for each run. Long series (N>5000 values) were constructed in order to ensure a stable solution for the computed bedload probability distribution. Finally, the simulated bedload samples $q_s(\tau^*, F_s)$ were averaged and the result $\overline{q_s(\tau^*, F_s)} = \frac{1}{N} \sum_N q_s(\tau^*, F_s)$ was compared to the transport rate calculated with the mean input data $q_s(\overline{\tau}^*, \overline{F}_s)$.

The variance in shear stress was represented with a dissymmetric gamma probability function (Paola, 1996; Nicholas, 2000; Bertoldi et al., 2009):

$$p(\tau) = \frac{\alpha^{\alpha} \hat{\tau}^{\alpha-1} e^{-\alpha\hat{\tau}}}{\overline{\tau} \Gamma(\alpha)}$$

(65)

Where $\hat{\tau} = \tau / \overline{\tau}$, $\overline{\tau}$ is the average bed shear stress, and α is a parameter describing the width of the distribution. The lower its value, the larger the variance in τ. A value $\alpha=1$ was found to be a limiting value for highly irregular sections (Paola, 1996; Nicholas, 2000) in braided streams. Larger values would be representative for single tread irregular channels, and α tends to infinity for a rectangular section. A comparison with the field data set allowed to describe α with the following function (Figure 49):

$$\alpha = 5 \frac{\overline{\tau}^*}{\overline{\tau}_c^*}$$

(66)

Where $\overline{\tau}^*$ and $\overline{\tau}_c^*$ are calculated for $\overline{D}_{84}$. Variation of the parameter α with the flow strength was an expected result (Nicholas, 2000), and this function gives values in the range $5<\alpha<10$ which are consistent with other results for single tread channels (Tunnicliffe et al., 2012). Hypotheses on the variance of other parameters ($\overline{F}_s, \overline{D}_{84}$) are discussed in Recking (sub.).
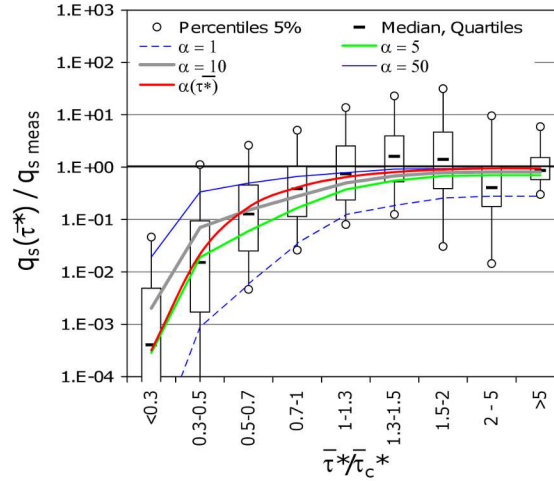
Figure 49 : Comparison between the Monte Carlo approach used with Eq.63-65 and several shape parameter α and the field bedload measurements

Results shows that the under-prediction is greater for low transport stages and decreases with increasing shear stress, as *Ferguson* [2003] also concluded. This can be explained by a reduced variance in the shear stress when the flow increases, because depth variations with the local bed topography may become relatively negligible with regard to the mean flow depth (this is particularly true for moveable beds becoming flatter with increasing transport stage).

Equations 65 and 66 were used for computing the distribution of the local transport stage τ/τ_c, for different values of the mean transport stage $\bar{\tau}/\bar{\tau}_c$. The results indicate that for $\bar{\tau}/\bar{\tau}_c$ ratios as low as 0.3, the shear stress may locally be higher than the critical shear stress for mobility of the bed surface ($\tau/\tau_c > 1$). This means that local armour break-up can always exist to some degree, exposing the subsurface material to the flow. This is consistent with the observation that even in the presence of a coarse armour, with a zero sand fraction at the bed surface (Fs = 0), the bedload GSD is always much finer than the surface GSD and equivalent to the subsurface GSD. This was, for instance, the case for several of the Idaho streams [*King, et al.*, 2004], for which bedload was measured for very low transport stages. However, the bedload material may also include upstream sediment supply that is not accounted for in the current analysis. Consequently, the sand fraction measured at the bed surface at rest could be an incorrect indicator of sediment availability for bedload computation.

5. OUTLOOK

Several developments are still needed to confirm the methods presented in this manuscript. It includes additional theoretical developments of the equations and their relations with the bed morphologies, flume and field experiments on mechanisms governing the sediment mobility, an analysis of uncertainties and variance in flow and bed parameters, with new field measurements obtained with highly reliable techniques.

5.1. Linking bedload transport and channel morphodynamics

Sediment transport is only a means to an end but not the final objective of my research, which is linking processes of sediment transport, channel morphodynamics and connectivity at the drainage basin scale (Liebault and Piegay, 2001; Piégay et al., 2008).

A first step would concern the derivation of a fractional version of Eq.60. Indeed, knowing the size of the transported particles is of primary importance for understanding the river morphodynamics and for modeling aspects (Ferguson and Church, 2009). One difficulty of the fractional approach is that the results are closely dependent on the grain size distribution used for computation. Unfortunately, sediments at the bed surface are usually dispatched into distinct patches of similar grain size and sorting, which interact in very complex manners (Buffington and Montgomery, 1999b; Laronne et al., 2001; Dietrich et al., 2006; Recking et al., 2009b; Nelson et al., 2010) and the variance associated with the smaller sizes can be very high, spatially and temporally (Laronne et al., 2001). In some circumstances the sand fraction can even be absent at the bed surface whereas it is abundant in bedload transport, as discussed above. On the other hand, the new bulk equation (Eq.60), which considers the transport of finer fractions in an implicit manner, as a function of the mobility of diameters D_{84}, is very robust. This is why instead of calculating directly the transport for each class as usually done, with large uncertainties on the grain size curve, and to compute the bulk transport by summing the results obtained for each class, the inverse could be done. The results of the bulk calculation (with Eq.60) could serve as a basis for the calculation, and be degraded into a series of individual transports corresponding to each grain size. The quality of the results would be closely dependent on the quality of the data used to derive the function $\tau_{mi}^{*} = \Psi(\tau_{m}^{*}, D_i, \text{Slope}\ldots)$ for each size class. A better understanding of τ_m^* implies a better understanding of mechanisms acting on bed clustering and the transition between partial and full transport.

The bedload equation also needs to be adapted to specific environments. For instance, the slope exponent in τ_m* was introduced to reduce bedload transport rates on steep slopes, for given shear stress and grain size distribution, as a consequence of supply limitation of fine materials when the bed develops lag formations such as stone clusters, pavements, and step-pools, whose effects are increased on steep slopes (Pitlick et al., 2008). Such a correction is statistically representative only when considering a continuity of the river reach as part of a whole system progressively evolving in grain size distribution and grain arrangement in the streamwise direction, a given reach being supplied by the bed sediment of the upstream reach. However, it was shown in a recent publication (Recking, 2012) that the correction is not representative anymore for the low-order mountain streams where lateral inputs become an additional independent parameter (depending on the connexion to the sediment source), and the slope exponent must be adapted in Eq.61.

Figure 50 : Braiding river in flume experiment (Pauline Leduc phD thesis)

Similar analysis is required for various flow environments, including the effects of vegetation on flow resistance, bedload transport and associated morphodynamics (Piegay et al., 2004). For instance using the bedload equation (Eq.60) with flow and sediment data averaged over the total section would certainly lead to large underprediction in braiding rivers (Figure 50), because of the large variance in shear stress (§4.3.3). Adapting the equation

would certainly necessitate a new formulation for τ_m* (transition between partial transport and full mobility) as a function not only of the slope and grain size distribution, but also as a function of additional morphometric parameters (Piégay et al., 2009) such as the braiding index of the river. The relations between bedload transport and morphodynamics has been investigated in flume experiments (Metivier and Meunier, 2003), but new technologies, such as RFID (passive transponders, Figure 51) can also help to better understand sediment mobility in the field (Reid et al., 2007; Liebault et al., 2012).
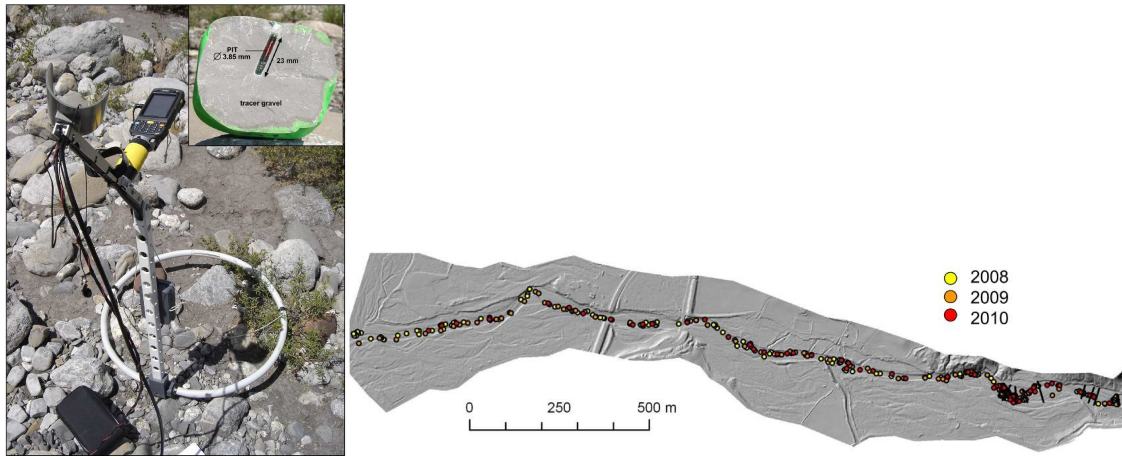
Figure 51 : (a) Passive transponder inserted in a cobble, and the antenna used for detection (photo Liénault) (b) RFID migration from their injection point, from 2008 to 2010.

More generally, the flow and transport equations may serve to develop morphological tools (Metivier and Barrier, 2010; Pitlick et al., sub.), and to implement morphodynamics numerical models (Paquier and Khodashenas, 2002; Lane et al., 2009; Leduc, 2010; Raven et al., 2011).

5.2. Grain scale study of sediment mobility

A better understanding of mechanisms governing the sediments mobility is also crucial. Indeed, the adequacy of the proposed bedload equations (Eq.60) depends on the value $\tau*_m$, for which bed clusters are assumed to disappear. Equation 61 was obtained by interception between a field-derived function for low transport (by similarity collapse of a large field data set from Idaho rivers) and a flume-derived function for full mobility (Recking et al., 2008). Compared to Eq.40, it gives a ratio of $\tau*_m / \tau*_{c84} \approx$ 1.5-2.0 for slopes within the range (0.005-0.01). These values are consistent with Wilcock and McArdell (1997), who concluded (for similar slopes) that mobilisation of grain size in a size fraction increases from

10 to 90% over a range of $\tau*$ by a factor of 2. This is also consistent with Church and Hassan (1998) who observed that stone cells start to develop when the Shields stress is lower than twice the critical Shields stress for the bed armour, and to Strom et al. (2004) who observed with glass particles that clusters disappear when the shear stress is higher than $2\tau_c*$. More generally, Rickenmann (2001) reported that values in the $2\text{-}5\tau_c*$ range were reported for the transition to full mobility in the literature: this range corresponds to what is obtained with the $\tau*_m / \tau*_{c84}$ ratio when the exponent describing supply limitation is varied for taking into account sediment supply conditions (Recking, 2012).

More generally, a grain scale study of mechanisms governing bedload transport is of first importance (Lajeunesse et al., 2009). It concerns the effects of grain sorting, and more particularly the role of the finer fractions of the grain size distribution, which plays an important role in bedload transport not only because it permits non-threshold transport, with a progressive supply when the discharge is progressively increased from zero to bankfull, but also because it increases the transport efficiency of the coarser fractions. These effects concern the initiation of motion and transport. In low-flow conditions, fine sediments increase bed instability by allowing destabilisation of boulders by scouring effects (Rosport and Dittrich, 1995; Church and Zimmerman, 2007; Curran, 2007, 2012; Recking et al., 2012b). As a consequence, vertical sorting is less effective and fine sediments of the subsurface are more easily released. For higher flows, when the transport is effective, several experiments have demonstrated that the transport efficiency of the coarser fraction was increased when used in a mixture with a finer faction (Gilbert, 1914; Iseya and Ikeda, 1987; Curran and Wilcock, 2005; Recking et al., 2009b). This was attributed to smoother bed surfaces produced when fine sediments filled interstices between coarser sediments (Gilbert, 1914). Grain sorting and its effects on sediment mobility can be studied in flume experiments (Recking et al., 2009b; Bacchi, 2011). However, as discussed in this report, reproducing the full complexity of field bedload transport necessitate to work with appropriate grain size distributions and to adapt the measurement techniques. Image analysis can provide useful tools for a grain scale approach (Frey et al., 2003).

5.3. Variance and uncertainties

The variance in shear stress was discussed in § 4.3.3 and additional research is needed to better define the probability distribution functions, more especially for irregular sections such as in braiding rivers. Similar research is needed for all other parameters such as the bed surface grain size distribution which can vary with morphological units such as riffle, pools,

bars (Buffington and Montgomery, 1999a; Bunte and Abt, 2001) and other external factors, such as the hydraulic roughness (Buffington and Montgomery, 1999c). The variance of coarse sediments present in a given reach has been poorly documented. On the basis of multi pebble counts (Wolman, 1954) involving 2500-4700 particles on three reaches of the Williams Fork river (CO, USA), Segura et al. (2010) concluded that the variance in D_{50} was very small (<10%) for the study reaches in question. To the best of my knowledge, no extensive field studies have described similar results for D_{84}, but variance in D_{84} is usually considered lower than for smaller diameters (Bunte and Abt, 2001).

But in addition to the variance, uncertainties attached to the input averaged data need to be better evaluated; these uncertainties may be particularly important when the flow strength used for computation differs notably from the conditions that prevailed (usually low flow) when these input data were collected:

(i)   The grain size distribution is usually poorly defined, and the procedures used for sampling the surface can also considerably impact the results of bedload computation (Bunte and Abt 2001). Changes in grain size distribution with increasing flow strength could also affect the results, despite available measurements suggesting that the value of D_{84} measured at low flows may be persistent during flooding (Wilcock and DeTemple, 2005; Clayton and Pitlick, 2008).

(ii)   Only the average bed slope of the river reach is usually measured, whereas the energy slope could be different, especially for high flows (Smart, 1999).

(iii)   The active width (the part of the width that effectively participates to transport) is still difficult to estimate.

Improving the quality of the data also supposes to improve the measurement techniques, especially for ungauged basins (Laronne and Gray, 2007; Piégay et al., 2007; Villar et al., 2012). For instance, because of the small orifice of the standard Helley-Smith sampler, its use should be preferentially limited to sand bed rivers or at very-low-transport stages in gravel bed rivers. When possible, other techniques such as sediment traps should be developed, allowing a continuous measurement of the combined bedload and hydraulics values (Reid et al., 1996; Garcia et al., 2000; Laronne et al., 2002; Laronne and Gray, 2007). A sediment trap was recently installed to the Irstea's experimental catchment in Draix.

REFERENCES

Aberle, J., Smart, G.M., 2003. The influence of roughness structure on flow resistance on steep slopes. Journal of Hydraulic Research, 41(3): 259-269.

Abrahams, A.D., Gao, P., 2006. A bed-load transport model for rough turbulent open-channel flows on plane beds. Earth Surface Processes and Landforms, 31: 910-928.

Ackers, P., White, W.R., 1973. Sediment transport; new approach and analysis. Journal of the Hydraulics Division, 99(11): 2041-2060.

Aguirre-Pe, J., Fuentes, R., 1990. Resistance to flow in steep rough streams. Journal of Hydraulic Engineering, 116(11): 1374-1387.

Aksoy, S., 1973. The influence of relative depth on threshoàld of grain motion, IAHR, Bangkok, Thailand, pp. 359-370.

Andrews, E.D., 1983. Entrainment of gravel from naturally sorted riverbed material. Geological Society of America Bulletin, 94(10): 1225-1231.

Armanini, A., Gregoretti, C., 2005. Incipient sediment motion at high slopes in uniform flow condition. Water Resources Research, 41(W12431): 1-8.

Ashida, K., Bayazit, M., 1973. Initiation of motion and roughness of flows in steep channels, IAHR, proceedings of the 15th congress, Istambul, Turkey, pp. 475-484.

Ashworth, P.J., Ferguson, R., 1989. Size-selective entrainment of bed load in gravel bed streams. Water Resources Research, 25(4): 627-634.

Bacchi, V., 2011. Etude experimentale de la dynamique sedimentaire d'un systeme a forte pente soumis a des conditions hydrauliques faibles, Université Joseph fourier, Grenoble, 209 pp.

Bagnold, R.A., 1977. Bed load transport by natural rivers. Water Resources Research, 13(2): 303-312.

Bagnold, R.A., 1980. An empirical correlation of bedload transport rates in flumes and natural rivers. Proc. R. Soc. Lond., A372: 453-473.

Baiamonte, G., Ferro, V., 1997. The influence of roughness geometry and Shields parameter on flow resistance in gravel-bed channels. Earth Surface Processes and Landforms, 22: 759-772.

Barzilai, R., Laronne, J.B., Reid, I., 2012. Effects of changes in fine grained matrix on bedload sediment transport in a gravel-bed river. Earth Surface Processes and Landforms, DOI 10.1002/esp 3288

Bathurst, J.C., 1985. Flow resistance estimation in mountain rivers. Journal of Hydraulic Engineering, 111(4): 625-643.

Bathurst, J.C., 1987. Critical conditions for bed material movement in steep, boulder-bed streams, Erosion and Sedimentation in the Pacific Rim. AIHS Pub. N°165, Proceedings of the Corvallis Symposium, pp. 309-318.

Bathurst, J.C., 1988. Velocity profile in high-gradient, boulder-bed channels, IAHR, Proc Int. Conf. on Fluvial Hydraulics, Budapest, Hungary, pp. 29-34.

Bathurst, J.C., 2007. Effect of coarse surface layer on bed-load transport. Journal of Hydraulic Engineering (ASCE), 133(11): 1192-1205.

Bathurst, J.C., Li, R.-M., Simons, D.B., 1981. Resistance equation for large-scale roughness. Journal of the Hydraulics Division, 107(HY12): 1593-1613.

Bathurst, J.C., Graf, W.H., Cao, H.H., 1982. Initiation of sediment transport in steep channels with coarse bed material, Euromech 156: Mechanics of sediment transport, Istanbul, pp. 207-213.

Bayazit, M., 1976. Free surface flow in a channel of large relative roughness. Journal of Hydraulic Research, 14: 115-126.

Bergeron, N.E., Carbonneau, P., 1999. The effect of sediment concentration on bedload roughness. Hydrological Processes, 13: 2583-2589.

Bertoldi, W., Ashmore, P., Tubino, M., 2009. A method for estimating the mean bed load flux in braided rivers. Geomorphology, 103: 330-340.doi:10.1016/j.geomorph.2008.06.014.

Bettess, R., 1984. Initiation of sediment transport in gravel streams. Proc., Institute of the Civil Engineering, 77, Part 2, March: 79-88.

Bogardi, J., 1970. Sediment transportation in alluvial streams (International Post-Graduate Course on Hydrological methods for developping water resources management), Research Institute for Water Research Development / UNESCO, Budapest, Hungary, 133 pp.

Boussinesq, J., 1872. Theorie des ondes et des remous qui se propagent le long d'un canal rectangulaire horizontal. . Journal Mathematique Pure et Applique 2(17): 55-108.

Bridge, J.S., Jarvis, J., 1982. The dynamic of a river bend: a study in flow and sedimentary processes. Sedimentology, 29(2): 499-541.

Bridge, J.S., Bennett, S., 1992. A model for the entrainment and transport of sediment grains of mixed sizes, shapes and densities. Water Resources Research, 28(2): 337-363.

Brown, C.B., 1950. Sediment transportation., Engineering Hydraulics. H.Rouse, New York, Wiley, pp. 769-857.

Buffington, J.M., Montgomery, D.R., 1997. A systematic analysis of eight decades of incipient motion studies, with special reference to gravel-bedded rivers. Water Resources Research, 33(8): 1993-2027.

Buffington, J.M., Montgomery, D.R., 1999a. A procedure for classifying textural facies in gravel-bed rivers. Water Resources Research, 35(6): 1903.

Buffington, J.M., Montgomery, D.R., 1999b. Effects of sediment supply on surface textures of gravel-bed rivers. Water Resources Research, 35(11): 3523.

Buffington, J.M., Montgomery, D.R., 1999c. Effects of hydraulic roughness on surface textures of gravel-bed rivers. Water Resources Research, 35(11): 3507.

Buffington, J.M., Dietrich, W.E., Kirchner, J.W., 1992. Friction angle measurements on a naturally formed gravel streambed: implications for critical boundary shear stress. Water Resources Research, 28(2): 411-425.

Bunte, K., 1992. Particle number grain size composition of bedload in a mountain stream. In: P.Billi, R.D.H., CR Thorne & P. Tacconi (Editor), Dynamics of gravel bed rivers. John Wiley & Sons Ltd, Chichester, pp. 55-68.

Bunte, K., Abt, S.R., 2001. Sampling surface and subsurface particle-size distributions in Wadable and cobble bed streams for analyses in sediment transport, hydraulics and streambed monitoring, USDA Report RMRS-GTR-74, 450 pp.

Bunte, K., Abt, S.R., 2005. Effect of sampling time on measured gravel bed load transport rates in a coarse-bedded stream. Water Resources Research, 41(W11405): 12 pp.

Byrd, T.C., Furbish, D.J., 2000. Magnitude of deviatoric terms in vertically averaged flow equations. Earth Processes and Landforms, 25: 319-328.

Byrd, T.C., Furbish, D.J., Warburton, J., 2000. Estimating depth-averaged velocities in rough channels. Earth Surface Processes and Landforms, 25: 167-173.

Calomino, F., Gaudio, R., Miglio, A., 2004. Effect of Bed-Load Concentration on Friction Factor in Narrow Channels, River Flow. IAHR, Napple, Italy, pp. 279-285.

Camenen, B., Holubova, K., Lukac, M., Le Coz, J., A., P., 2011. Assessment of methods used in 1D models for computing bedload transport in a large river: the Danube River in Slovakia. Journal of Hydraulic Engineering, 137(10): 1190-1199.

Campbell, L. et al., 2005. Bed-Load Effects on Hydrodynamics of Rough-Bed Open-Channel Flows. Journal of Hydraulic Engineering, 131(7): 576-585.

Carbonneau, P., Bergeron, N.E., 2000. The effect of bedload transport on mean and turbulent flow properties. Geomorphology, 35: 267-278.

Carling, P.A., 1983. Threshold of coarse sediment transport in broad and narrow natural streams. Earth Surface Processes and Landforms, 8: 1-18.

Carollo, F.G., Fero, V., Termini, D., 2005. Analyzing Turbulence Intensity in Gravel Bed Channels. Journal of Hydraulic Engineering, 131(12): 1050-1061.

Chepil, W.S., 1958. The use of evenly spaced hemispheres to evaluate aerodynamic forces on a soil surface. Eos Trans AGU, 39(3): 397-404.

Chiew, Y.M., Parker, G., 1994. Incipient sediment motion on non horizontal slopes. Journal of Hydraulic Research, 32: 649-660.

Childers, D., 1999. Field Comparisons of six pressure-difference bedload samplers in high-energy flow, USGS report N°92-4068, 59 pp.

Christensen, B.A., 1971. Incipient motion on cohesionless channel banks, Sedimentation: symposium to honor Hans Albert einstein:1971.06.17-19, Berkeley, California, pp. Chapter 4, pp.1-22.

Church, M., 1978. Palaeohydrological reconstructions from a holocene valley fill. Fluvial Sedimentology, A.D. Mial, Mem. Can. Soc. Pet. Geol., 5: 743-772.

Church, M., Hassan, M.A., 1998. Stabilizing self-organized structures in gravel-bed stream channels: field and experimental observations. Water Resources Research, 34(11): 3169-3179.

Church, M., Zimmerman, A., 2007. Form and stability of step-pool channels: Research progress. Water Resources Research, 43(W03415): 1-21.

CIRIA/CUR/CETMEF, 2007. The Rock Manual. The use of Rock in hydraulic engineering (2nd Edition), C683, 1302 pp.

Clayton, A., Pitlick, J., 2008. persistence of the surface texture of a gravel-bed river during a large flood. Earth Surface Processes and Landforms, 33: 661-673.doi: 10.1002/esp.1567.

Coleman, N.L., 1967. A theoritical and experimental study of drag and lift forces acting on a sphere resting on a hypothetical streambed. In: IAHR (Editor), Proceedings of 12th IAHR Congress. 3, Madrid, pp. 185-192.

Comiti, F., Mao, L., Wilcox, A., Wohl, E., Lenzi, M., 2007. Field-derived relationships for flow velocity and resistance in high-gradient streams. Journal of Hydrology, 21(3)

Cudden, J.R., Hoey, T.B., 2003. The causes of bedload pulses in a gravel channel: the implications of bedload grain-size distribution. Earth Surface Processes and Landforms, 28: 1411-1428.

Curran, J.C., 2007. Step-pool formation models and associated step spacing. Earth Surface Processes and Landforms, 32: 1611-1627.doi: 10.1002/esp.1589.

Curran, J.C., 2012. Examining individual step stability within step-pool sequences, in Church, M., Biron, P. and Roy, A.G., editors, Gravel-bed Rivers 7: Processes, Tools, Environments. Chichester, Wiley-Blackwell. 378-385.

Curran, J.C., Wilcock, P.R., 2005. Effects of sand supply on transport rates in a gravel-bed channel. Journal of Hydraulic Engineering, 131(11): 961-967.

Day, T.J., 1977. Aspects of flow resistance in steep channels having coarse particle beds, Research in Fluvial Geomorphology: Proceedings of The 5th Guelph Symposium on Geomorphology, pp. 45-48.

Dey, S., 2003. Threshold of sediment motion on combined transverse and longitudinal sloping beds. Journal of Hydraulic Research, 41(4): 405-415.

Dietrich, A., Koll, K., 1997. Velocity field and resistance of flow over rough surfaces with large and small relative submergence. International Journal of Sediment Research, 12(3): 21-33.

Dietrich, W.E. et al., 2006. Sediment patches, sediment supply and channel morphology, In: River, Coastal and Estuarine: Morphodynamics,Parker, G., and Garcia, M. H. (Eds.), Taylor and Francis/Balkema, Lisse, The Netherlands, pp. 79-90.

Duan, J.G., Scott, S., 2007. Selective bedload transport in Las Vegas wash, a gravel-bed stream. Journal of Hydrology, 342: 320-330.

DuBoys, 1879. Le Rhône et les rivières à lit affouillable. Annales des Ponts et Chaussées, 18(5)

Einstein, H.A., 1950. The bed-load function for sediment transportation in open channel flows, United States Department of Agriculture - Soil Conservation Service, Washington, 71 pp.

Einstein, H.A., El-Samni, E.-S.A., 1949. Hydrodynamic forces on a rough wall. Reviews of modern physics, 21(3): 520-524.

Einstein, H.A., Barbarossa, N.L., 1952. River channel roughness. American Society of Civil Engineers, Paper N°2528: 1121-1146.

Emmett, W.W., 1980. A field calibration of the sediment-trapping characteristics of the Helley-Smith bedload sampler, USGS Report N°1139, 44 pp.

Engelund, F., Hansen, E., 1967. A monograph on sediment transport in alluvial streams, Technical University of Denmark, 62 pp.

Ergenzinger, P. et al., 1994. Short term temporal variations in bedload transport rates: Squaw Creek, Montana, USA and Nahal Yatir and Nahal Estemoa, Israel, Dynamics and Geomorphology of Mountain Rivers. Lecture Notes in Earth Sciences. Springer Berlin / Heidelberg, pp. 251-264.

Fenton, J., Abbott, J.E., 1977. Initial movement of grains in a stream bed: The effect of relative protrusion. Proc. Roy. Soc., Ser A, 352: 523-537.

Ferguson, R., 2007. Flow resistance equations for gravel and boulder bed streams. Water Resources Research, 43(W05427): 1-12.

Ferguson, R., 2012. River channel slope, flow resistance, and gravel entrainment thresholds. Water Resour. Res., 48(W05517): 1-13.

Ferguson, R., Church, M., 2009. A critical perspective on 1-D modeling of river processes: Gravel load and aggradation in lower Fraser River. Water Resour. Res., 45

Ferguson, R.I., 2003. The missing dimension: effects of lateral variation on 1-D calculations of fluvial bedload transport. Geomorphology, 56: 1-14.

Ferro, V., Baiamonte, G., 1994. Flow velocity profiles in gravel-bed rivers. Journal of Hydraulic Engineering, 120(1): 60-80.

Fienberg, K., Singh, A., Foufoula-Georgiou, E., Jerolmack, D.J., Marr, J., 2010. Theoretical Framework for Interpreting and Quantifying the Sampling Time Dependence of Gravel Bedload Transport Rates (http://pubs.usgs.gov/sir/2010/5091/papers/) 171-184 pp.

Franca, M., 2005. A field study of turbulent flows in shallow gravel-bed rivers, PhD thesis n° 3393, Ecole Polytechnique Fédérale de lausanne, 210 pp.

Frey, P., Church, M., 2011. Bedload: a granular phenomenon. Earth Surface Processes and Landforms, 36: 58-69.DOI: 10.1002/esp.2103.

Frey, P., Ducottet, C., Jay, J., 2003. Fluctuations of bed load solid discharge and grain size distribution on steep slopes with image analysis. Experiments in fluids, 35: 589-597.

Gao, P., Abrahams, A.D., 2004. Bedload transport resistance in rough open-channel flows. Earth Surface Processes and Landforms, 29: 423-435.

Garcia, C., Laronne, J.B., Sala, M., 2000. Continuous monitoring of bedload flux in a mountain gravel-bed river. Geomorphology, 34: 23-31.

Gaydou, P., 2012. Quelle méthodologie pour étudier les potentialités de restaurer la dynamique fluviale du Rhône?, IsRivers, Lyon, pp. " pp.

Gessler, J., 1971. Beginning and ceasing of incipient motion, River Mechanics, Chp7. Shen, H.W., Fort Collins, Collorado, USA.

Gilbert, G.K., 1914. The Transportation of Debris by Running Water, US Geological Survey, Washington Government Printing Office, 263 pp.

Gimenez-Curto, L.A., Cornerio, M.A., 2006. Comment on "Characteristic dimensions of the step-pool bed configuration: an experimental study" by Joanna C.Curran and Peter Wilcock. Water Resources Research, 42.doi:10.1029/2005WR004296.

Gomez, B., 1983. Temporal variations in bedload transport rates: the effects of progressive bed armouring. Earth Surface Processes and Landforms, 8: 41-54.

Gomez, B., Richard, L.N., Hubbell, D.W., 1989. Temporal variations in bedload transport rates associated with the migration of bedforms. Earth Surface Processes and Landforms, 14: 135-156.

Graf, W.H., Suszka, L., 1987. Sediment transport in steep channels. Journal of Hydrosciences and Hydraulic Engineering, 5(1): 11-26.

Gregoretti, C., 2000. The initiation of debris flow at high slopes: experimental results. Journal of Hydraulic Research, 38(2): 83-88.

Habersack, H., Nachtnebel, H.P., Laronne, J.B., 2001. The continuous measurement of bedload discharge in a large alpine gravel bed river. Journal of Hydraulic Research, 39(2): 125-133.

Hey, R.D., 1979. Flow resistance in gravel bed rivers. Journal of the Hydraulics Division (ASCE), 105(4): 365-379.

Hu, S., Abrahams, A.D., 2005. The effect of bed mobility on resistance to overland flow. Earth Surface Processes and Landforms, 30: 1461-1470.

Hubbell, D.W., Stevens, H.H., 1986. Factors affecting accuracy of bedload sampling, Proc, 4th Federal Interagency Sedimentation Conf., Subcomm. on Sedimentation, Interagency Advisory Commitee on Water Data, Las Vegas.

Ikeda, H., 1982. Incipient motion of sand particles on side slopes. Journal of the Hydraulics Division, 108(HY1): 95-114.

Inokuchi, M., Takayama, S., 1973. Incipient motion of pebbles on the bed of small streams, University of Tsukuba, Institute of Geoscience, Ibaraki, Japan, 157-169 pp.

Iseya, F., Ikeda, H., 1987. Pulsations in bedload transport rates induced by a longitudinal sediment sorting: a flume study using sand and gravel mixture. Geografiska Annaler, 69A(1): 15-27.

Jackson, W.L., Beschta, R.L., 1982. A model of two-phase bedload transport in an Oregon coast range stream. Earth Surface Processes and Landforms, 7: 517-527.

Jarrett, R.D., 1990. Hydrologic and Hydraulic Research in Mountain Rivers. Water Resour. Bull., 26: 419-429.

Johnson, J.W., 1942. The importance of side-wall friction in bed-load investigations. Civil Eng., 12(6): 329-331.

Karim, F., Kennedy, J.F., 1990. Menu of couple velocity and sediment discharge relations for rivers. Journal of Hydraulic Engineering, 116(8)

Katul, G., Wiberg, P., Albertson, J., Hornberger, G., 2002. A mixing layer theory for flow resistance in shallow streams. Water Resources Research, 38(11): 32-40.

Kellerhalls, R., 1970. Runoff routing through steep natural channels. ASCE Journal of the Hydraulics Division, 96: 2201-2217.

Kellerhalls, R., 1973. Hydraulic performance of mountain streams, IAHR, 15th Congress, Istanbul. Proceedings v.1, pp. 467-473.

Keulegan, G.B., 1938. Laws of turbulent flow in open channels. Journal of Research of the National Bureau of Standards, 21(Research Paper 1151): 707-741.

Komar, P.D., 1987. Selective entrainment by a current from a bed of mixed sizes: a reanalysis. Journal of Sedimentary Petrology, 57(6): 203-211.

Kuhnle, R.A., 1992. Fractional transport rates of bedload on Goodwin Creek. In: P.Billi, Hey, R.D., Thorne, C. and Tacconi, P. (Editors), Dynamics of gravel bed rivers. John Wiley & Sons, pp. 141-155.

Lajeunesse, E., Malverti, L., Charru, F., 2009. Bedload transport in turbulent flow at the grain scale: experiments and modeling. J. Geophys. Res., 115.F04001, doi:10.1029/2009JF001628. .

Lamb, M.P., Dietrich, W.E., Venditti, J.-G., 2008. Is the critical Shields stress for incipient sediment motion dependent on channel-bed slope? J. Geophys. Res., 113(F02008, doi:10.1029/2007JF000831)

Lane, S.L., Tayefi, V., Reid, S.C., Yu, D., Hardy, R.J., 2009. The spatial and temporal patterns of aggradation in a temperate , upland, gravel-bed river. Earth Surface Processes and Landforms, 34: 1181-1197.

Lanzoni, S., 2000. Experiments on bar formation in a straight flume 2. Graded sediment. Water Resources Research, 36(11): 3351.

Laronne, J., Lekach, J., Cohen, H., Alexandrov, Y., 2002. Experimental Drainage Basins in Israel: Rainfall, Runoff, Suspended Sediment and Bedload Monitoring. In: in Renard, K.G., McElroy, S.A., Gburek, W.J., Canfield, H.A., and Scott, R.L. (eds.): First Interagency Conference on Research in the Watersheds, Benson, AZ., 753pp. (Editor), pp. 168-172.

Laronne, J.B., Reid, l., 1993. Very high rates of bedload sediment transport by ephemeral desert rivers. Nature, 366(6451): 148-150.

Laronne, J.B., Gray, J.R., 2007. Formation of a Bedload Research International Coorerative, BRIC Context Document (http://www.nced.umn.edu/BRICPortal.html), pp. 7.

Laronne, J.B., garcia, C., reid, I., 2001. Mobility of patch sediment in gravel bed streams: patch character and its implications for bedload, Gravel Bed Rivers V, pp. 249-290.

Lawrence, D.S.L., 1997. Macroscale surface roughness and frictional resistance in overland flow. Earth Surface Processes and Landforms, 22: 365-382.

Leduc, P., 2010. Etude hydro-sédimentaire des rivières en tresses: modélisation numérique du Bès, Master2 Sciences de la Terre et de l'Environnement, UJF Grenoble, 59 pp.

Lenzi, M.A., Mao, L., Comiti, F., 2006. When does bed load transport begin in steep boulder - bed streams? Hydrological Processes, 20: 3517-3533.

Liebault, F., Piegay, H., 2001. Assesment of channel changes due to long term bedload supply decrease, Roubion river, France. Geomorphology, 36: 167-186.

Liebault, F., Laronne, J.B., 2008. Evaluation of bedload yield in gravel-bed rivers using scour chains and painted tracers: the case of the Esconavette Torrent (Southern French Prealps). Geodinamica Acta, 21(1-2): 23-34.

Liebault, F., Bellot, H., Chapuis, M., Klotz, S., Deschates, M., 2012. Bedload tracing in a high sediment load moutain stream. Earth Surface Processes and Landforms, 37: 385-399.

Lisle, T.E., 1995. Particle size variations between bed load and bed material in natural gravel bed channels. Water Resources Research, 31(4): 1107-1118.

Luque, R.F., Van Beek, R., 1976. Erosion and transport of bed-load sediment. Journal of Hydraulic Research, 14(2): 127-144.

Madej, M.A., Ozaki, V., 1996. Channel response to sediment wave propagation and movement, Redwood Creek, california, USA. Earth Surface Processes and Landforms, 21: 911-927.

Mahdavi, A., Omid, M., 2004. The effect of bed roughness on velocity profile in open channels. In: IAHR (Editor), River Flow Conference, Napple, Italy, pp. 295-300.

Manes, C., Pokrajac, D., McEwan, I., 2007. Double-averaged open-channel flows with small relative submergence. Journal of Hydraulic Engineering-Asce, 133(8): 896-904.

Marchand, J.P., Jarret, R.D., Jones, L.L., 1984. Velocity profile, water-surface slope, and bed material size for selected streams in colorado, Open file report, N°84-773, US Geological Survey, 82 pp.

Metivier, F., Meunier, P., 2003. Input and output mass flux correlations in an experimental braided stream. Implications on the dynamics of bed load transport. Journal of Hydrology, 271(1-4): 22-38.

Metivier, F., Barrier, L., 2010. Alluvial landscape evolution: what do we know about metamorphosis of gravel bed meandering and braided streams. Actes de GBR7

Meyer-Peter, E., Mueller, R., 1948. Formulas for bed-load transport, Procedings 2d Meeting IAHR, Stockholm, pp. 39-64.

Miller, M.C., McCave, I.N., Komar, P.D., 1977. Threshold of sediment motion under unidirectional currents. Sedimentology, 24: 507-527.

Mizuyama, T., 1977. Bedload transport in steep channels, PhD thesis Dissertation, Kyoto University, Kyoto, 118 pp.

Mueller, E.R., Pitlick, J., Nelson, J.M., 2005. Variation in the reference Shields stress for bed load transport in gravel-bed streams and rivers. Water Resources Research, 41: W04006 (1-10).

Nakagawa, H., Tsujimoto, T., Shimizu, Y., 1988. Velocity profile of flow overrough permeable bed, 6th Congress Asian and Pacific Regional Division of IAHR (1988.06.20-22), Kyoto, Japan, pp. 449-456.

Nelson, P.A., Dietrich, W.E., Venditti, J.G., 2010. Bed topography and the development of forced surface patches. Journal of Geophysical Research –Earth Surface, 115, F04024

Nicholas, A.P., 2000. Modelling bedload yield in braided gravel bed rivers. Geomorphology, 36: 89-106.

Nikora, V.I., Goring, D., McEwan, I., Griffiths, G., 2001. Spatially averaged open-channel flow over rough bed. Journal of Hydraulic Engineering, 127(2): 123-133.

Nikora, V.I., Koll, K., McEwan, I., McLean, D.G., Dittrich, A., 2004. Velocity distribution in the roughness layer of rough-bed flows. Journal of Hydraulic Engineering, 130(10): 1036-1042.

Nikuradse, J., 1933. Strömungsgesetze in rauhen Rohren (Laws of Flow in Rough Pipes). Forschungsheft Verein Deutscher Ingenieure N°361

Nowell, A.R., Church, M., 1979. Turbulent flow in a depth-limited boundary layer. Journal of Geophysical research, 84(C8): 4816-4824.

noWiberg, P.L., Smith, J.D., 1991. Velocity distribution and bed roughness in high-gradient streams. Water Resources Research, 27(5): 825-838.

O'Loughlin, E.M., Annambhotla, V.S.S., 1969. Flow phenomena near rough boundaries. Journal of Hydraulic Research, 7(2): 231-250.

Omid, M., Mahdavi, A., Narayanan, R., 2003. Effects of bedload transport on flow resistance in rigid boundary channels, IAHR, Tessalonic, pp. 641-646.

Paige, A.D., Hickin, E.J., 2000. Annual bed-elevation regime in the alluvial channel of Squamish River, Southern British Columbia, Canada. Earth Surface Processes and Landforms, 25: 991-1009.

Paintal, A.S., 1971. Concept of Critical Shear Stress in Loose Boundary Open Channels. Journal of Hydraulic Research, 1: 90-113.

Paola, C., 1996. Incoherent structures: turbulence as a metaphor for stream braiding. Coherent Flow Structures in Open Channel Flows. In Ashworth, P.J., Bennet, S.J., Best, J.L., McLelland, S.J. (Eds), John Wiley and sons, 706-723 pp.

Papanicolaou, A.N., Dermisis, D.C., Elhakeem, M., 2011. Investigating the Role of Clasts on the Movement of Sand in Gravel Bed Rivers. Journal of Hydraulic Engineering, 137(9): 871-883.ISSN: 0733-9429.

Paquier, A., Khodashenas, S.R., 2002. River bed deformation calculated from boundary shear stress. Journal of Hydraulic Research, 40(5): 603-609.

Parker, G., 1978. Self-formed straight rivers with equilibrium bank and mobile bed. Part 2 : the gravel river. Journal of Fluid mechanics, 89(1): 127-146.

Parker, G., 1979. Hydraulic geometry of active gravel rivers. Journal of Hydraulic Engineering (ASCE), 105(9): 1185-1201.

Parker, G., 1990. Surface-based bedload transport relation for gravel rivers. Journal of Hydraulic Research, 28(4): 417-428.

Parker, G., Klingeman, P.C., 1982. On why gravel bed streams are paved. Water Resources Research, 18(5): 1409-1423.

Parker, G., Klingeman, P.C., McLean, D.G., 1982. Bedload and size distribution in paved gravel-bed streams. Journal of the Hydraulics Division (ASCE), 108(HY4): 544-571.

Parker, G., Seminara, G., Solari, L., 2003. Bed load at low Shields stress on arbitrarily sloping beds: Alternative entrainment formulation. Water Resources Research, 39(7): 1183.

Parker, G., Wilcock, P.R., Paola, C., Dietrich, W.E., Pitlick, J., 2007. Physical basis for quasi-universal relations describing bankfull hydraulic geometry of single-thread gravel bed rivers. J. Geophys. Res., 112(F4): F04005.

Patnaik, P.C., Vittal, N., Pande, P.K., 1994. lift coefficient of stationary sphere in gradient flow. Journal of Hydraulic Research, 32(3): 471480.

Peirson, W.L., Cameron, S., 2006. Design of Rock Protection to Prevent Erosion by Water Flows Down steep Slopes. Journal of Hydraulic Engineering, 132(10): 1110-1114.

Petit, F., 1994. Dimensionless critical shear stress evaluation from flume experiments using different gravel beds. Earth Surface Processes and Landforms, 19: 565-576.

Piegay, H. et al., 2004. Contemporary changes in sediment yield in an alpine mountain basin due to afforestation (the upper Drôme in France). Catena (Elsevier), 55: 183-212.

Piégay, H., H., H., M., R., 2007. Field monitoring of bedload transport and particle entrainment : calibration efforts and new developments. Geodinamica Acta.

Piégay, H., Alber, A., Slater, L., Bourdin, L., 2009. Census and typology of the braided rivers in the French Alps Aquatic Sciences, 71(3): 371-388.

Piégay, H., Hupp, C.R., Citterio, A., Moulin, B., Walling, D.E., 2008. Spatial and temporal variability in sedimentation rates associated with cutoff channel infill deposits: Ain River, France. Water Resour. Res., 44(W05420).doi: 10.1029/2006WR005260 (IF: 2.154).

Pitlick, J., 1992. Flow resistance under conditions of intense gravel transport. Water Resources Research, 28(3): 891-903.

Pitlick, J., Van Steeter, M., 1998. Geomorphology and endangered fish habitats of the upper Colorado River. 2 Linking sediment transport to habitat maintenance. Water Resour. Res., 34(2): 303-316.

Pitlick, J., Marr, J., Pizzuto, J., sub. Width adjustment in experimental gravel-bed channels caused by overbank flows. J. Geophys. Res.

Pitlick, J., Mueller, E.R., Segura, C., Cress, R., Torizzo, M., 2008. Relation between flow, surface layer armoring and sediment transport in gravel bed rivers. Earth Surface Processes and Landforms, DOI:10.1002/esp.1607: 18.

Raven, E., ferguson, R., Lane, S.L., 2011. A coupled sediment routing and lateral migration model for gravel bed rivers. Hydrological processes, 25: 1887-1898.

Recking, A., 2006. An Experimental Study of Grain Sorting Effects on Bedload, PhD Thesis Cemagref (http://cemadoc.cemagref.fr/), Lyon, 261 pp.

Recking, A., 2007. Variation du nombre de Shields critique avec la pente, SHF, Lyon.

Recking, A., 2009. Theoretical development on the effects of changing flow hydraulics on incipient bedload motion. Water Resources Research, 45, W04401: 16.doi:10.1029/2008WR006826.

Recking, A., 2010. A comparison between flume and field bedload transport data and consequences for surface based bedload transport prediction. Water Resources Research, 46: 1-16.doi:10.1029/2009WR008007.

Recking, A., 2012. Influence of sediment supply on mountain streams bedload transport rates. Geomorphology: 12 p.doi: 10.1016/j.geomorph.2012.07.005.

Recking, A., in press. A simple method for calculating reach-averaged bedload transport. Journal of Hydraulic Engineering, doi: 10.1061/(ASCE)HY.1943-7900.0000653

Recking, A., sub. An analysis of non-linearity effects on bedload prediction. Journal of Geophysical Research - Earth Surface

Recking, A., Pitlick, J., in Press. Shields versus Isbach. Journal of Hydraulic Engineering

Recking, A., Bacchi, V., Naaim, M., Frey, P., 2009a. Antidunes on steep slopes. Journal of Geophysical Research, Earth Surface, F04025, doi:10.1029/2008JF001216: 1-11.doi:10.1029/2008JF001216.

Recking, A., Frey, P., Paquier, A., Belleudy, P., 2009b. An experimental investigation of mechanisms responsible for bedload sheet production and migration. J. Geophys. Res., 114, F03010,.doi:10.1029/2008JF000990.

Recking, A., Liébault, F., Peteuil, C., Jolimet, T., 2012a. Testing several bed load transport equations with consideration of time scales. Earth Surface Processes and Landforms.doi: 10.102/esp.3213.

Recking, A., Leduc, P., Liébault, F., Church, M., 2012b. A field investigation of the influence of sediment supply on step-pool morphology and stability. Geomorphology, 139-140: 53-66.doi:10.1016/j.geomorph.2011.09.024.

Recking, A., Frey, P., Paquier, A., Belleudy, P., Champagne, J.Y., 2008. Feedback between bed load and flow resistance in gravel and cobble bed rivers. Water Resources Research, 44: 21.doi:10.1029/2007WR006219.

Reid, I., Laronne, J.B., 1995. bedload sediment transport in an ephemeral stream and a comparison with seasonal and perennial counterparts. Water Resour. Res., 31(3): 773-781.

Reid, I., Frostick, L.E., Brayshaw, A.C., 1985. The incidence and nature of bedload transport during flood flows in coarse-grained alluvial channels. Earth Surface Processes and Landforms, 10: 33-44.

Reid, I., Powell, M., Laronne, J.B., 1996. Prediction of bed load transport by desert flash floods. Journal of Hydraulic Engineering ASCE, 122(3): 170-173.

Reid, S.C., Lane, S.N., Berney, J.M., Holden, J., 2007. The timing and magnitude of coarse sediment transport events within an upland, temperate gravel-bed river. Geomorphology, 83(1-2): 152-182.

Rickenmann, D., 1990. Bedload transport capacity of slurry flows at steep slopes, Der Versuchsanstalt fuer Wasserbau, Hydrologie und Glaziologie, der Eidgenössischen Technischen Hochschule Zürich, 249 pp.

Rickenmann, D., 1991. Hyperconcentrated flow and sediment transport at steep slopes. Journal of Hydraulic Engineering (ASCE), 117(11): 1419-1439.

Rickenmann, D., 1994. An alternative equation for the mean velocity in gravel-bed rivers and mountain torrents, In GV Cotroneo & R.R. Rumer (Eds), Proceedings ASCE, National Conference on Hydraulic Engineering, Buffalo, NY USA, pp. 672-676.

Rickenmann, D., 2001. Comparison of bed load transport in torrents and gravel bed streams. Water Resources Research, 37(12): 3295.

Rickenmann, D., Recking, A., 2011. Evaluation of flow resistance in gravel-bed rivers through a large field dataset. Water Resources Research, 47: 1-23.doi: 10.1029/2010WR009793.

Robert, A., 1991. Boundary roughness in coarse-grained channels. Progress in physical geography, 14: 42-70.

Rosport, M., Dittrich, A., 1995. step-pool formation and stability - A flume study. In: CVJ Varma, A.R. (Editor), Sixth International Symposium on River Sedimentation, New Dehli, India, pp. 525-532.

Ryan, S., Porth, L., 1999. A field comparison of three pressure-difference bedload samplers. Geomorphology, 30: 307-322.

Ryan, S.E., Porth, L.S., Troendle, C.A., 2002. Defining phases of bedload transport using piecewise regression. Earth Surface Processes and Landforms, 27: 971-990.

Ryan, S.E., Porth, L., Troendle, C., 2005. Coarse sediment transport in mountain streams in Colorado and Wyoming, USA. Earth Surface Processes and Landforms, 30: 269-288.

Saad, M.B.E.A., 1989. Critical shear stress of armour coat. In: ASCE (Editor), Sediment Transport Modelling. ASCE, New Orleans, USA, pp. 308-313.

Saldi-Caromile, K., Bates, K., Skidmore, P., Barenti, J., Pineo, D., 2004. Stream Habitat Restoration Guidelines: Final Draft. Co-published by the Washington Departments of Fish and Wildlife and Ecology and the U.S. Fish and Wildlife Service. Olympia, Washington, 715 pp.

Schmitt, L., Trémolières, M., C., N., E., D., Pfarr, U., 2012. 30 years of restoration works on the two sides of teh Upper Rhine River: feddback and future challenges, IsRiver, Lyon, pp. 3 pp.

Schoklitsch, A., 1962. Handbuch des Wasserbaus (in German), Springer Verlag (3rd edition), Wien.

Segura, C., McCutchan, J.H., Lewis, W.M., Pitlick, J., 2010. The influence of channel bed disturbance on algal biomassin a Colorado muntain stream. Ecohydrology: 11.DOI:10.1002/eco.142.

Seminara, G., Solari, L., Parker, G., 2002. Bedload at low shield stress on arbitrarily sloping bed Part1 : Failure of the Bagnold hypothesis. Water Resources Research, 38(11): 31.1-31.16.

Shields, A., 1936. Anwendung der Aehnlichkeitsmechanik und der Turbulenzforschung auf die Geschiebebewegung, Mitteilungen der Preussischen Versuchsanstalt fur Wasserbau und Schiffbau, Berlin, Heft 26, English Translation by WP Ott and JC Van Uchelen, USDA Soil Conservation Service Cooperative Laboratory, California Institute of Technology, Pasadena, Ca, Hydrodynamics Laboratory Publication N°167, 36 pp.

Shvidchenko, A., Pender, G., 2000. Flume study of the effect of relative depth on the incipient motion of coarse uniform sediments. Water Resources Research, 36(2): 619-628.

Shvidchenko, A., Pender, G., Hoey, T.B., 2001. Critical shear stress for incipient motion of sand/gravel streambeds. Water Resources Research, 37(8): 2273.

Sime, L.C., Ferguson, R., Church, M., 2007. Estimating shear stress from moving boat acoustic Doppler velocity measurements in a large gravel bed river. Wat. Resour. Res., 43(W03418): 1-12.

Singh, A., Fienberg, K., Jerolmack, D.J., Marr, J., Foufoula-Georgiou, E., 2009. Experimental evidence for statistical scaling and intermittency in sediment transport rates. J. Geophys. Res., 114(F01025): 1-16.doi:10.1029/2007JF000963

Smart, G., 1999. Turbulent velocity profiles and boundary shear in gravel bed rivers. Journal of Hydraulic Engineering, 125(2): 106-116.

Smart, G.M., Jaeggi, M.N.R., 1983. Sediment transport on steep slopes. Mitteilungen n°64, Der Versuchsanstalt fuer Wasserbau, Hydrologie und Glaziologie, Eidg. Techn. Hochschule Zuerich, Zurich, 89-191 pp.

Song, T., Chiew, Y.M., Chin, C.O., 1998. Effects of bed-load movement on flow friction factor. Journal of Hydraulic Engineering, 124(2): 165-175.

Sterling, M.S., Church, M., 2002. Sediment trapping characteristics of a pit trap and the Helley-Smith sampler in a cobble gravel bed river. Water Resour. Res., 38(1144): 1-19.

Strickler, K., 1923. Beiträge zur Frage der Geschwindigkeitsformel und der Rauhigkeitszahlen für Ström, Kanäle und geschlossene Leitungen, Eidgenössisches Amt für Wasserwirtschaft, N°16, Bern, Switzerland.

Strom, K., Papanicolaou, A., Evangelopoulos, N., Odeh, M., 2004. Microforms in Gravel Bed Rivers: Formation, Disintegration, and Effects on Bed Load Transport. Journal of Hydraulic Engineering, 130(6): 554-567.

Suszka, L., 1991. Modification of transport rate formula for steep channels. Earth Sciences (Lecture Notes), 37: 59-70.

Tabata, S., Ichinose, Y., 1971. An Experimental Study on Critical Tractive Force of Cobble Gravels. Journal of the Japan Society of Erosion Control Engineering, SHIN-SABO, Vol.23, No.4, Ser. No.79: 12-20.

Torri, D., Poesen, J., 1988. Incipient motion conditions for single rock fragments in simulated rill flow. Earth Surface Processes and Landforms, 13: 225-237.

Tsujimoto, T., 1991. Bed-load transport in steep channels. Fluvial Hydraulics of Mountain Regions, Lect; Notes Earth Sci. ser., 37: 89-102.

Tunnicliffe, J. et al., 2012. Use of 2D hydraulic models to develop and improve parameterized 1D models of sediment transport EGU 2012 (Poster Session), Vienna, Austria.

USACE, 1991. Hydraulic Design of Flood Control Channels, EM 1110-2-1601, US Army Corps of Engineers, 183 pp.

Van Rijn, L.C., 1984. Sediment transport, Part I: Bedload transport. Journal of Hydraulic Engineering, 110(10): 14311457.

Vanoni, V.A., Brooks, N.H., 1957. Laboratory studies of the roughness and suspended load of alluvial streams, Report N°E-68, Sedimentation Laboratory, California Institute of Technology, Passadena, California, 120 pp.

Vanoni, V.A. et al., 1966. Sediment transportation mechanics: initiation of motion. Journal of the Hydraulics Division, 92(HY2): 291-314.

Vericat, D., Church, M., Batalla, R.J., 2006. Bedload bias: comparison of measurements obtained using two (76 and 152 mm) helley-Smith samplers in a gravel bed river. Water Resour. Res., 42(W01402): 1-13.

Villar, R.E. et al., 2012. The integration of field measurements and satellite observations to determine river solid loads in poorly monitored basins. Journal of hydrology, 444-445: 221-228.

Vollmer, S., Kleinhans, G., 2007. Predicting incipient motion, including the effect of turbulence pressure fluctuations in the bed. Water Resources Research, 43(W05410): 1-16.

Wang, J., Dong, Z., Chen, C., Xia, Z., 1993. The effects of bed roughness on the distribution of turbulent intensities in open channel flow. Journal of Hydraulic Research, 31(1): 89-98.

Whitaker, A.C., Potts, D.F., 2007. Analysis of flow competence in an alluvial gravel bed stream, Dupuyer Creek, Montana. Water Resources Research, 43(W07433): 1-16.

White, C.M., 1940. The equilibrium of grains on the bed of a stream. Proc. Roy. Soc., A 174: 322-338.

Whiting, P., Dietrich, W.E., Leopold, L.B., Drake, T.G., Sherve, R.L., 1988. Bedload sheets in heterogenous sediments. Geology, 16: 105-109.

Wiberg, P., Smith, J.D., 1987. Calculation of the critical Shear stress for motion of uniform and heterogeneous sediments. Water Resources Research, 23(8): 1471-1480.

Wiberg, P., Smith, J.D., 1991. Velocity distribution and bed roughness in high-gradient streams. Water Resources Research, 27(8): 825-838.doi:10.1029/90WR02770.

Wilcock, P., 2001. Toward a practical method for estimating sediment-transport rate in gravel-bed rivers. Earth Surface Processes and Landforms, 26: 1395-1408.DOI: 10.1002/esp.301.

Wilcock, P., Pitlick, J., Cui, Y., 2009. Sediment transport primer, Estimating bed-material transport in gravel-bed rivers, Gen Tech Rep RMRS-GTR-226. Fort Collins, CO: U.S. Department of Agriculture, Forest service, Rocky Mountain Research Station, 78 pp.

Wilcock, P.R., 1993. Critical shear stress of natural sediments. Journal of Hydraulic Engineering, 119(4): 491-505.

Wilcock, P.R., Southard, J.B., 1988. Experimental study of incipient motion in mixed-size sediment. Water Resources Research, 24(7): 1137-1151.

Wilcock, P.R., McArdell, B.W., 1993. Surface-based fractional transport rates: Mobilization thresholds and partial transport of a sand-gravel sediment. Water Resources Research, 29(4): 1297-1312.

Wilcock, P.R., McArdell, B.W., 1997. Partial transport of a sand/gravel sediment. Water Resources Research, 33(1): 235.

Wilcock, P.R., Crowe, J.C., 2003. Surface-based transport model for mixed-size sediment. Journal of Hydraulic Engineering (ASCE), 129(2): 120-128.

Wilcock, P.R., DeTemple, B.T., 2005. Persistence of armor layers in gravel-bed streams. Geophysical Research Letter, 32(L08402): 1-4.

Wilcock, P.R., Kenworthy, S.T., Crowe, J.C., 2001. Experimental study of the transport of mixed sand and gravel. Water Resources Research, 37(12): 3349.

Wolman, M.G., 1954. Method of sampling coarse river bed material. Transactions of the American Geophysical Union,, 35: 951-956.

Wong, M., Parker, G., 2006. Re-analysis and correction of bed load relation of Meyer-Peter and Muller using their own database. Journal of Hydraulic Engineering, 132(11): 1159-1168.

Yager, E.M., Kirchner, J.W., Dietrich, W.E., 2007. Calculating bed load transport in steep boulder bed channels. Water Resources Research, 43(W07418): 1-24.

Yager, E.M., Dietrich, W.E., Kirchner, J.W., McArdell, B.W., 2012. Prediction of sediment transport in step-pool channels. Water Resour. Res., 48(1): W01541.

Yalin, M.S., 1963. An expression for bedload transportation. Journal of Hydraulic Engineering, ASCE, 89(3): 221-250.

Yalin, M.S., Karahan, E., 1979. Inception of sediment transport. Journal of the Hydraulics Division, HY11: 1433-1443.

Yang, C.T., 1984. Unit stream power equation for gravel. Journal of Hydraulic Engineering, 110(12): 1783-1797.

Yen, B.C., 2002. Open channel flow resistance. Journal of Hydraulic Engineering, 128(1): 20-38.

Zimmermann, A., 2010. Flow resistance in steep streams: an experimental study. Water Resour. Res., 46: W09536, doi:10.1029/2009WR007913.

Abstract

Because it is difficult to measure bedload sediment transport in rivers during flooding, flume experiments have been widely used for studying the mechanisms involved and for constructing bedload transport equations. However, flume experiments usually involve several simplifications concerning the sediment material (usually a uniform grain size distribution is used) and the flow conditions (usually maintained high for one-dimensional transport and no bed meandering), which can have strong consequences when the flume-derived equations are used in the field. This manuscript presents the results of my research on this topic and aims to fill the gap between the flume and the field. The three parts of the manuscript concern the hydraulics, the threshold conditions for bedload transport, and bedload transport rates. It is shown that large diameters such as D_{84} are recommended for matching the results obtained in the flume and in the field, both for flow resistance and threshold dimensional shear stress. The comparison is less trivial for bedload transport as (i) most flume bedload transport were measured for high shear stress and almost full mobility of the bed sediments, whereas in the field, measurements usually correspond to partial transport (the finer fractions are transported whereas the coarsest fractions are maintained at rest) and (ii) because of nonlinearity, 1D flume derived equations tend to underestimate bedload transport when they are used with width averaged data.

Résumé

En raison de la difficulté à mesurer le charriage dans les rivières en crue, l'expérimentation en canal a très largement été utilisée pour étudier les mécanismes impliqués et pour élaborer des équations. Cependant, les expériences en canal impliquent généralement plusieurs simplifications concernant les sédiments (généralement une distribution uniforme est utilisée) et les conditions d'écoulement (généralement maintenues élevées pour un transport unidimensionnel), ce qui peut avoir des conséquences fortes lorsque les équations qui en sont issues sont utilisées sur le terrain. Ce manuscrit présente les résultats de ma recherche sur ce sujet et vise à faire le lien entre le laboratoire et le terrain. Les trois parties du manuscrit concernent l'hydraulique, les conditions de début de mouvement, et la modélisation du charriage. Il est montré que les grands diamètres tels que le D_{84} sont recommandés pour comparer les résultats obtenus au laboratoire et sur le terrain, à la fois pour la résistance à l'écoulement et pour la contrainte adimensionnel de mise en mouvement. La comparaison est moins triviale pour charriage car (i) le charriage au laboratoire a souvent été mesuré pour des contraintes de cisaillement fortes et une mobilité quasi totale des sédiments du lit alors que sur le terrain, les mesures correspondent habituellement à un transport partiel (les fractions les plus fines sont transportées alors que le fractions plus grossières sont maintenus au repos) et (ii) en raison de la non-linéarité du phénomène, les équations 1D issues du canal ont tendance à sous-estimer le charriage lorsqu'elles sont utilisées sur le terrain avec grandeurs moyennées sur la section.